ADDIS ABABA UNIVERSITY

SCHOOL OF POST GRADUATE STUDIES

ADDIS ABABA INSTITUTE OF TECHNOLOGY

SCHOOL OF ELECTRICAL AND COMPUTER ENGINEERING

Satellite Tracking Microwave Phased Array Antenna.

By

Eyob Habte

Advisor

Dr. Murad Ridwan (Ph.D.)

This thesis is submitted to Addis Ababa University, School of Post Graduate Studies, Addis Ababa Institute of Technology, School of Electrical and Computer Engineering in Partial Fulfillment for a Degree of Masters of Science in Communication Engineering.

August 10, 2016.
Addis Ababa, Ethiopia.

ADDIS ABABA UNIVERSITY

SCHOOL OF POST GRADUATE STUDIES

ADDIS ABABA INSTITUTE OF TECHNOLOGY

SCHOOL OF ELECTRICAL AND COMPUTER ENGINEERING

Satellite Tracking Microwave Phased Array Antenna.

By

Eyob Habte

Advisor

Dr. Murad Ridwan (Ph.D.)

August 10, 2016.

Approval by Board of Examiner committee

Chairman Department Graduate committee	**Date and Signature**
Dr. Murad Ridwan (Ph.D.)	
Advisor	**Date and Signature**
Internal Examiner	**Date and Signature**
External Examiner	**Date and Signature**

Abstract

Satellite based communication and the utilization of wideband frequency spectrum are essential to military, aerospace communication and navigation. It will also enhance the terrestrial communication to meet the required coverage, quality and data rate. So its implementation is inevitable in the near/future Ethiopian communication engineering advancement. Satellite tracking is one of the important issue in fulfilling the complete satellite based communication. The challenges in tracking methods such as, the need to rotate large dish antenna with the aid of Programmable Logic Controller, its applicability to only single target and drawbacks related with pointing accuracy are some of them.

This thesis investigates both adaptive phased array antenna within microwave frequency spectrum and satellite constellation theories to verify the ability of phased array antenna in tracking multiple targets by using single Tracking, Telemetry Commanding and Monitoring station at the sub-satellite point. The thesis also presents adaptive signal processing algorithms to demonstrate their tracking capability of two satellites' directional beacons.

In this thesis, Matlab software has been used to simulate adaptive signal processing. The analysis of the satellites' constellation using the six orbital element sets and the directional beacon signal from two satellites in the Line of Sight direction is performed. The where about of the satellites are extracted from the beacon signal angle of arrival. It is then used by the steering vector to point the maxima towards the targets and the nulls towards the interferer. The error vector is generated by the difference between the reference signal and the array output and used to derive the weight control block. The simulation is within Ka and C – band frequency spectrum, which is performed by implementing various numbers of elements and spacing. Based on the simulation result, we have concluded that the optimum elemental spacing in microwave frequency spectrum is 0.5λ at a cost of 20 times more elements than that was simulated for 10 elements. Generally, by controlling the inter element spacing and array number; it is possible to track multiple moving satellites.

Keywords: Adaptive phased antenna, Steering vector, Error vector, Satellite Constellation and Six orbital element sets.

Declaration

I, the undersigned, declare that this research work has not been submitted before as a fulfillment for Masters of Science degree in communication Engineering in this or any other university, and all the materials referred by this research has been fully acknowledged.

Eyob Habte _____

Name **Date and Signature**

Date of Submission: _____

This research work has been submitted to board of examiner for examination with the approval as a university advisor.

Dr. Murad Ridwan (Ph.D.) _____

Advisor **Date and Signature**

Dedication

Dedicated to my parents.

Table of Contents

Acknowledgment

First and the most I thank God for all of the courage and patience he gave me to work on this research, next my deepest gratitude goes to Dr. Murad Ridwan for his valuable support and guidance towards the thesis objectives.

I would also like to express my deepest gratitude to all of the AAiT School of Electrical and Computer Engineering staffs and my friends.

List of Abbreviations

Abbreviations	Definitions
ADC	Analog – to – Digital converter
AOA	Angle of Arrival
Az	Azimuth
BER	Bit Error Rate
CG	Constant Gradient
C – band	Compromise band
DBF	Digital Beamforming
DMI	Direct Matrix Inversion
DSP	Digital Signal Processor
E – Plane	Electric field vector Plane
El	Elevation
ESPRIT	Estimation Signal Parameters Rotation Invariance Technique
FNBW	First Null Beam Width
GLONASS	Global Navigation Satellite System
GPS	Global Positioning Satellite
GS	Ground Station
H – Plane	Magnetic field plane
HPBW	Half Power Beam Width
IEEE	International Electrical Electronics Engineering
IF	Intermediate Frequency
Inmarsat	International Marine/Maritime Satellite
ISL	Inter – Satellite Link
Ka	Kurth above band

Kbps	Kilo Bit per Second
Ku	Kurth under band
Lat	Latitude
L – band	Frequency spectrum range
LEO	Lower Earth Orbit
LMS	Least Mean Square
LOS	Line of sight
LP	Linear Prediction
LS – CMA	Least Square – Constant Modulus Algorithm
ME	Maximum Entropy
MEO	Medium Earth Orbit
ML	Maximum Likelihood
MMSE	Minimum Mean Square Error
MN	Minimum Norm
MSE	Mean Square Error
MUSIC	Multiple Signal Classification
MV	Minimum Variance
MVDR	Minimum Variance Distortion Less response
NLMS	Normalized Least Mean Square error
Opt	Optimum
Pdf	Probability Density Function
PHD	Pisareko Harmonic Decomposition
PLC	Programmable Logic Controller
PLL	Phased Locked Loop
QPSK	Quadrature Phase – Shift keying

RAAN	Right Ascension Ascending Node.
RF	Radio Frequency
RLS	Recursive Least Square
LS - CMA	Recursive Least Square Constant Modulus Algorithm
SAT	Satellite
SINR	Signal – to – Interference plus Noise Ratio
SLC	Side Lobe Canceller
SMI	Sample Matrix Inversion
SNR	Signal – to – Noise ratio
SOI	signal of Interest
SONI	Signal of Not Interest
SVE	Steering Vector Error
TDMA	Time Division Multiple Access
TTC&M	Tracking, Telemetry, Commanding and Monitoring
WVE	Weighting Vector Error
2D	Two Dimensional

List of Symbols

Symbols	Definitions
G	Array Gain
t	Time
k	Discrete time instant
R	Antenna region radius scalar value
L	Antenna physical length scalar value
E	Electric field vector
H	Magnetic field vector
L	Linear Array vector element number
M	Array element number in X – axis in 2 D array matrix
N	Array element number in Y – axis in 2 D array matrix
d_x	Infinitesimal spacing in x - direction
d_y	Infinitesimal spacing in y - direction
$\boldsymbol{K}$	**K** sources vector located in the far field of the space
θ_{el}	Elevation angle
ϕ_{az}	Azimuthal angle
τ	Time delay on the element from the reference element
$\mathbf{r}(\theta_{el}, \phi_{az})$	Radial distance vector from the element to the source
$\mathbf{v}(\theta_{el}, \phi_{az})$	Unit vector in the direction of wave front arrival angle $\mathbf{r}(\theta_{el}, \phi_{az})$
C	Speed of light wave electromagnetic disturbance
$\boldsymbol{X}$	Electrical induced signal vector or matrix on the array
m_k	Modulating low pass signal from the source
f_c	Carrier signal radio frequency

l	Elemental index number in x – axis of rectangular array
k	Elemental index number in y – axis of rectangular array
λ	Wave length
$\boldsymbol{S}$	Steering vector or matrix with a Vandermonde vector structure
$\boldsymbol{W}$	Weighting vector or matrix
Y	Total array scalar output
$W_{m,n}$	Elemental weight in rectangular array weight matrix
$S_{l,k}$	Component of steering matrix
$y_i(t)$	Scalar array output due to the i^{th} source
$\boldsymbol{e}(k)$	Error vector at the k^{th} sampling instant
$X_{m,n}$	The induced signal on the $(m,n)^{th}$ element
$P_{m,n}$	The M, N index power
$\mathbf{X}^*$	Conjugate of the induced signal vector
$\boldsymbol{X}^H$	Hermittian of the induced signal vector or matrix
$\boldsymbol{W}^H$	Hermittian of the weighting vector or matrix
P	Scalar output power or the magnitude square of the array output signal
$\mathbf{R}$	Covariance matrix of the total induced signal including interference and noise
$\boldsymbol{R_{SS}}$	Signal covariance matrix
$\boldsymbol{R}_{II}$	Interference signal covariance matrix
$\boldsymbol{R}_{NN}$	Noise covariance matrix
P_S	Source signal power
P_I	Interference signal power
P_N	Noise power
P_B	Periodogram Bartlet

P_C	Periodogram Capon
P_{LPM}	Periodogram Linear Prediction
P_{ME}	Periodogram Maximum Entropy
P_{PHD}	Periodogram Pisareko Harmonic Decomposiotion
P_{MN}	Periodogram Minimum Norm
$\boldsymbol{E}_N$	Noise sub space eigen vector
$\boldsymbol{E}_N^H$	Hermittian of Noise sub space eigen vector
P_{MUSIC}	Periodogram MUSIC
$P_{ROOT-MSIC}$	Periodogram Root MUSIC
Z_i	Root of the denominator of the Root MUSIC periodogram
$k = \frac{2\pi}{\lambda}$	Wave number
d	Elemental spacing
$\boldsymbol{\phi}$	Doublet phase shift vector
$\boldsymbol{R}_{11}$	The first doublet array correlation matrix
$\boldsymbol{R_{22}}$	The second doublet array correlation matrix
u	Unwanted signal for minimum variance beamforming
λ	The Lagrange multiplier of the minimum variance beamforming
$\boldsymbol{W}_{MV}$	Weighting vector for minimum variance beamforming
Δ_W	Gradient of the least mean square error function with respect to weight
$\boldsymbol{J}$	Cost function or least mean square error vector
R_{nn}	Noise covariance matrix
σ_n^2	Noise variance
$L(x)$	Log – likelihood function
$\mathbf{W}_{ML}$	Maximum likely – hood weight vector

β	*Forgetting factor*
$\overline{\boldsymbol{W}}$	Estimated weight matrix or vector
Γ	Weighting or steering vector error model
r_{si}	Radius or length of the elliptical orbit
e	Eccentricity value range from 0 to 1
E	Angular value eccentricity anomaly
M	Angular value mean anomaly
η_{Ui}	The i^{th} satellite signal AOA in the line of sight derived from the true anomaly
t_0	The initial time when the target satellite is exactly at the perigee altitude.
C_6	The six orbital element set of a satellite in a constellation
i	The orbital plane inclination from the equatorial plane
Ω	*Right Ascension ascending node measured from radius of sun to the first crossing node*
ω	Argument of perigee
η_i	True anomaly/the true angular position of the i^{th}satellite from radius of Perigee
$\boldsymbol{W}_{opt}$	Wiener optimum weighting vector
$\mathbf{r}(t)$	Reference signal vector
L_{GSi}	The Longitude of the ground station in tracking the i^{th}satellite.
Δ_i	Difference in longitude between the ground station and i^{th} satellite
R_{si}	Slant range of the i^{th} satellite in the direction of $\mathbf{v}(\theta, \phi)$
M	*Sub - satellite point coordinate value on the Earth*
$\boldsymbol{e}$	Error vector to drive the adaptive weight control block
d	Desired signal vector
$\boldsymbol{r}_{xd}$	Cross correlation matrix between the induced signal and the desired signal
μ	*Convergence time or learning rate*

λ_i	The i^{th} eigen value of the array correlation corresponds to the i^{th}source signal
λ_{max}	The maximum eigen value of the array correlation matrix
R_e	Radius of the Earth
a	Major axis orbital radius
γ	Central angle at the Earth center or true anomaly when $\theta_{el} = 0$
h_o	Orbital altitude of the satellite above the Earth surface.

List of Figures

List of Tables

Chapter One

Introduction

1.1 Motivation and Background

By the authors' opinion, the future of Ethiopian technological advancement in the fields of Telecommunication, navigation and surveillance, deep space interplanetary exploration, regional as well as national security will deal inevitably with the utilization of wideband frequency spectrum and satellite based communication. In addition, the classical or the older satellite based navigation and communication are employed with less integrated technology and poor performance [1].

Poor performances such as beam pointing error due to wind vibration, system deterioration in rotating large dish antenna and its applicability to single target tracking are some of them.

Adaptive phased array antenna is an antenna array which is aided by digital signal processor. The digital signal processor controls the transmitted and received directional signals. In this thesis, linear antenna array lattice, the DSP, the ADC, the RF and IF processing hardware have been taken in to account. Given the controlling parameters in these hardware that, their effect on the performance measuring metrics has direct as well as indirect influences.

The term adaptive is given for phased array antenna, such that the weighting applied on each channel is not at the time of initial antenna system design. The weighting process rather adapts to the signal environment. The adaptive control of the signal shall be performed on the received data rather than on signal beam space by using DSP. The DSP includes two fundamental blocks called the AOA estimator and the digital adaptive beam former.

1.2 Statement of the Problem

In the past, a single space craft was sufficient to perform most of the space mission. However, a single space craft cannot fulfill most of the space mission objectives [32]. One way

to fulfill the mission objective is through the use of a series or a number of satellites on the same or different orbital paths and it is known as Satellite Constellation.

There are different constellation theories, which are applicable for different space mission objective. In the past, satellite constellation concept has been proposed for broad range of uses. Initially, starting from navigation and positioning (GPS and GLONASS), Satellite constellation theory [32] spines out in to Telecommunication (Iridium, Global star, Teledesic and Inmarsat etc.).

Taking both adaptive phased array antenna and satellite constellation theories into account; can the theories in these fields be investigated in parallel for multiple moving signal source tracking? Can the adaptive DSP performance measuring metrics be evaluated using the two theories' concept? Can the adaptive phased array antenna be tested in tracking two targets at polar orbit? What are the effect of SVE, WVE and variation in input SINR on the antenna array Gain (G)? If the above research questions are answered, can phased array antenna be applied for multiple targets tracking?

1.3 General Objective

The main objective of the thesis is to study the adaptive phased array antenna and satellite constellation theories. Next to that, investigating if satellite constellation and adaptive phased antenna be analyzed and applied to multiple beacon signal sources tracking which are moving on their orbits. In addition, it includes the following points.

1. Study the performance of adaptive beamforming algorithms such as LMS, SMI or DMI, RLS, LS – CMA, based on (beam steering, nullifying, computational complexity and convergence) for linear array geometry.
2. Investigating the output SINR and the signal processor gain with respect to weighting vector error (WVE) and steering vector error (SVE) for linear array configuration.
3. Investigating/study the beam pointing accuracy of the adaptive phased array antenna for linear array geometry.

1.4 Specific Objectives

1. Investigating adaptive beamforming for two specific constellations i.e. for Walker star and Delta.
2. Investigating the effects of varying antenna element number and inter – element spacing on the performance of signal processor in tracking the directional beacon signals which are transmitted from two target satellites using linear array configuration within microwave frequency spectrum.
3. Investigating how to adjust the effect of antenna array number and spacing within the operating microwave frequency spectrum.

1.5 Methodology

The methods which we follow to achieve the aim and objectives of this research are illustrated as follows.

1. Reading books, Journal Papers, Conference Papers, Proceedings, Reviews and Articles which are related to Satellite Tracking, Adaptive Beamforming, Digital Signal Processing, Satellite Constellation Theory and implementation method. Reading simulation toolbox documentation and any research papers which are related to the topics.
2. System Mathematical Modeling: Mathematical formulation of the AOA of the signals in LOS direction from two target satellites.
3. Simulation: Simulation of uniform linear array and adaptive phased array antenna beamforming algorithms for two targets satellite constellation.
4. Analysis and interpretation of the simulation result which is obtained by simulating two targets beacon of the Iridium and Global star satellites. Comparing the tracking performance of the adaptive beamforming algorithm based on main beam steering toward the direction of the targets and placing deep nulls toward the interferer.

1.6 Research tools and equipment

Matlab phased array antenna tool box and Microsoft office software on Intel(R) ™ i3–3240 processor with Windows 7 service pack 1 operating system have been used.

1.7 Contribution of the thesis

This thesis contributes to the field of navigation and communication through the investigation of both satellite constellation theory and the adaptive antenna's multiple moving beacon sources tracking. In such a way that the two theories have been analyzed through a mathematical modeling and then the phased array antenna tracking analysis has been simulated through adaptive beamforming algorithms to measure their performance in tracking multiple targets' beacon which are transmitted from two target satellites on same orbital path.

1.7.1 Specific contribution of the thesis:

- It has verified the ability of phased array antenna, which is operating within microwave frequency spectrum and located at the sub - satellite point in tracking multiple targets.
- It provides an easy and smart method of satellite tracking by a reduced cost through the use of adaptive signal processing.

1.8 Literature review

Many research papers and articles have been published regarding adaptive phased array antenna, satellite constellation and tracking theory. The literatures reviewed in this thesis are categorized specifically those of which are related with adaptive antenna array signal processing and satellite constellation theory.

[1], [2], [3], [4] present the basic model of determining the AOA of the incoming signal's from a certain direction. [2], [3], [4], [5], [6], [7] present antenna array beam forming and adaptive beam forming algorithms which are used currently in array signal processing. [10] discusses the self-steering capability of adaptive antenna array and demonstrates its ability to track Satellite as it moves across the sky. It has further been summarized that in satellite communication system adaptive antenna array main beam can be steered to track the desired

signal by using LMS algorithm [3], [9], [10], and this has performed by changing the number of element and changing the main beam steering angle.

[1], [11], [12] review a number of tracking systems in satellite communication. [1] presents the past 25 years tracking methods which have been employed in satellite communication systems to sensing error in amplitude and phase; among these two of error sensing methods are prevalent. They may be described as monopulse and step tracking. In monopulse [1], [13], [14] the received wave front from the target satellite processed and the error is sensed to derive the pointing information to track the target satellite.

The reviews by Hawkin [1] summarized that by sensing higher order wave front both in amplitude and phase an error sensing less than 0.005^0 can be achieved using monopulse tracking method [13], [14]. Unfortunately, the monopulse technique relies on at least two channel coherent receivers [1] for its operation and to process the received higher order wave front and this incurs additional mass and expense. This factor can be absorbed in terms of ground station operation but presents a penalty in terms of space craft consideration; as a result a monopulse ground station system reduces the effective communication payload on the space segment.

[1], [11] and [12] presents about the step track method, in the case of step track a relatively simple non coherent receiver is employed and it is cheaper to implement than the monopulse system. While the performance of the communication link is sacrificed a minimum signal to noise ratio of 30 dB is required for satisfactory operation of the step track as compared to the monopulse system which is 15 dB. As the error detection system is not "*real – time*" the system suffers from the dynamic lag.

In the early eighties electronic beam squint tracking method had emerged and it appeared to overcome the problem associated with the early tracking systems [1]. The tracking accuracy and the dynamic performance are comparable with the monopulse tracking method and relatively cheap to implement as it require only single channel receiver which yields simple system.

In this thesis as we have surveyed in the literature, the tracking system has employed dish antenna and also the system has been used for single target tracking. In addition, the error in amplitude and phase has attained to a minimum value of 0.005^0 .

This thesis has investigated the tracking ability of adaptive phased antenna and contributed to the satellite tracking method. In such a way that it demonstrates the ability of phased array antenna in tracking multiple target satellites at polar orbit. The simulation result obtained, using the adaptive signal algorithms shows the optimal elemental spacing is 0.5λ at a cost of 20 times more element than that was simulated for 10 elements.

1.9 Assumption made in the thesis

1. The target satellites are equipped with space borne adaptive antenna.
2. Array element coupling and Doppler shift are assumed to be suppressed.
3. The ground and the space borne antenna initially locked at time $t = t_0$ using a reference signal.
4. The effect of the signal propagation from space borne antenna to the ground antenna is a pure time delayed.
5. The signals are propagated in the line of sight direction.
6. The ground station, where the adaptive phased array antenna to be deployed in, is assumed to be located exactly at the sub satellite point of the target. The target orbit of inclination is approximated to polar. As a result the longitude of the satellites and the ground station are assumed to be equal at any instant t. The orbital planes of the target satellites are perpendicular to equatorial plane. The orbital planes can be considered as **XZ** or **YZ** plane in Cartesian coordinate.

1.10 Thesis Overview

Chapter one presents the motivation and background, the general and specific objectives, methodology and the literature reviewed by the thesis. Moreover, assumptions taken by the thesis and the thesis contribution have been also discussed.

Chapter two covers a brief explanation about the fundamental parameters, definitions and standard terms used in antenna theory which are defined by IEEE standard and other literatures.

In Chapter three fundamental to antenna array theory, terminologies used in an antenna array and the fundamental types of antenna array have been defined and discussed. Adaptive antenna historical background, rectangular array signal modeling, rectangular array steering vector and weighting, introduction to two dimensional LMS algorithm, measuring metrics and terminologies used in adaptive signal processing have been also discussed.

Chapter four presents satellite constellation theory and the ground station TTC and M mathematical modeling where the adaptive phased array antenna to be deployed in. The chapter presents the derivation of AOA equation of the signals from the i^{th} satellites. The analysis of satellite tracking in conjunction with adaptive signal processing have been discussed and simulated for two targets on the same orbital path.

Chapter five presents and discusses the two target tracking simulation results, which is performed by simulating uniform linear antenna array for 16 different element number and spacing combinations within Ka and C – band operating frequency spectrum. Chapter Six summarized and concluded the thesis and finally it presents the recommendations for future work.

Chapter Two

Fundamental Parameters of Antenna

2.1 Introduction

IEEE's standard definitions for terms (IEEE Std 145 – 1983) defines antennas or aerials as "a means of radiating or transmitting and/or receiving Electromagnetic or radio waves." There are different types of antennas such as wire antennas, aperture antennas, micro strip patch antennas, reflector antennas and lens antennas. The history of antennas [9] dates back to James Clerk Maxwell who had unified the theory of Electricity and Magnetism, and described their relationship through the famous equation called Maxwell's equations. Maxwell had also showed that light was Electromagnetic waves, and both light and electromagnetic waves travels by the same speed of wave disturbance. In 1886 professor Henrich Rudolph Hertz had discovered a spark of electromagnetic waves, whose wavelength was 4 meters, between two half wave transmitting dipoles and detected its presence around a loop and it was the first wireless electromagnetic system. In 1901 Marconi had demonstrated signal transmission over large distance; he had sent the first transatlantic signals from Poldhu, Cornwell, England to St. John new found Land. From Marconi's' inception up to 1940s; prior to the second World War antenna elements were wire type (long wire, dipoles, Helices, Rhombus and fans). From 1960s up to 1990s major advances in antennas technology were made; during 1960s advanced evolution on an antenna technology had maximized the bandwidths to 40:1. Early in 1970s micro strip patch antennas was introduced and it was antennas advancement for a millimeter waves; today antenna can easily be integrated with passive and active microwave circuits to form a monolithic type. The basic antenna parameters which are defined below are derived from the IEEE standard definitions of terms for antennas (IEEE std 145 - 1983).

2.2 Radiation Pattern

Radiation pattern of an antenna [3], [9] is defined as "the mathematical or graphical representation of the radiation properties of an antenna as a function of angular space coordinates. Some of these radiation properties include Radiation Power flux, Radiation Power

density, Radiation Intensity, Electric or Magnetic field strength, Directivity, Phase or Polarization." The received electric or magnetic field of an antenna at distance of constant radius is called amplitude field pattern, whereas the angular distribution of the radiation power density over a surface of constant radius is called Power field pattern. In other words the field pattern of an antenna is defined as the plot or representation of the magnitude of either the electric field or magnetic field as a function of angular space coordinate [3], [9] and by similar explanation power pattern of an antenna is the plot or representation of the square of either the electric or magnetic field as a function of angular space coordinate. Amplitude field pattern and power pattern are usually normalized by their maximum value and are called *normalized field or power pattern*, respectively. Logarithmic scale usually called decibels (dB) used, which is used to scale those parts of the pattern which have very small values.

2.2.1 Radiation Pattern Lobes

Different parts of the antenna pattern are called lobes. Lobes can be major or main lobe, minor, side and back lobes.

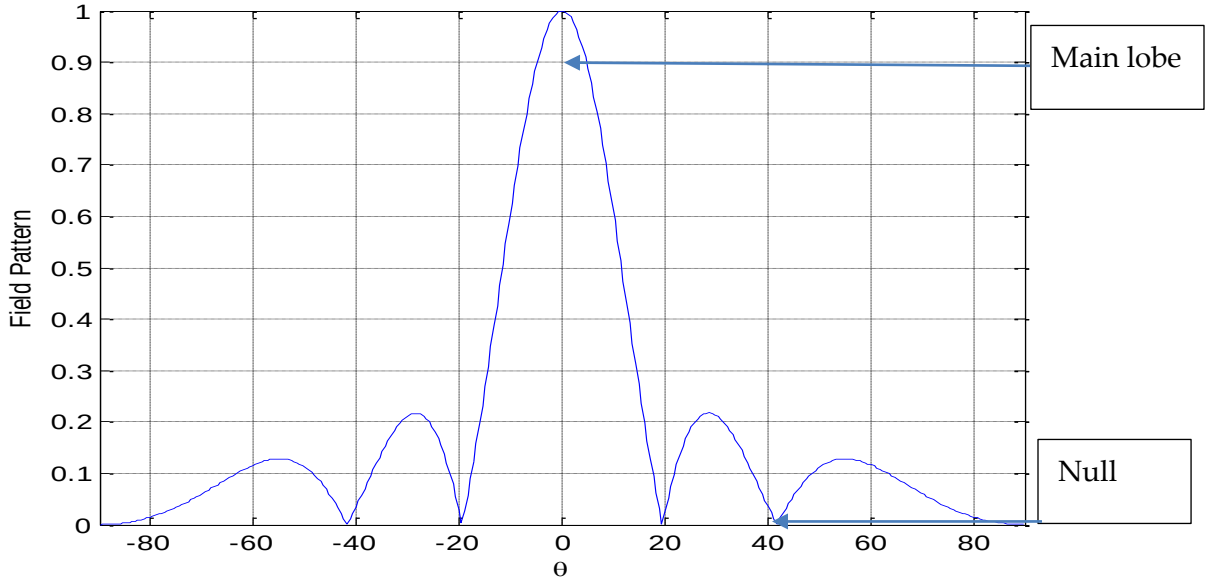

Figure (2.1) Azimuth cut line plot of Major,Minor, and side lobes in rectangular coordinate [3].

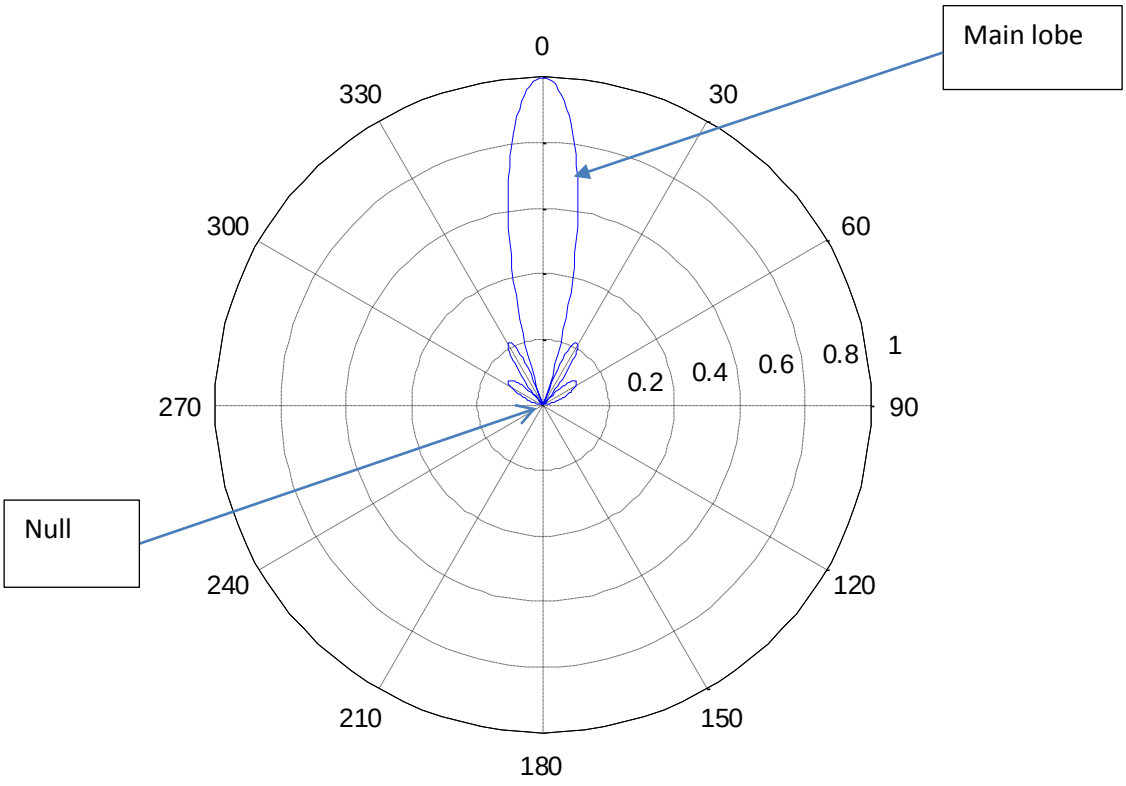

Figure (2.2) Azimuth cut polar plot of Major,Minor, and side lobes in polar coordinate [3].

2.3 Antenna regions

The space surounded by an antenna is known as antenna regions. There are three different antenna regions [3], [9], the reactive near field region, the radiating near field region and the far field region. The physical surrounding of antenna wherein the the electromagnetic wave power and energy half of the physical length the antenna can be defined as the physical antennas region. The reactive near field region is defined as ”that part of antennas region which predominately consists of the reactive energy.” The reactive energy does not radiated and it can be described as the energy stored on the imaginary part of the antenna terminal impedance.

That part of the antenna region, whrer it is between the reactive near field and the far field region is said to be radiating near field or the fresnel region. Similarly, that part of the antennas region beyond the radiating near field region is called the far field region. The energy within the far field region is independent of the distance from the antenna and it is also refered as the frauhnofer region [9].

2.4 Power density

Electromagnetic wave is used to transport information from one point to another in a wireless as well as in guided medium [9]. It is naturally evident that electromagnetic wave contains energy and power. The quantity to express the energy associated with the electromagnetic wave is through the use of the vector cross product between the electric field vector with the magnetic field vector [3], [9]. This quantity is defined as the poynting vector or radiation power density. The average power radiated by the antenna over a closed surface can be obtained by integrating the normal component of the instantneous average real power density over entire radiation surface. It is obvious that the power density associated with the imaginary part is the reactive or stored energy [9]. The power density associated with electromagnetic field in the far field is purely real and refered to as radiation power density.

2.5 Power Intensity

In order to describe power intensity a spherical geometry term called sterdian or one unit of solid angle has to be defined. One sterdian is the spherical angular meaured value of spherical area of r^2 where r is the sphere radius. Since the total spherical area is $4\pi r^2$ then there are 4π sterdian in a closed sphere. Having in mind the solid angle, power intensity in a given direction is defined as *" power radiated from the antenna per unit solid angle*." Since the observation is made on large sphere of constant radius which is extending to the far field then radiation intensity at the far field is simply defined by multiplying the average real power density by the square of the distance and it is the far field antenna's parameter.

2.6 Directivity

Isotrophic, omnidirectional and directional radiators are usually described along with directivity of antenna [9] and defined as follows. A hypothetical loseless antenna which radiates the electromagnetic wave equally in all direction is termed as Isotrophic. It is not exist in practice but it is used as a reference to measure the directivity of others radiator. Whereas directional radiator is defined as a directional antenna which can transmit and receive the electromagnetic wave in certain direction. Its directivity is usually greater than unity. The term

is usually defined for antennas whose directivity is more than the directivity of dipole wire antenna, which is used commoly as a reference for directivity meaurement. Omni directional radiator can be defined as "a special case of directional antenna,which radiates the electromagnetic wave in either azimuth or elevation plane omnidirectionaly but not on both plane."

The authors of the 1973 IEEE's *standard definitions of Terms for antennas* uses Directivity gain of antenna rather than Directivity of antenna. But the authors of the 1983 IEEE's *standard definitions of Terms for antennas* revised the term directivity gain. Having in mind the revised term and the three radiators, the directivity of antenna [3], [9] defined as the *"ratio of radiation intensity in a given direction to radiation intensity averaged over all direction."* Directivity is a unitless antenna parameter. The average radiation intensity is the power radiated divided by 4π. If the direction of intensity is not given then the direction of the maximum intensity is used.

For antenna with orthogonal polarization componets, there is a directivity called partial directivity [9] and defined as "part of radiation intensity to the given polarization component divided by the radiation intensity averaged over all direction." The total directivity includes both of the directivity of the two orthogonal polarization components.

2.7 Antenna Gain

Antenna gain is a modification of antenna directivity so as to include the effects of antenna eficiency or another term usually defined along with directivity. It is the measurment of the antenna directivity in terms of its efficiency [3], [9] and it separately takes into account the antenna input power along with its radiation efficiency so as to compare with the radiated power. Antenna gain for antenna arrays can be defined as the ratio of output SINR of the array to the input SINR [2].

2.8 Plane waves

E – plane of the electromagnetic wave is defined as the plane containing the electric field vector and the direction of the maximum power radiation, on the other hand the H – plane is

defined as the plane containing the magnetic field vector and the direction of the maximum power radiation.

2.9 Beamwidth

The beamwidth of the antenna pattern is defined as the angular separation between two identical points on the opposite sides of the antenna pattern maximum [9]. There are a number of beamwidth on antenna pattern, it can be Half power beam width (HPBW) which is defined by IEEE " *in the plane containing the direction of the maximum of the beam, the angular separation between two points in which the radiation intensity is half of the maximum*." There is also a beamwidth called First Null Beamwidth (FNBW) or approximately twice of the HPBW [3], [9], which is the angular separation between the first nulls of the antenna pattern maximum. The beam width is an important figure of merit and it is used as a trade of between the antenna pattern beamwidth and the side lobe level. When the beam width of the main lobe decreases then the beamwidth of the side lobe increases and vice versa [9]. The resolution capablity of an antenna to separate two sources is half of the first null beamwidth.Two adjcent sources or targets separated by angular distance equal or greater than half of the FNBW can be resolved.

2.10 Bandwidth

The bandwidth of an antenna is defined as the "range of frequency within which the performance of the antenna with respect to some specified characterstics cofirmed to some standard [9]." In other words it can be defined as the range of frequency between either sides of the center frequency (resonant frequency for dipole antenna) wherein some characterstics of the antenna (antenna terminal impedance, pattern, phase or polarization, side lobe level, gain, beam, and beam efficiency) remain constant [3],[9].

2.11 Polarization

The polarization of antenna in a given direction is defined as " the polarization of the electromagnetic wave transmitted by the antenna." If the direction is not specified then the polarization of the antenna is taken as the polarization of the maximum gain."

2.12 Antenna boresight

Antenna boresight is defined as the physical aiming direction of the antenna, or it can be defined as the direction of the maximum gain or the centeral axis of the main lobe [3], [9].

2.13 Reciprocity

Antenna can radiate or transmit power in prefered direction, similarly antenna can receive power in the same direction, this priciple is known as "reciprocity."

2.14 Friis equation

Harald Friis devised a formula which relates the powers radiated and received by two distance antenna and this famous equation relates the power received and transmitted by a satellite transmitter with the ground station antenna system, and it includes the signal attenuation model due to atmospheric layer, rain and other enviromental conditions.

$$P_r = P_t G_t G_r \frac{\lambda^2}{4\pi(d)^2} \qquad (2 - 1)$$

Chapter Three

Fundamentals of Antenna Array

3.1 Introduction

Specific antenna radiation pattern requirements cannot be achieved by a single antenna element alone, because single antenna element has wide radiation pattern and low directivity. To increase the directivity of single antenna element it is usually necessary to increase the electrical size of the antenna and increasing the electrical size of the antenna accompanied by increasing the associated mechanical problems. One way of increasing the directivity is achieved through an aggregation of a multiple clones of this single radiating element in a particular geometric lattice called Antenna Array.

Antenna array can be defined in its geometrical lattice in space; antenna array can be defined from a simple two element linear array up to a complex geometrical lattice such as circular, spherical, hexagonal and cylindrical type.

3.2 Fundamental Parameters of Antenna Arrays

Antenna array in a particular geometrical configuration has different parameters such as element number, element spacing, its geometrical configuration in space, its freedom to put the maxima and the null to the preferred direction, the input SINR, the output SINR and its gain.

3.3 Linear array

An arrangement of antenna in a straight line is defined as linear array; the simplest number of antenna element in linear array is two. Linear array is important since it helps to have an insight to analyze even a large number of array elements and it can be linear or nonlinear.

3.4 Rectangular array

An antenna array element arranged in two dimensional Cartesian coordinate is called rectangular array [9]. In such lattice the element spacing, element number and the array factor is defined in the respective two coordinate directions.

3.5 Array factor

In antenna array theory, steering vector can be defined as propagation vector and the sum of the steering vector in the array system is called array factor [2], [3], [9]. In a rectangular array the array factor is along the x and the y axis direction.

3.6 Array freedom and array weighting

The gain and phase applied to the signal derived from antenna element can be considered as a complex quantity and it is called the weighting applied to the antenna array element. For a single antenna element, the weighting applied to the antenna element will not vary the antenna pattern and parameter as we require; but for two element array the weight of one element can vary with respect to the other, so that the pattern can be varied to desired direction; that is the pattern maxima to one place and the null to the other place. For L element antenna array, the antenna pattern can be placed at L – 1 different position; which is implemented by changing the weight applied to the single element with respect to the other; therefore, we call the flexibility of the antenna array to place the pattern at L– 1 place array freedom [2].

3.7 Array weighting

The weighting technique [2], [3], [9] which is applied on the antenna array can be used for specific antenna array design purpose. For example, array weighting such as Binomial, Black man, kaisser – Bessel, Hamming and Gaussian.

3.8 Shading

Array shading in antenna is defined as a technique which is applied in the antenna radiation pattern so as to suppress the side lobe level to a certain defined amount which is measured in logarithmic scale, so that the desired radiation pattern amplified to a certain

amount. In phased array antenna there are different kind of shading such as Taylor, Chebyshev, Hann, Kaiser and Hamming.

3.9 Optimal Antenna

The noise component, in a communication system which is operating in an environment at which both the signal and the interferer works at the same carrier frequency, cannot be removed by filtering. In such a case the noise component can be optimally reduced by maximizing the signal to interference plus noise ratio such a communication system devised antenna called optimal antenna [2].

3.10 Adaptive Antenna

The name adaptive antenna is given for a phased antenna array such that the weighting process of the antenna element is not performed at the time of design rather the weighting process is performed dynamically on the time of signal processing and such a communication system employed an antenna array called adaptive antenna [2].

The historical background of adaptive antenna dates back to Van Atta [3] who has theorized the principles of operation of retro directive antenna which is used to retransmit signal in the direction of reception and it can be viewed as a reflector antenna by using phased antenna array concept. The advancement of the retro directive antenna through the use of closed loop system had stepped the antenna array research forward to the current advancement level i.e.; the phased – locked – loop (PLL) improves the self – phasing ability of the retro directive antenna system. Adaptive side lobe canceller (SLC) which was proposed by Howells in the retro directive antenna system improves the interference nulling ability so that it stepped the research in the adaptive antenna forward, there by SLC maximized signal – to – interference ratio (SNR).

By using the generalized side lobe canceler which was applied to maximize the SNR, Apple Baum developed an algorithm which is governing the adaptive interference cancellation and known as Howells Apple Baum algorithm, at the same time Widrow developed least mean Square algorithm (LMS), both the Howell - Apple Baum and Widrow's algorithm converges to

the optimum wiener solution. The convergence of the algorithm depends on the eigen value spread of the signal correlation matrix.

The involvement of adaptive algorithm in the phased locked closed loop system which had been researched and devised by Widrow and Apple Baum comprised not only the antenna array but also a signal processing unit. This signal processing unit is used to retro direct the transmitted signal towards the signal source, and includes sampling and digitizing, signal auto correlation sequence operation on the received digitized data. So that the generated array correlation matrix of the received signal, the estimated array weight using the statistical signal processing final output are applied to adaptive beam forming so as to manipulate signal source tracking.

3.10.1 Rectangular Array Lattice

In two dimensional array, the number of antenna elements are **M** and **N**, and spacing $\boldsymbol{d_x}$ and $\boldsymbol{d_y}$ in **X** and **Y** axis respectively as shown in Figure 3.1. Having taken into account rectangular array lattice, spatial array's digital signal processing always needs to define the following: signal model, media of propagation, constitute antenna elemental model, assumed signal bandwidth, effects of propagation in the modeled media.

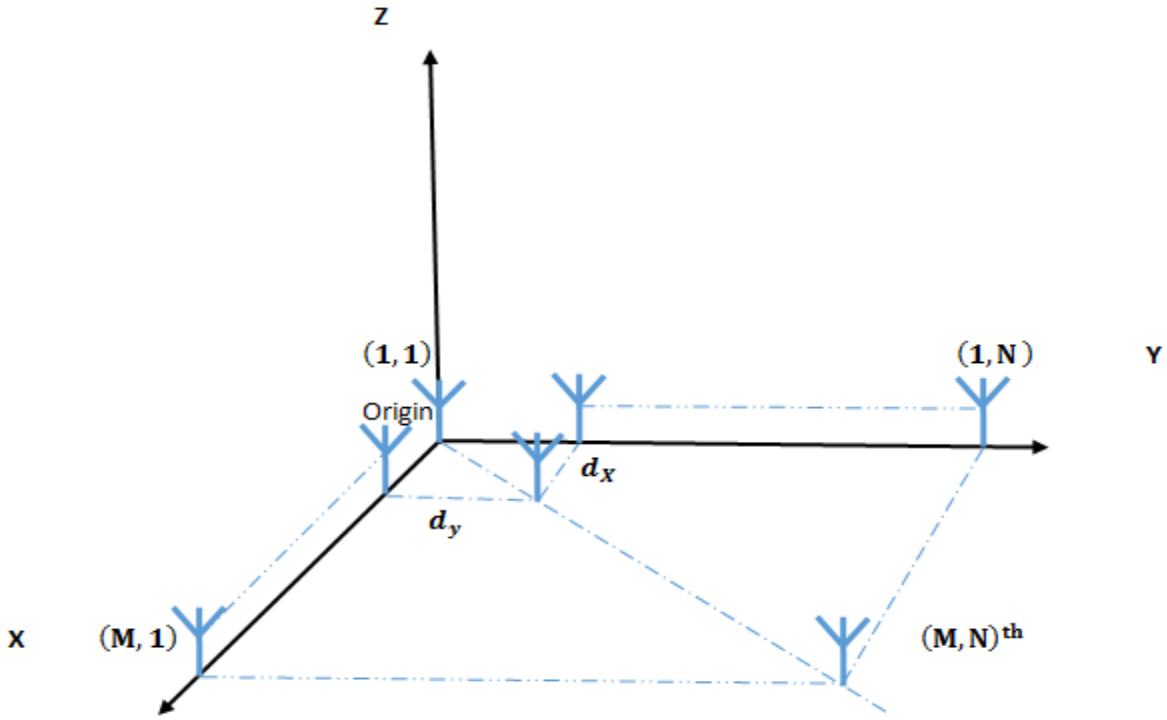

Figure (3.1) Rectangular array coordinate system models [14].

Which are the corresponding parametric digital signal processing terminology to the rectangular array lattice given that the initial hypothetical assumption towards a formulation of a mathematical equation that shall be applied to multiple moving signal source tracking.

3.10.1.1 Signal Model

The incident directional signals coming from a moving source located at the farthest distance from the antenna array can be considered as a plane wave, and the propagation media between the $\mathbf{K}^{th}$ source and the antenna array modeled as homogenous non dispersive, and the antenna array element modeled as distortion free omnidirectional.

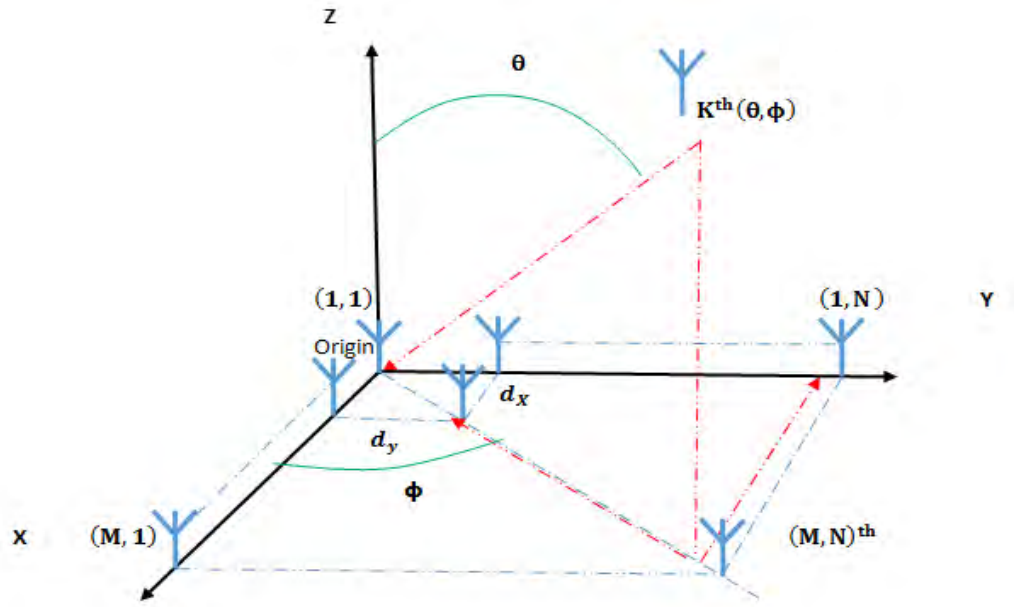

Figure (3.2) signal model in rectangular array [14].

If it is so then the effect of propagation from the source to antenna array is purely time delayed. Consider a rectangular Cartesian coordinate system in Figure (3.2) at which the antenna array element located at the origin taken as a time reference element. Having in mind the reference element at the origin, the time required by the plane wave front coming from the $\mathbf{K}^{th}$ source to the $(\mathbf{M},\mathbf{N})^{th}$ element is given by.

$$\tau_{(M,N)^{th}}(\theta_{el},\phi_{az}) = \frac{r_{(M,N)} * \mathbf{v}(\theta_{el},\phi_{az})}{c} \quad seconds \quad (3-1)$$

Where $r_{(M,N)}$ is the radial distance measured from the $(\mathbf{M},\mathbf{N})^{th}$ element located on the array to the moving signal source, $\mathbf{v}(\theta_{el},\phi_{az})$ is the unit vector in the direction of $\boldsymbol{r}_{(\boldsymbol{M},\boldsymbol{N})}$ and c is the speed of electromagnetic wave disturbance. The signal induced on the array element by the $\mathbf{K}^{th}$ source can be modeled using the following complex notation.

$$x(t) = m_k(t)e^{(j2\pi f_c t)} \quad (3-2)$$

Where $m_k(t)$ is the modulating signal of the $\mathbf{K}^{th}$ source which is modeled as a complex low pass process with zero mean, stationary process with variance of the signal source power and f_c is the carrier microwave carrier frequency assigned for satellite communication. The signal induced on the $(\mathbf{M},\mathbf{N})^{th}$ element delayed by $\tau_{(\mathrm{M,N})^{\mathrm{th}}}(\theta_{el},\phi_{az})$ seconds before it arrives on the reference element at the origin of the array coordinate and it is given by [14], [2], [4].

$$x(t) = m_k(t)\, \mathrm{e}^{\left(\mathrm{j2\pi f_c}\left(\mathrm{t}+\tau_{(\mathrm{M,N})^{\mathrm{th}}}(\theta_{el},\phi_{az})\right)\right)} \qquad (3-3)$$

The signal from the source is assumed narrowband and the antenna array size is smaller enough so that the modulating signal in the propagation time which is during $\tau_{(\mathrm{M,N})^{\mathrm{th}}}(\theta_{el},\phi_{az})$ seconds remain undistorted, i.e. $m_k(t) = m_k\left(t + \tau_{(\mathrm{M,N})^{\mathrm{th}}}(\theta_{el},\phi_{az})\right)$.

The signal induced on the arbitrary element on the array shown in the Figure. (3.2) let it be on the element indexed $(\mathrm{m} = \mathrm{l})$and $(n = k)$ is given by the following general equation [14], [2], [4].

$$x(t) = m_k(t)\mathrm{e}^{\left(\mathrm{j2\pi f_c}\left(\mathrm{t}+\tau_{(\mathrm{M,N})^{\mathrm{th}}}(\theta_{el},\phi_{az})\right)+2\pi(\mathrm{d_{l,k}})\,((\sin\theta_{el}))\left(\cos\left(\phi_{az}(\mathrm{t})-\tan^{-1}\frac{(\mathrm{k}-1)}{(\mathrm{l}-1)}\right)\right)\right)} \qquad (3-4)$$

Where θ_{el} is the array physical elevation angle towards the targets to be tacked, $\phi_{az}(t)$ is the instantaneous azimuth angular displacement of the sources signal which are coming from the target satellites and we can say the main beam is pointing towards the target at angle of (θ_{el},ϕ_{az}) where $(90^0-\theta_{el})$ is the slant range angle and $\phi_{az}(t)$ is the instantaneous true angular pointing direction of the antenna towards the target satellite beacon signal source. And the distance $d_{l,k}$ is given by

$$d_{l,k} = \sqrt[2]{\left(\left((l-1)\frac{d_x}{\lambda}\right)^2+\left((k-1)\frac{d_y}{\lambda}\right)^2\right)} \qquad (3-5)$$

3.10.1.2 Two dimensional steering vectors

The total induced signal matrix of the rectangular array $\mathbf{X(t)}$ due the $\mathbf{K^{th}}$ sources will look like.

$$\mathbf{X}(t) = [\ (\mathbf{X}(t)_1),\ (\mathbf{X}(t)_2),\ \cdots,\ (\mathbf{X}(t)_k)\ ] \qquad (3-6)$$

Where $\mathbf{X(t)}_{\mathbf{k}}$ is M by N induced signal matrix for the k^{th} source which is impinged at the two dimensional direction (θ_{el}, ϕ_{az}) on the rectangular array. Now let us assume the signal induced by single source alone on the arrays shown in Figure (3.2) therefore the steering matrix due to single signal source located in the far field from the antenna array is given as follows [14], [2], [4].

$$\mathbf{X}(t) = m_k(t)e^{\left(j2\pi f_c\left(t+\tau_{(M,N)^{th}}(\theta_{el},\phi_{az})\right)+2\pi(d_{l,k})\,((\sin\theta_{el}))\left(\cos\left(\phi_{az}(t)-\tan^{-1}\frac{(k-1)}{(l-1)}\right)\right)\right)}$$

$$= m_k(t)e^{j2\pi f_c\left(t+\tau_{(M,N)^{th}}(\theta_{el},\phi_{az})\right)}e^{j2\pi(d_{l,k})\,((\sin\theta_{el}))\left(\cos\left(\phi_{az}(t)-\tan^{-1}\frac{(k-1)}{(l-1)}\right)\right)}$$

$$= m_k(t)e^{j2\pi f_c\left(t+\tau_{(M,N)^{th}}(\theta_{el},\phi_{az})\right)}\mathbf{S}(\theta_{el},\phi_{az}) \qquad (3-7)$$

$$\text{Where } \mathbf{S_{l,k}}(\theta_{el},\phi_{az}) = e^{j2\pi(d_{l,k})\,((\sin\theta_{el}))\left(\cos\left(\phi_{az}(t)-\tan^{-1}\frac{(k-1)}{(l-1)}\right)\right)}$$

Where the two dimensional steering vector is given by the general formula in Eq. (3 - 8) and the first, second and the M, N column steering vector components of the two dimensional steering vector is given by Eq. (3 - 9), Eq. (3 - 10) and Eq. (3 - 11) respectively.

$$\mathbf{S}(\theta_{el},\phi_{az}) = [\ \mathbf{S_{M,1}}(\theta_{el},\phi_{az(l,k)}),\ \mathbf{S_{M,2}}(\theta_{el},\phi_{az(l,k)}),\ \ldots,\ \mathbf{S_{M,N}}(\theta_{el},\phi_{az(l,k)})\ ] \qquad (3-8)$$

$$\mathbf{S_{M,1}}(\theta_{el},\phi_{l,k}) = \begin{bmatrix} \mathbf{1} \\ e^{j2\pi(d_{2,1})\,((\sin\theta_{el}))(\cos(\phi_{az}(t)))} \\ \vdots \\ e^{j2\pi(d_{M,1})\,((\sin\theta_{el}))(\cos(\phi_{az}(t)))} \end{bmatrix} \qquad (3-9)$$

$$\mathbf{S_{M,2}}(\theta_{el},\phi_{l,k}) = \begin{bmatrix} e^{j2\pi(d_{1,2})\,((\sin\theta_{el}))\left(\cos\left(\phi_{az}(t)-\tan^{-1}\frac{(m-1)}{(l-1)}\right)\right)} \\ e^{j2\pi(d_{2,2})\,((\sin\theta_{el}))\left(\cos\left(\phi_{az}(t)-\tan^{-1}\frac{(m-1)}{(l-1)}\right)\right)} \\ \vdots \\ e^{j2\pi(d_{M,2})\,((\sin\theta_{el}))\left(\cos\left(\phi_{az}(t)-\tan^{-1}\frac{(m-1)}{(l-1)}\right)\right)} \end{bmatrix} \qquad (3-10)$$

$$\mathbf{S_{M,N}}(\theta_{el},\phi_{l,k}) = \begin{bmatrix} e^{j2\pi(d_{1,N})\,((\sin\theta_{el}))\left(\cos\left(\phi_{az}(t)-\tan^{-1}\frac{(m-1)}{(l-1)}\right)\right)} \\ e^{j2\pi(d_{2,N})\,((\sin\theta_{el}))\left(\cos\left(\phi_{az}(t)-\tan^{-1}\frac{(m-1)}{(l-1)}\right)\right)} \\ \vdots \\ e^{j2\pi(d_{M,N})\,((\sin\theta_{el}))\left(\cos\left(\phi_{az}(t)-\tan^{-1}\frac{(m-1)}{(l-1)}\right)\right)} \end{bmatrix} \qquad (3-11)$$

3.10.1.3 Two dimensional weight matrix

In two dimensional arrays processing the beam former output is obtained by multiplying each element induced signal of the array by its elemental weight $w_{m,n}$ and then summed together.

$$W = [w_{1,1} \quad w_{2,1} \quad \dots \quad w_{M,1} \quad w_{1,2} \quad w_{2,2} \quad \dots \quad w_{M,2} \quad w_{1,N} \quad w_{2,N} \quad \cdots \quad w_{M,N}]^H \qquad (3-12)$$

Therefore, the beam former output $y(t)$ for single signal source $X(t)$ is given by the weighted sum of each array element induced signal and is given by [2], [4], [14].

$$y(t) = \sum_{n=1}^{N}\sum_{m=1}^{M}\left(w_{m,n}\left(m_k(t)e^{j2\pi f_c\left(t+\tau_{(M,N)^{th}}(\theta_{el},\phi_{l,k})\right)}\mathbf{S}(\theta_{el},\phi_{l,k})\right)\right) \qquad (3-13)$$

Then the beam former output due to k directional moving sources is the individual sum of the beam former output for the corresponding arrived signals in the direction of (θ_i, ϕ_i) and is given by the following equation.

$$y(t) = \sum_{i=1}^{K} y_i(t) \qquad (3-14)$$

For a rectangular planar array lattice of M by N elements, d_x and d_y inter – element spacing along the x and y axes, the two dimensional adaptive LMS algorithm [16] is described as follows. The error signal between the array output and the estimated output at the k^{th} discrete time instant is given.

$$e(k) = y(k) - \sum_{n=0}^{N}\sum_{m=0}^{M} w_{mn}^{*}(k)x_{mn}(k) \qquad (3-15)$$

Then the least mean square error will be derived by squaring the norm of the above equation eq.$(3-15)$.

$$|e(k)|^2 = \left| y(k) - \sum_{n=0}^{N}\sum_{m=0}^{M} w_{mn}^{*}(k)x_{mn}(k) \right|^2 \qquad (3-16)$$

$$|e(k)|^2 = \left(y(k) - \sum_{n=0}^{N}\sum_{m=0}^{M} w_{mn}^{*}(k)x_{mn}(k) \right)\left(y(k) - \sum_{n=0}^{N}\sum_{m=0}^{M} w_{mn}^{*}(k)x_{mn}(k) \right)^{*}$$

$$|e(k)|^2 = |\, y(k)|^2 - \sum_{n=0}^{N}\sum_{m=0}^{M} x_{mn}^{*}(k)\, y(k)\, w_{mn}(k) - \sum_{n=0}^{N}\sum_{m=0}^{M} x_{mn}(k) y^{*}(\,k) w_{mn}^{*}(k)$$

$$+ \left(\sum_{q=0}^{N}\sum_{p=0}^{M}\sum_{n}^{N}\sum_{m}^{M} x_{mn}(k) w_{mn}(k) x_{pq}^{*}(k) w_{pq}^{*}(k) \right) \qquad (3-17)$$

The gradient of the least mean square error is obtained by partial derivative of the mean square error Eq. $(3-17)$ with respect to elemental weight and it is given by [2], [14], [16].

$$\frac{\partial\, E[|e(k)|^2]}{\partial\, w_{mn}(k)} = -2\, E[e(k)\, x^{*}(k)] \qquad (3-18a)$$

$$w_{mn}(k+1) = w_{mn}(k) - \frac{\mu}{2}\frac{\partial\, E[|e(k)|^2]}{\partial\, w_{mn}(k)}$$

$$w_{mn}(k+1) = w_{mn}(k) + E[e(k)\,x^*(k)] \qquad (3-18b)$$

Substituting Eq. $(3-15)$ in to Eq. $(3-18a)$ then adaptive weight at the discrete instant $(k+1)$ is given by the following equation.

$$w_{mn}(k+1) = w_{mn}(k) + \mu\left(y(k)\,x^*(k) - \sum_{n=0}^{N}\sum_{m=0}^{M} w_{mn}(k)x_{mn}(k)x^*(k)\right) \qquad (3-19)$$

The gradient of the least mean square error is then used in the entire reference signal based adaptive algorithm [3], [16] that is the LMS, SMI and RLS in order to calculate the minimum least mean square error between the reference and the array output which in turn used to calculate the adaptive optimal weight in the direction of signal of interest from the target satellite.

3.10.1.4 Phased Array Power output

Define the array correlation matrix **R** which includes the summation of the array correlation matrix due to the desired target signals, undesired target signal which can be considered as unwanted interferer and the array correlation matrix due to the background and electronics noise. The output power of the array at any time t is obtained by the magnitude square of the array beam former output $y(t)$ which is given by Eq. $(4-14)$.

$$P(t) = |y(t)|^2$$

$$P(t) = |y(t)y^*(t)|$$

$$P(t) = \left|w^H\mathbf{X}(t)\mathbf{X}^*(t)\,w\right| \qquad (3-20)$$

Since the signal is modeled as zero mean stationary process then taking the expectation of the instantaneous power output $P(t)$ of the array will give us the mean output power of the array which includes the power output due to the desired target signals, unwanted target interference and power output due to the electronics and background noise which is generated on the phased array antenna system.

$$P(w) = w^H\mathbf{R}\,w \qquad (3-21)$$

The mean output power of the array is given by Eq. $(4-21)$ clearly shows that the performance of the array can be measured in terms of the weighting method and it is application dependent.

Output power due to K moving sources, the undesired interference and the total noise is given by the following mean output power equation, respectively.

$$P_s(w) = w^H \mathbf{R_{ss}} w \qquad (3-22)$$

$$P_I(w) = w^H \mathbf{R_I} w \qquad (3-23)$$

$$P_N(w) = w^H \mathbf{R_N} w \qquad (3-24)$$

3.10.1.5 Signal to interference plus noise Ratio (SINR)

$$SINR = \frac{P_s(w)}{P_I(w) + P_N(w)} \qquad (3-25)$$

$$SINR = \frac{w^H \mathbf{R_{ss}} w}{w^H \mathbf{R_I} w + w^H \mathbf{R_N} w} \qquad (3-26)$$

3.10.1.6 Performance measurement indices

Performance indices to measure the effect of error on the array system include array gain, measure the depth of the deep null, interference rejection capability, measure of change of the side lobe level and bias on the estimation of the angle of arrival of the signal. Array gain in antenna is defined as the ratio of the output SINR to the input SINR [2]

3.10.1.7 Weighting vector error (WVE)

Array weights [2] are calculated using an ideal assumption and it is stored in the memory. Array weighting is implemented using amplifier and phase shifter to vary the amplitude and the phase of the elements respectively. The theoretical performance of an array system is measured by assuming the error free – weights; however the actual system performance measure is dependent on the actual array weight implemented on. Having this facts in mind, the difference in the actual and theoretical system performance is arise due to errors caused at different point on the array systems; starting from the assumption of the plane wave arrival at the array, imperfect knowledge of the element position and characteristics, steering vector and

reference signal error in calculating the weight, quantization error in converting the analog weight to digital form, error during implementation which is caused by variation in components.

The effect of random weight fluctuation is reduction in the array gain [2]. The reduction in array gain is very much dependent on the number of elements in the array system and the error free gain.

For an array with large number of elements the effect of random weight fluctuation cause the array gain to unity, which implies the output SINR is equal to the input SINR, as a result no array gain is obtained.

It is assumed that the estimated weight $\bar{\mathbf{W}}$ is different from the optimal weight by the additive random error component and the random weight fluctuation $\boldsymbol{\Gamma}$ can be modeled as M by N matrix with the following statistical properties.

$$\overline{\mathbf{w}} = \mathbf{w_{op}} + \boldsymbol{\Gamma} \qquad (3-27)$$

$$E[\Gamma_{ij}] = 0 \text{ for } i,j = 0,1 \qquad (3-28)$$

$$E[\Gamma_{ij}\,\Gamma^{*}_{mn}] = \begin{cases} \sigma_n^2, & \text{for } i,m \neq n,j \\ 0, & \text{for } i,\ m = n,j \end{cases} \qquad (8-29)$$

3.10.1.7.1 Output signal power

$$P_s(\mathbf{w}) = \overline{w}^{H}\mathbf{R_{ss}}\overline{w} = P_s\overline{\mathbf{w}}^{\mathbf{H}}\mathbf{S_0}\mathbf{S_0^H}\,\overline{\mathbf{w}} \qquad (3-30)$$

Substituting Eq. $(3-27)$ in to Eq. $(3-30)$ the output signal power is given by eq. $(3-31)$

$$P_s(\mathbf{w}) = P_s\overline{\mathbf{w}}^{\mathbf{H}}\mathbf{S_0}\mathbf{S_0^H}\,\overline{\mathbf{w}} = P_s(\mathbf{w_{op}} + \boldsymbol{\Gamma})^{H}\mathbf{S_0}\mathbf{S_0^H}(\mathbf{w_{op}} + \boldsymbol{\Gamma}) \qquad (3-31)$$

3.10.1.7.2 Output interference plus Noise power

$$P_N(\mathbf{w}) = \overline{\mathbf{w}}^{H}\mathbf{R_{NN}}\overline{\mathbf{w}} = P_n\overline{\mathbf{w}}^{H}\mathbf{S_N}\mathbf{S_N^H}\,\overline{\mathbf{w}} \qquad (3-32)$$

Substituting Eq. (3 − 27) in to Eq. (3 − 32) the Output interference plus Noise power is given by Eq. (8 − 33) below.

$$P_N(\mathbf{w}) = P_n(\mathbf{w_{op}} + \boldsymbol{\Gamma})^H \mathbf{S_N S_N^H} (\mathbf{w_{op}} + \boldsymbol{\Gamma}) \qquad (3-33)$$

3.10.1.7.3 Output SINR

The ratio of eq. (3 − 31) to eq. (3 − 33) and given by eq. (3 − 34) below.

$$\text{SINR} = \frac{P_s (\mathbf{w_{op}} + \boldsymbol{\Gamma})^H \mathbf{S_0 S_0^H} (\mathbf{w_{op}} + \boldsymbol{\Gamma})}{P_n (\mathbf{w_{op}} + \boldsymbol{\Gamma})^H \mathbf{S_N S_N^H} (\mathbf{w_{op}} + \boldsymbol{\Gamma})} \qquad (3-34)$$

3.10.1.7.4 Array gain (G)

Dividing Eq. (3 − 34) by the input SINR gives us the gain (G) of the phased array antenna.

3.10.1.8 Steering vector error

Steering vector may be erroneous due to factors such as imperfect knowledge of the element position and due to finite word size arithmetic, it is assumed that each components of the estimated steering vector $\bar{\boldsymbol{S}}$ different from $\boldsymbol{S_0}$ by the additive random error component and it can be modeled as follows [2].

$$\bar{\mathbf{S}} = \mathbf{S_0} + \boldsymbol{\Gamma} \qquad (3-35)$$

$$E[\Gamma_i] = 0 \text{ for } i = 0, 1,$$

$$E[\Gamma_i \Gamma_j^*] = \begin{cases} \sigma_n^2, & \text{for } i \neq j \\ 0, & \text{for } i = j \end{cases} \qquad (3-36)$$

3.10.1.8.1 Output signal power

$$P_s(\mathbf{w}) = \mathbf{w^H R_{ss} w}$$

$$= P_s \mathbf{w^H} \bar{\mathbf{S}}\, \bar{\mathbf{S}}^{\mathbf{H}} \mathbf{w} \qquad (3-37)$$

Substituting eq. (3 − 35) in to eq. (3 − 37) the output signal power is given by eq. (3 − 38)

$$P_s(w) = P_s \boldsymbol{w^H} (\mathbf{S_o} + \boldsymbol{\Gamma})(\mathbf{S_o} + \boldsymbol{\Gamma})^{\boldsymbol{H}} \mathbf{w} \qquad (3-38)$$

3.10.1.8.2 Output interference plus Noise power

$$P_N(\boldsymbol{w}) = \boldsymbol{w^H R_{II} w}$$

$$= \mathrm{P_{IN}} \mathbf{w^H \overline{S}\ \overline{S}^H w}$$

$$= \mathrm{P_{IN}}\, \boldsymbol{w^H}(\mathbf{S_I} + \ \boldsymbol{\Gamma}\ )(\mathbf{S_I} + \ \boldsymbol{\Gamma}\ )^{\boldsymbol{H}}\mathbf{w} \qquad (3-39)$$

3.10.1.8.3 Output SINR

$$\mathrm{SNR} = \frac{\mathrm{P_S}\, \boldsymbol{w^H}(\mathbf{S_o} + \ \boldsymbol{\Gamma}\ )(\mathbf{S_o} + \ \boldsymbol{\Gamma}\ )^{\boldsymbol{H}}\, \mathbf{W}}{\mathrm{P_{IN}}\, \boldsymbol{w^H}(\mathbf{S_I} + \ \boldsymbol{\Gamma}\ )(\mathbf{S_I} + \ \boldsymbol{\Gamma}\ )^{\boldsymbol{H}}\, \mathbf{W}} \qquad (3-40)$$

3.10.1.8.4 Array gain(G)

G is obtained by dividing both sides of the output SINR in Eq. $(3-40)$ by input SINR.

3.11 Angle of Arrival Estimation

Adaptive antenna estimates the direction of arrival of the incoming wave front based on the statistical operation on the induced signals; the two known approaches so as to determine the angle of arrival (AOA) of the signals arrived from a certain directions are based on spectral estimation and the eigen structure of the corresponding superposed induced signal.

The methods of angle of arrival estimation [2], [3], [11], [18], [19] which is based on spectral estimation techniques are Bartlet AOA Estimation, Capon AOA estimation, linear prediction AOA estimation, Maximum Entropy AOA Estimation, PHD AOA estimation. Multiple Signal Classification (MUSIC) and Estimation of Signal Parameters via Rotation Invariance (ESPRIT) are the two AOA estimation techniques which are based on the eigen structure of the incoming superposed signal.

3.11.1 Spectral Estimation

The goal of spectral estimation or angle of arrival (AOA) estimation is to define a function that gives the angle of arrival of the wave front which is coming from the moving target beacon sources at some discrete time snap shot k which is based on the maxima and angular dependent and independent variable.

3.11.1.1 Bartlett AOA Estimation

It is a spatial version of averaged periodogram [3] and it can simply be considered as spatial finite Fourier transform of all signals arrived on the antenna array; equivalently the periodogram can be considered as adding all array factors for each angle of arrival and then finding the absolute value squared.

$$P_B(\theta) = S^H(\theta) R_{xx} S(\theta) \qquad (3-41)$$

3.11.1.2 Capon AOA Estimation

It is known as Minimum Variance distortion less response (MVDR) and it is a maximum likelihood estimate of signal power coming from one direction and considering all other sources as an interferer [3]. The goal is to maximize the SINR while passing signal of interest undistorted in phase and amplitude. The maximized SINR is accomplished by a set of array weights which is given by the weight vector.

$$\mathbf{W} = \frac{\mathbf{R_{xx}^{-1}S}(\theta)}{\mathbf{S}^H(\theta)\mathbf{R_{xx}^{-1}S}(\theta))} \qquad (3-42)$$

$$\mathbf{P_c}(\boldsymbol{\theta}) = \frac{\mathbf{1}}{\mathbf{S^H}(\boldsymbol{\theta})\mathbf{R_{xx}^{-1}S}(\boldsymbol{\theta}))} \qquad (3-43)$$

3.11.1.3 Linear Prediction (LP) AOA Estimation

The goal of LP is to minimize the prediction error [3] between the output of the m^{th} sensor and the actual output of the array. The m^{th}weights to minimize the mean squared prediction error are given by the weight vector components.

$$\mathbf{w_m} = \frac{\mathbf{R_{xx}^{-1}u_m}}{\mathbf{u_m^T R_{xx}^{-1}u_m}} \qquad (3-44)$$

$$P_{LPm}(\theta) = \frac{(\mathbf{R_{xx}^{-1}u_m})^2}{\left|\mathbf{u_m^T R_{xx}^{-1}S}(\theta)\right|^2} \qquad (3-45)$$

3.11.1.4 Maximum Entropy AOA Estimation

Maximum Entropy AOA estimation is also called Autoregressive Method [3]. It defines a function that maximizes the entropy; the pseudo spectrum is given by.

$$P_{MEj}(\theta) = \frac{1}{\mathbf{S}^{H}(\theta)C_j \ \mathbf{C_j^H u_m^T}} \qquad (3-46)$$

Where C_j is the j^{th} column of the inverse of array correlation matrix (R_{xx}^{-1}).

3.11.1.5 PHD AOA Estimation

The PHD performs the pseudo spectrum estimation based on the minimum mean squared error of the array output under the constraint such that the norm of the weight vector is unity [3]. The constraint to the unity weight vector is achieved by choosing the smaller eigen vector of the array correlation matrix which is corresponds to smallest eigen value. It minimizes the MSE and is given by eq.$(3-47)$.

$$P_{PHD}(\theta) = \frac{1}{|\mathbf{S}^{H}(\theta)\,\boldsymbol{e}_1)|^2} \qquad (3-47)$$

Where e_1 is the signal subspace eigen vector corresponds to the smallest eigen value, θ is the instantaneous arrival angle of the signal.

3.11.1.6 Minimum Norm (MN) AOA Estimation

The MN spectral estimation [3] is based on solving optimization problem for calculating the array weight vector such that the following is set [2], [3].

$$P_{MN}(\theta) = \frac{\left|\mathbf{U_1 E_N E_N}^{H}\mathbf{U_1}^{T}\right|^2}{\left|\mathbf{S}^{H}(\theta)\mathbf{E_N E_N}^{H}\mathbf{U_1}^{T}\right|^2} \qquad (3-48)$$

Where θ the angle of arrival of signal, $\mathbf{U_1}$ is is the first column of the M by M Cartesian matrix, and E_N is the noise subspace eigen vector matrix which is given by [2], [3].

$$\mathbf{E_N} = [\mathbf{E}_1 \quad \mathbf{E}_2 \quad \cdots \quad \mathbf{E}_{M-D}] \qquad (3-49)$$

Where M is the number of element, then normalizing the pseudo spectrum expression above will give us the following spectral estimation equation [2], [3].

$$P_{MN}(\theta) = \frac{1}{\left|\mathbf{S}^{H}(\theta)\mathbf{E}_{N}\mathbf{E}_{N}{}^{H}\mathbf{U}_{1}{}^{T}\right|} \qquad (3-50)$$

3.11.2 Eigen structure AOA Estimation

The AOA Estimation method which is categorized in the eigen structure [2], utilizes the following properties of the array correlation matrix (1) the space spanned by the eigen vectors can be separated into signal sub space and noise sub space (2) the signal sub space is orthogonal to the space spanned by the noise eigen vector.

3.11.2.1 Multiple Signal Classification (MUSIC)

Music AOA estimation promises to provide the number signals, angles of arrival and the strengths of the wave front [2]. If there are D signals arrived from D targets there are D signal eigen vector subspace; therefore. The noise eigen vector subspace $\mathbf{E}_N$ is M by (M-D) matrix such that it is orthogonal to the array steering vector. Using the orthogonality between the noise eigen vector subspace and the array steering vector then pseudo spectrum is given by eq. $(3-51)$.

$$P_{MUSIC}(\theta) = \frac{1}{\left|\mathbf{S}^{H}(\theta)\mathbf{E}_{N}\mathbf{E}_{N}{}^{H}\mathbf{S}(\theta)\right|} \qquad (3-51)$$

3.11.2.2 Root Multiple Signal Classification (Root MUSIC)

Root MUSIC [3] implies that the MUSIC algorithm is reduced to find the root of the denominator of the MUSIC pseudo spectrum in Eq. $(3-51)$. Such that a matrix C = $\mathrm{E}_{N}\mathbf{E}_{N}{}^{H}$ and the polynomial D(z) is the simplified sum equation which includes the product of the array steering vector by its Harmitian and the matrix **C**.

$$P_{RootMUSIC}(\theta) = \frac{1}{\left|\mathbf{S}^{H}(\theta)\mathrm{C}\,\mathbf{S}(\theta)\right|} \qquad (3-52)$$

Where C = $\mathrm{E}_{N}\mathbf{E}_{N}{}^{H}$

$$P_{RootMUSIC}(\theta) = \frac{1}{|D(z)\ |} \qquad (3-53)$$

The roots of D(z) whose norm has unity value are the exact zeros of D(z). The angle of arrival of the signal from the targets can be estimated by comparing roots: $Z_i = |Z_i|^{-jkd\sin(\theta)}$ and $Z_i = |Z_i|^{(\arg(Z_i))}$.

$$|Z_i|^{-jkd\sin(\theta)} = |Z_i|^{(\arg(Z_i)}$$

Then estimated angle of arrival from the targets are given by Eq. $(3-54)$

$$\theta_i = -\sin^{-1}\left(\frac{1}{kd\arg(Z_i)}\right) \qquad (3-54)$$

3.11.2.3 Constrained MUSIC

The constrained MUSIC [2] uses the direction of arrival of known source in order to estimate the angle of arrival of the unknown sources, in such AOA estimation the signal information of the known source is removed and used to determine the AOA of the unknown sources.

3.11.2.4 Beam – Space MUSIC

In previous section the data received by the antenna array element is simply received and directly processed by MUSIC algorithm but in the beam – space MUSIC the signal received by the antenna array element first processed by adaptive algorithm before it is taken and processed by MUSIC algorithm [2].

3.11.2.5 Estimation of Signal Parameter via Rotational Invariance Technique

ESPRIT exploits the rotational invariance of the signal subspace which is created by two arrays with translational invariance structure. ESPRIT is based on two arrays of identical structure called Doublets [3]; the arrays can be separate or composed of one large arrays and it is important to note that the arrays are displaced translationally not rotationally. The signal induced on the sub - arrays which are related translationally will be analyzed as follows. The row vector ϕ is the phase shift between the doublets at each angle of arrival therefore for the

two targets there are two arrival angles which is D = 2 and the phase shift is given in eq. $(3-59)$.

$$x_1(k) = \mathbf{S_1}(\theta)\, m_i(k) + n(k) \qquad (3-55)$$

$$x_2(k) = \mathbf{S_2}(\theta)\, m_i(k) + n(k) \qquad (3-56)$$

$$\begin{bmatrix} x_1(k) \\ x_2(k) \end{bmatrix} = \begin{bmatrix} \mathbf{S_1}(\theta) \\ \mathbf{S_2}(\theta) \end{bmatrix} m_i(k) + \begin{bmatrix} n(k) \\ n(k) \end{bmatrix} \qquad (3-57)$$

$$\mathbf{S_2}(\theta) = \Phi \mathbf{S_1}(\theta) \qquad (3-58)$$

$$\phi = [\, e^{jkdsin\theta_1} \quad e^{jkdsin\theta_2}] \qquad (3-59)$$

$$R_{11} = E[x_1(k)\, x_1(k)^H] \text{ and } R_{22} = E[x_2(k)\, x_2(k)^H]$$

Correlation matrix R_{11} and R_{22} are M by D with D signal eigen vectors each.

3.11.2.6 Closest AOA Estimation

This method employed to determine AOA in the selected source sector, CLOSEST AOA Estimation [2] is a generalization of the Minimum Norm method, and it is based up on element spacing rather than beam spacing and can be considered as an alternative to Beam – space MUSIC. The array weight is searched in noise sub space such that the steering vector which is CLOSEST to the direction of arrival of the signal is selected from the sector under consideration.

3.12 Beamforming

In signal processing, beamforming [3] can be broadly classified as conventional and digital beam forming, the conventional beamforming method is a simple technique by which the received signal is weighed and summed up together so as to generate the array output and it is also known as fixed weight beam forming. Digital beam forming rather involves a complex signal processor in order to manipulate the weighting process and the required parameter under specific application and it is known as Adaptive beamforming.

Digital beamforming ranges its application in mobile base station, in bio – medical, sonar and currently the older radar systems are also shifted to implement the digital beamforming techniques. Having in mind this; adaptive beamforming [2], [3], [11], [16], [20], [21], [22] is one

of the techniques in digital beamforming categories such that the signal received by the antenna array processed statistically so as to form the beam on the received signal rather than on space.

In adaptive antenna, pattern is controlled by using an adaptive algorithm based up on a certain criteria, the criteria might be maximizing signal to interference plus noise ratio, minimizing variance, minimizing the mean square error, steering the pattern towards signal of interest, putting the nulls of the antenna towards the interferer or signal of not interest and tracking moving signal sources.

Therefore, adaptive beamforming in satellite tracking involves receiving a beacon signal from a certain angular direction, while the arrival angles contain the where about information of the satellite in its orbital path; the AOA and the parameter which determine the where about of the satellite is derived from the initial satellite's constellation information and the instantaneous orbital – element of the satellite in space; therefore, adaptive beamforming in this thesis performs the beam on the data which is modeled by the six orbital element which will be discussed in the next chapter.

3.12.1 Fixed Beamforming

In fixed beamforming, the processor response ($w^H s_0$) in the direction of desired signal acquires value of unity so that the SINR will be maximized by putting the nulls in the direction of the interferer.

3.12.1.1 Maximum SINR

In fixed beamforming, the criteria to maximize SINR is performed by taking the derivative of the SINR equation in eq.(3 − 26) with respect to the weight w and then equate to zero substituting the evaluated weight vector into eq.(3 − 26) for maximum SINR value [2], [3].

$$\frac{d(\,SINR(w))}{dw} = \frac{d\left(\frac{w^H \mathbf{R_{ss}}\, w}{w^H \mathbf{R_I}\, w + w^H \mathbf{R_N}\, w}\right)}{dw} = 0$$

3.12.1.2 Minimum Variance

The minimum variance solution is the minimum variance distortion less response [3]; In MVDR the signal is remains undistorted after multiplication by the array weight vector. Here traditional array configuration block diagram in Figure (3.3) is considered and the mean of the unwanted signal is zero and the goal is to minimize the noise variance.

The array output:

$$y = w^H s_0 m + w^H u \qquad (3-60)$$

and putting the constrain $w^H s_0 = 1$,

$$y = m + w^H u \qquad (3-61)$$

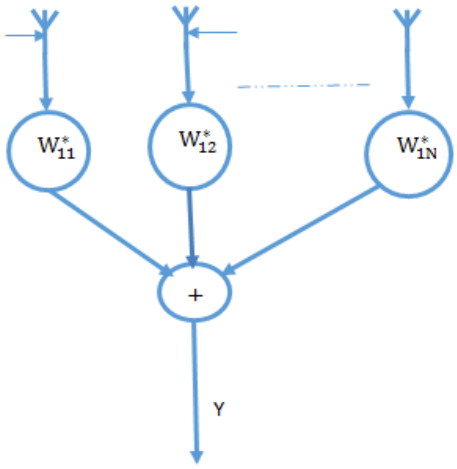

Figure (3.3) Conventional beamformer block diagram [3].

3.12.1.3 The mean and variance of the array output

Since the mean of the unwanted signal is zero that was initially assumed, then the mean of MV is the expected value of the array output, and given by.

$$Y = E[m + w^H u] = m \qquad (3-62)$$

The variance of the array output is given by such that [2], [3].

$$(\sigma_n^2) = \left[\left|m + w^H u\right|^2\right] = \frac{w^H R_{uu}^{-1} w}{2} \qquad (3-63)$$

The modified cost function is the linear combination of the variance and the constraint

$$J(w) = \frac{w^H R_{uu}^{-1} w}{2} + \lambda(1 - w^H s_0) \qquad (3-64)$$

The gradient of the modified cost function is given by Eq. $(3-65)$ and then the minimum of the gradient vector points out the weight vector to the minimum variance solution [3] and the minimum variance weight vector is given by Eq. $(3-66)$.

$$\nabla_w J(w) = w R_{uu}^{-1} - \lambda S_0 \qquad (3-65)$$

$$w_{MV} = \frac{\lambda s_0}{R_{uu}^{-1}} \qquad (3-66)$$

$$\lambda = \frac{R_{uu}^{-1} W_{MV}}{s_0} \qquad \text{Since } w^H s_0 = 1,\ W_{MV} = \frac{1}{s_0^H}$$

$$\lambda = \frac{R_{uu}^{-1}}{s_0 s_0^H} \qquad (3-67)$$

Substituting the Lagrange multiplier in Eq.$(3-67)$ in to the minimum variance weight vector Eq. $(3-66)$ then the weighting vector will be looked like below and it is unconstraint optimal beamformer weight vector.

$$w_{MV} = \frac{R_{uu}^{-1} s_0}{s_0^H R_{uu}^{-1} s_0} \qquad (3-68)$$

3.12.1.4 The maximum likelihood (ML)

The unknown desired signal x_s and the unwanted noise with zero mean, Gaussian distributed in which the mean of the noise is controlled by the desired signal and then traditional array configuration in Figure (3.3) is considered. The input vector signal X given by $\mathbf{X} = s_0 m + n$, and the maximum likelihood method estimates the desired signal by

manipulating the pdf of the joint distribution of the input vector **X** and the desired signal and it given by $\mathbf{p}\left(\boldsymbol{x}/\boldsymbol{x_s}\right)$ in Eq. $(3-69)$

$$\mathbf{p}\left(\boldsymbol{x}/\boldsymbol{x_s}\right) = \frac{e^{\left((x - s_0\mathrm{m}\ )^H \mathrm{R}_{\mathrm{nn}}^{-1}((x - s_0\mathrm{m}\ ))\right)}}{\sqrt{(\sigma_n^2)}} \qquad (3-69)$$

3.12.1.5 The log – likelihood of the joint pdf

$\mathrm{L}(x) = \mathrm{C}\left((x - s_0\mathrm{m}\ )^H \mathrm{R}_{\mathrm{nn}}^{-1}((x - s_0\mathrm{m}\ ))\right)$, C is a constant and the partial derivative of $\mathrm{L}(x)$ with respect to the estimated signal s is given by.

$$\frac{\partial \mathrm{L}(x)}{\partial m} = \frac{\partial\left((x - s_0\mathrm{m}\ )^H \mathrm{R}_{\mathrm{nn}}^{-1}((x - s_0\mathrm{m}\ ))\right)}{\partial m} = 0 \qquad (3-70)$$

$$\mathrm{x} = \frac{\mathrm{R}_{\mathrm{nn}}^{-1}\, s_0}{\mathrm{s}_0^{\mathrm{H}}\, \mathrm{R}_{\mathrm{nn}}^{-1}\, s_0}\,\mathrm{m}$$

$$\mathrm{w}_{\mathrm{ML}} = \frac{\mathrm{R}_{\mathrm{nn}}^{-1}\, s_0}{\mathrm{s}_0^{\mathrm{H}}\, \mathrm{R}_{\mathrm{nn}}^{-1}\, s_0} \qquad (3-71)$$

3.12.1.6 The minimum mean squared error (MMSE)

The adaptive control system array configuration in Figure 3.4 is considered for the evaluation of the optimum weight vector. Here desired signal can be used as a reference signal or signal which is highly correlated with the desired signal can also be taken, but if the reference signal is the desired then the MSE cannot be considered.

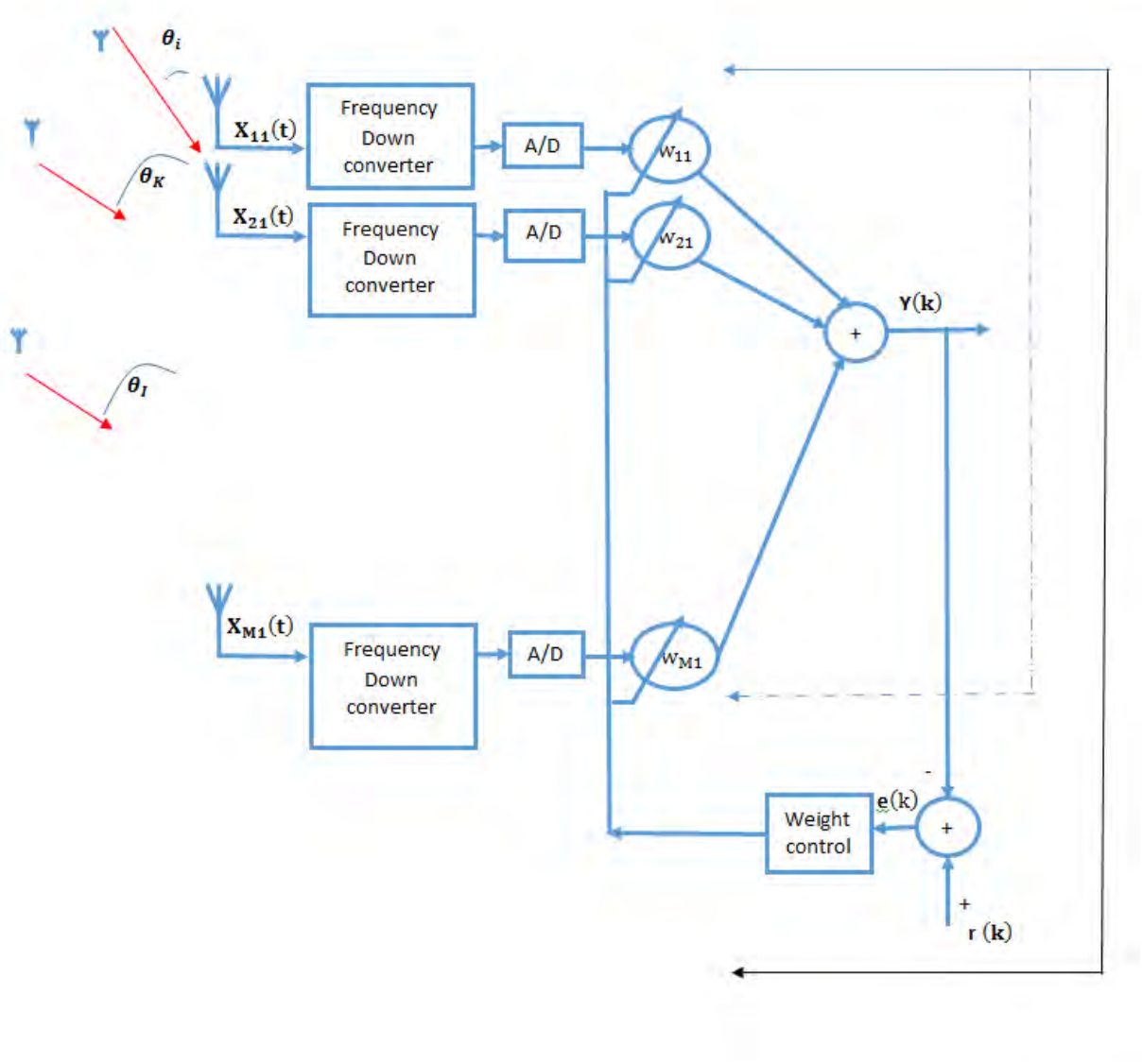

Figure (3.4) Beamforming with weight control and without weight control [4].

The output error is defined as: $e = |d - w^H x|$, then the mean – squared error is

$$|e|^2 = |d - w^H x|^2 = d^2 - 2w^H r_{xd} + w^H R_{xx} w = J(w) \qquad (3-72)$$

This function is called a cost function or sometimes performance surface, and it is a quadratic function of weight vector on M – dimensional space. The minimum of the MSE or the quadratic surface is found by the gradient of the cost function in Eq. $(3-72)$.

The Minimum of the performance surface changes as the AOA of the input vector changes and there by the array weight vector is updated for MSE between the desired signal and the reference signal.

$$\nabla_w J\,(w) = 2R_{xx}w_{MSE} - 2\ r_{xd} \qquad (3-73)$$

$$R_{xx}w_{MSE} - r_{xd} = 0$$

$$w_{MSE} = R_{xx}^{-1}r_{xd}\ , \text{since d = m}$$

$$w_{MSE} = mR_{xx}^{-1}x \qquad (3-74)$$

3.12.2 Adaptive Beamforming

The maximum SIR, maximum likelihood (ML) and the minimum variance (MV) methods are devised for fixed angle of arrival emitter such that the optimum array weight will not need to be adjusted by the receiver signal processor to adjust the continuous changing electromagnetic environment. If the angles of arrival of the incoming signals changing continuously then the receiver signal processor need to adjust or recalculate the optimum weight vector to adapt the changing electromagnetic environment, so that the signal processor need to devise an optimization method to continuously recalculating and adjusting the weight vector.

3.12.2.1 1D Least Mean square (LMS)

LMS is a quadratic performance surface based adaptive beamforming algorithm by using the gradient of the cost function; the performance surface is a quadratic function of the array weights and it is in the shape of the elliptical parabolic with one minima and a method to find the minimum is through the use of the gradient of the mean squared error.

$$e(k) = \left|d(k) - w^H(k)x(k)\right| \qquad (3-75)$$

The mean squared error function is given by:

$$|e(k)|^2 = \left|\left(d(k) - w^H(k)x(k)\right)\right|^2$$

The expected value of MSE:

$$E[|e(k)|^2] = E\left[\left|\left(d(k) - w^H(k)x(k)\right)\right|^2\right]$$

$$J(w) = E[|d(k)|^2 - 2\,w^H(k)\,x(k)\,d(k) + w^H(k)x(k)x^H(k)\,w(k)]$$

$$= D - 2\,w^H(k)r_{xd}(k) + w^H(k)R_{xx}(k)\,w(k)$$

Removing the independent variable

$$J(w) = D - 2\,w^H\,r_{xd} + w^H\,R_{xx}\,w \qquad (3-76)$$

The gradient of the cost or quadratic performance surface is given by

$$\nabla_{\mathbf{w}} J(w) = 2\,r_{xd} - 2\,wR_{xx} \qquad (3-77)$$

$$w_{opt} = R_{xx}^{-1}\,r_{xd} \qquad (3-78)$$

The optimum weight vector solution is predicted based on our knowledge of all signal statistics but actually we don't know the exact statistics of all signal so that the array correlation matrix and the signal correlation vector is estimated by taking the time average of all sample at some observation interval time of K, therefore the instantaneous array correlation matrix and signal correlation vector are given as follows.

$$\widehat{\mathbf{R}_{xx}}(k) = \frac{1}{K}\sum_{k=1}^{K} x(k)x^H(k) \approx R_{xx}(k) \qquad (3-79)$$

$$\widehat{\mathbf{r}_{xd}}(k) = \frac{1}{K}\sum_{k=1}^{K} x(k)d^H(k) \approx r_{xd}(k) \qquad (3-80)$$

The assumption for the above adaptive beamforming analysis is based on the known or exact statistics of the signal. But the exact statistics is approximated through the use of time average snapshot of the array correlation matrix and the signal vector as give in Eq. $(3-79)$and Eq. $(3-80)$.

Employing an iterative technique called method of steepest descent to approximate the gradient of the array weight quadratic performance surface, the direction of steepest descent is

opposite to the direction of the gradient vector. The steepest descent can be approximated in terms of weight using least mean square (LMS).

$$w(k+1) = w(k) - \frac{1}{2}\mu * \nabla_{w} J(w) \qquad (3-81)$$

Substituting the instantaneous array correlation matrix and signal correlation vector Eq. $(3-79)$and Eq. $(3-80)$ on to the gradient Eq. $(3-77)$ and then to Eq. $(3-81)$ next adaptive weight is given by

$$w(k+1) = w(k) - \frac{1}{2}\mu\left(2\, r_{xd}(k) - 2\, wR_{xx}(k)\right)$$

$$w(k+1) = w(k) - \mu\left(x(k)d^{H}(k) - w\, x(k)x^{H}(k)\right)$$

$$= w(k) + \mu\, x^{H}(k)\left(d(k) - w^{H}\, x(k)\right)$$

$$= w(k) + \mu\, x(k)\left(e^{H}(k)\right) \qquad (3-82)$$

The convergence time $t_i = \frac{1}{2\,\mu_i \lambda_i}$; and smaller step size μ_i makes the adaptation so slower that the signal processor will not track the time varying angle of arrival of the signal; in the same way larger step size makes the adaptation to overshot, such that the adaptation may oscillate above and below the optimum value.

Therefore, the step size μ has to be chosen in the interval $(1 < \mu_i < \frac{1}{\lambda_{max}})$, where λ_{max} is the largest eigen value of the array correlation matrix and it is selected approximately using trace of the array correlation matrix.

3.12.2.2 2D Adaptive signal processing

Adaptive algorithm can be classified into blind and non – blind type where the non – blind adaptive algorithm require a reference signal for adaptive weight control of the antenna array, algorithm such as LMS, SMI or DMI and RLS can be categorized in the non - blind type where as in the blind adaptive algorithm such as LS – CMA there is not a requirement for reference signal.

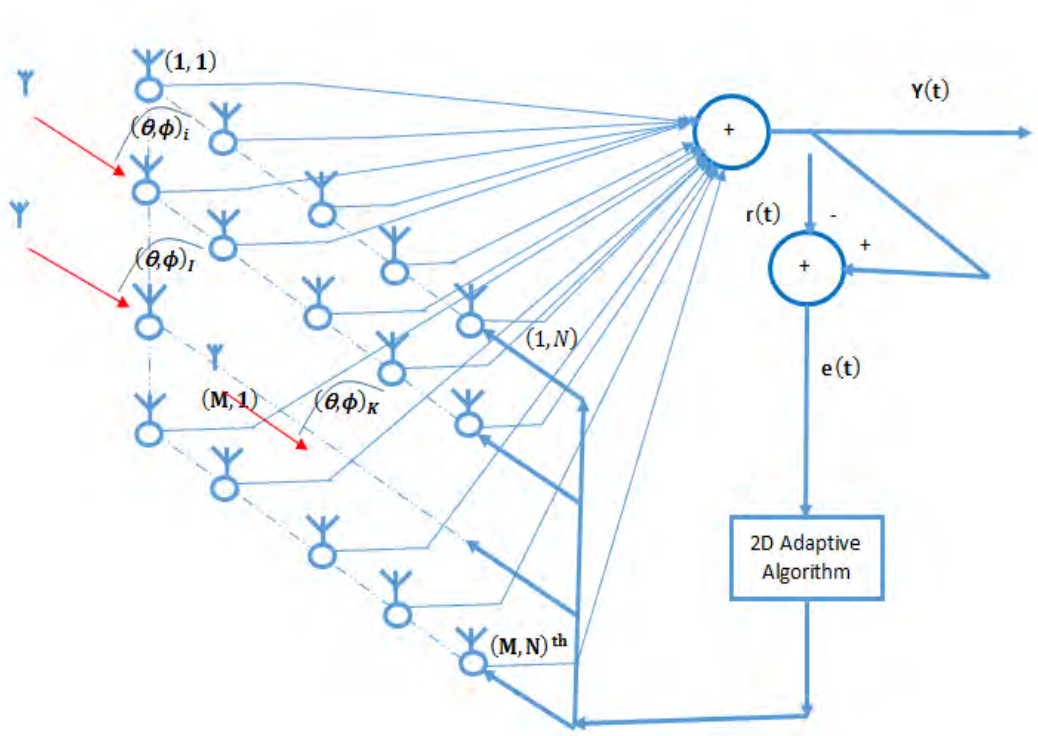

Figure (3.5) 2 dimensional array with adaptive weight control block [5], [14].

3.12.2.2.1 2D Least mean square (LMS)

Two dimensional weight adaptation which was given by eq. (3.19) in the previous section.

$$w_{mn}(k+1) = w_{mn}(k) + \mu\left(y(k)\,x^*(k) - \sum_{n=0}^{N}\sum_{m=0}^{M} w_{mn}(k)x_{mn}(k)x^*(k)\right)$$

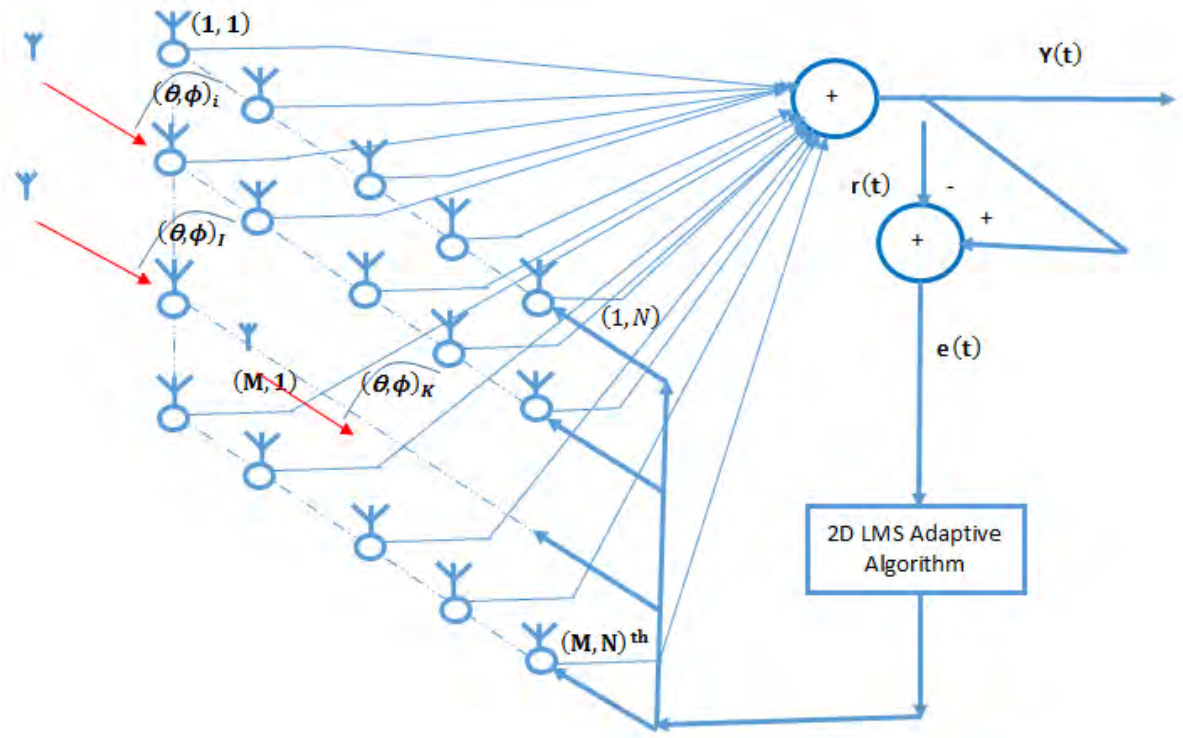

Figure (3.6) 2 dimensional array with 2D LMS adaptive weight control block [5]. [14].

3.12.2.2.2 2D Sample Matrix Inversion (SMI)

This method is also called direct matrix inversion [3] in such method of adaptive beam forming, the array correlation matrix and the signal vectors are approximated by time average snap shot of the sample; this method is used in order to avoid the LMS adaptive algorithm drawbacks of slower adaptation, which mean LMS requires more than half the period of the incoming wave front for adaptation. The SMI is faster than LMS [3] and it is a method based on block processing and has a drawback of matrix inverse error.

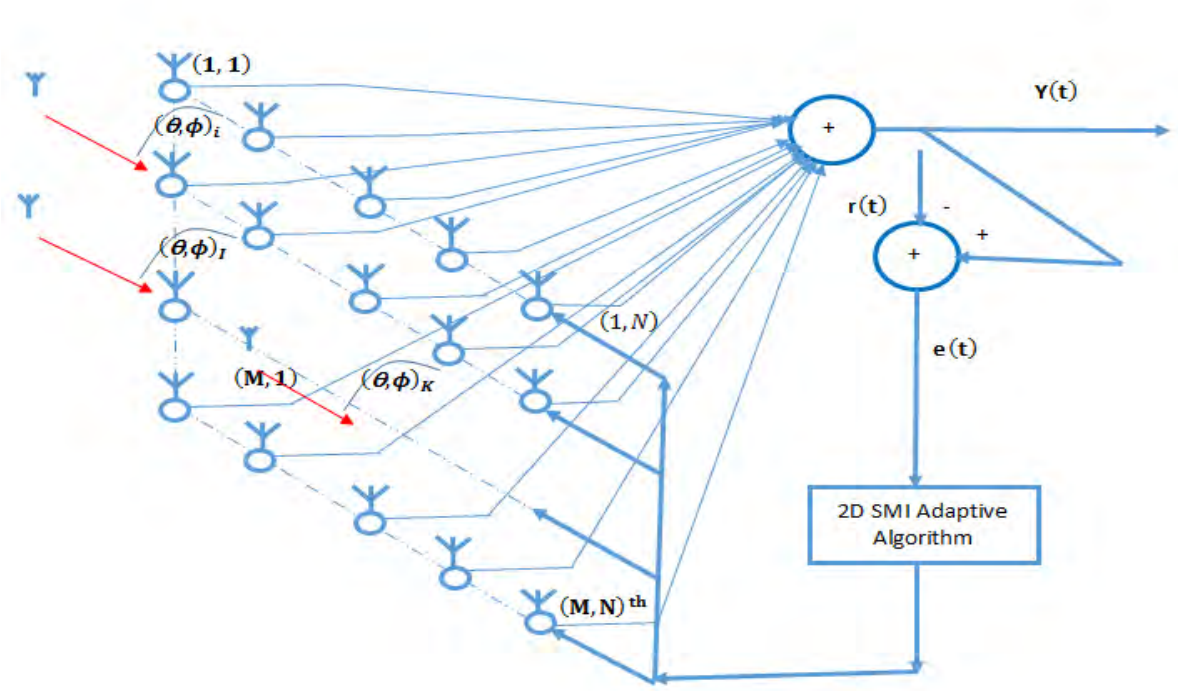

Figure (3.7) 2 dimensional array with 2D SMI adaptive weight control block [5], [14].

3.12.2 .2.3 2D Recursive Least Square (RLS)

This method devises a factor called forgetting factor ($0 < \beta^{k-1} < 1$) to ignore the earlier data samples performed through the process of adaptation of the electromagnetic environment. It has better performance when the eigen value spread is very large and if the forgetting factor is set to 1 then the RLS algorithm will return to LMS [3].

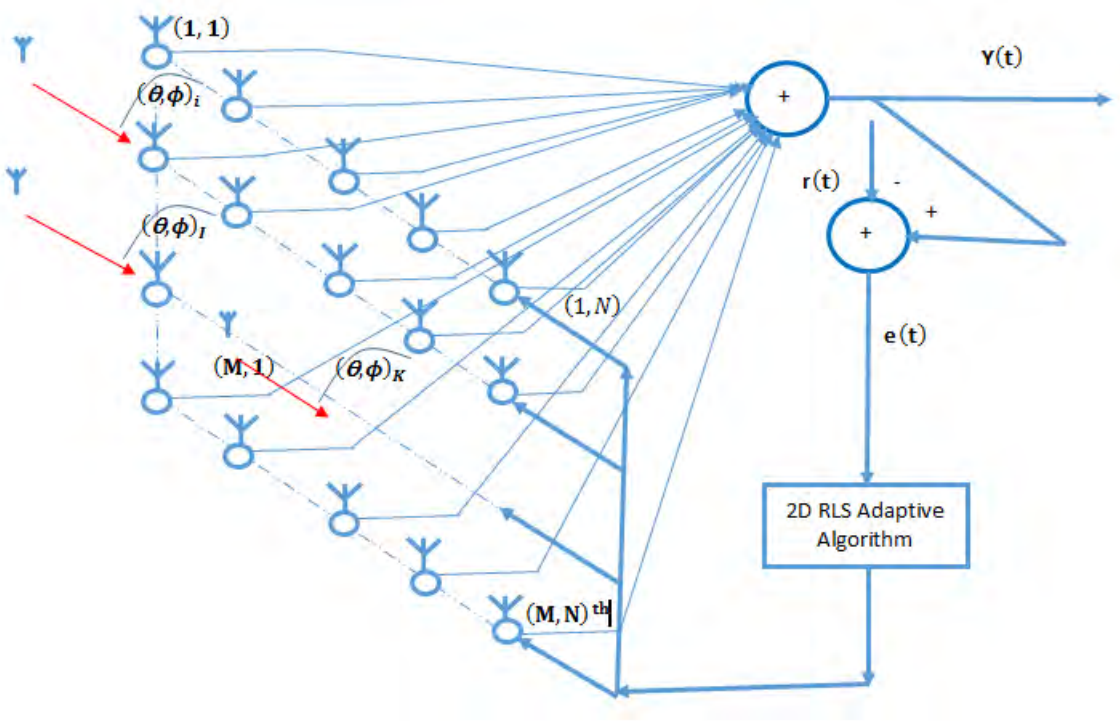

Figure (3.8) 2 dimensional array with 2D RLS adaptive weight control block [5], [14].

Chapter Four

Satellite Tracking and Constellation Theory

4.1 Introduction

The satellite constellation pattern theory [11], [12], [24] dates back to Clarke, in which by using geo-synchronous constellation pattern a complete equatorial coverage of the entire earth have been achieved using three satellites, which was proposed by Clarke. The simplest and the earliest class of satellite constellation was the *geosynchronous constellation* which was applied for most of communication and weather.

Due to the nature of geosynchronous orbit and increasing the number of satellites utilizing this orbit; another satellite constellation pattern has been studied. A constellation pattern which is based on orbital inclination and elliptical orbit has been studied and called a Tundra satellite constellation. The most known symmetric and regular class of satellite constellation called the Walker satellite constellation; after the great contribution of J.G Walker [25]. Walker has used three satellite constellation parameters the total number of satellites, the number of total orbital planes, and the phasing rule which are used to specify and systematize satellite coverage. The two known Walker's constellations are the Star and Delta. The Satellite constellation at orbital inclination close to 90^0 i.e., polar orbit constellation pattern and used by Iridium is called walker star. Another walker type of constellation called the Rosetta constellation which provides best global coverage using multiple satellites above the ground station. Most of the satellite constellation pattern theory which was discussed above have been analyzed based on Earth – Centered – Inertial frame, but new satellite constellation theory called Flower constellation have been proposed in Texas university, the Flower constellation unlike the previous constellation it creates a repeating ground track using Planet – Centered – planet – fixed rotating reference frame.

4.2 Two bodies motion system Model

The two bodies are defined as the Earth – Satellite relative motion [25], [26], [27]; in orbital science, System model is required to specify the orbital motion of the satellite. For bodies in space two – body's motion can completely describe the orbital motion of the body to a fair degree of accuracy, having this fact in mind; orbital elements are defined as the parameters which are used to describe the basics of two – bodies motion of the orbiting body. The classical orbital element (C_6) sets used Earth – Centered – inertial frame and six parameters to completely describe the orbit of the body in space, and these six parameters are shown in Table. (4.1); orbiting satellites in space governed by using the C_6 sets [25], [26], and these sets are grouped as parameters which describe the orbit size (*a [major axis], e [eccentricity]*) and orbital plane orientation (*i[inclination], Ω[Right ascension ascending node], ω[argument of perigee], η[true anomaly]*). The six orbital elements define the where about of the target and each i^{th} satellite in the constellation has its own C_6 sets.

4.3 Ground Station Model

In satellite communication, the space segment and the ground segment plays a vital role so as to fulfill the complete satellite communication as well as navigation service requirement. Therefore, the adaptive phased array system which is hypothesized to be deployed in the Earth station (TTC and M), which is aimed initially to track multiple beacon sources, needs to consider different measurement geometries.

4.3.1 Geometric distance of bodies in the tracking system Model

1. The distance between the i^{th} satellite and the ground station as illustrated in Figure.4.1 is called the slant range R_{Si} (t) and it is given by eq. (4 – 1) [11].

$$R_{Si}(t) = \sqrt[2]{(R_e^2 + r_{si}(t)^2 - 2R_e r_{si}(t)\cos(\eta_i(t)))} \qquad (4-1)$$

Since $\theta_{el} = 0$ then $\gamma = \eta_i$ (t) is the central angle at the Earth center, R_e is radius of the Earth and $r_{si}(t)$ is the orbital radius of the i^{th} satellite and given by eq. (4 – 3) and they are shown in Figure (4.1).

2. The azimuth and elevation angle, collectively called the look angle (θ_{el}, ϕ_{az}). The look angle is defined as the angular coordinate by which the ground station (GS) antenna pointed to communicate with the satellite. The azimuth ϕ_{azi} is the angle by which the ground station disk pointed to the horizon, and the elevation angle θ_{eli} [11] is the angle at which the antenna bore sight axis must be rotated up to lock on to the i^{th} satellite [11], [12].

$$\theta_{eli} = \tan^{-1} \frac{\left(\cos L_{GS\,i} \cos \Delta_i - \frac{R_e}{r_{si}(t)}\right)}{\sqrt[2]{(1 - \cos^2(L_{GS\,i}) \cos^2(\Delta_i))}} \qquad (4-2)$$

3. G is defined as the location point of the ground station on the earth surface as illustrated in Figure (4.1).
4. S is the position of the satellite on the space as illustrated in Figure (4.1).
5. The geometric locations of the Earth which are exactly perpendicular to the satellite position are called the sub satellite point.
6. L_{GSi} is the latitude of the ground station and it is positive for earth station located in north of the equator and negative for ground station located in south of the equator and used in eq. (4-2) to calculate the elevation angle towards the i^{th}satellite.
7. L_{SATi} is the latitude of the i^{th}satellite and used in eq. (4-2) to calculate the elevation angle towards the i^{th}satellite.
8. Δ_i is the difference in longitude between the ground station and the i^{th}satellite, used in eq. (4-2) to calculate the elevation angle towards the i^{th}satellite.
9. Note the assumption in this thesis, i.e. the location of the ground station is exactly on to the sub satellite point such that the longitude of G and S are equal at any instant and $\eta_i(t) = \gamma$; meaning the central angle is assumed equivalent to the true anomaly of the satellite; which is in turn used to derive the azimuth angle of arrival of the beacon signal from the target satellite i.e. $\eta_{ui}(t)$.
10. r_{si} is the orbital radius of the i^{th} satellite from the center of the earth as illustrated in Figure (4.1) and it is given by eq. (4 – 3) [11], [12], [25].

$$r_{si}(t) = \frac{a(1 - e^2)}{(1 + e \cos \eta_i(t))} \qquad (4-3)$$

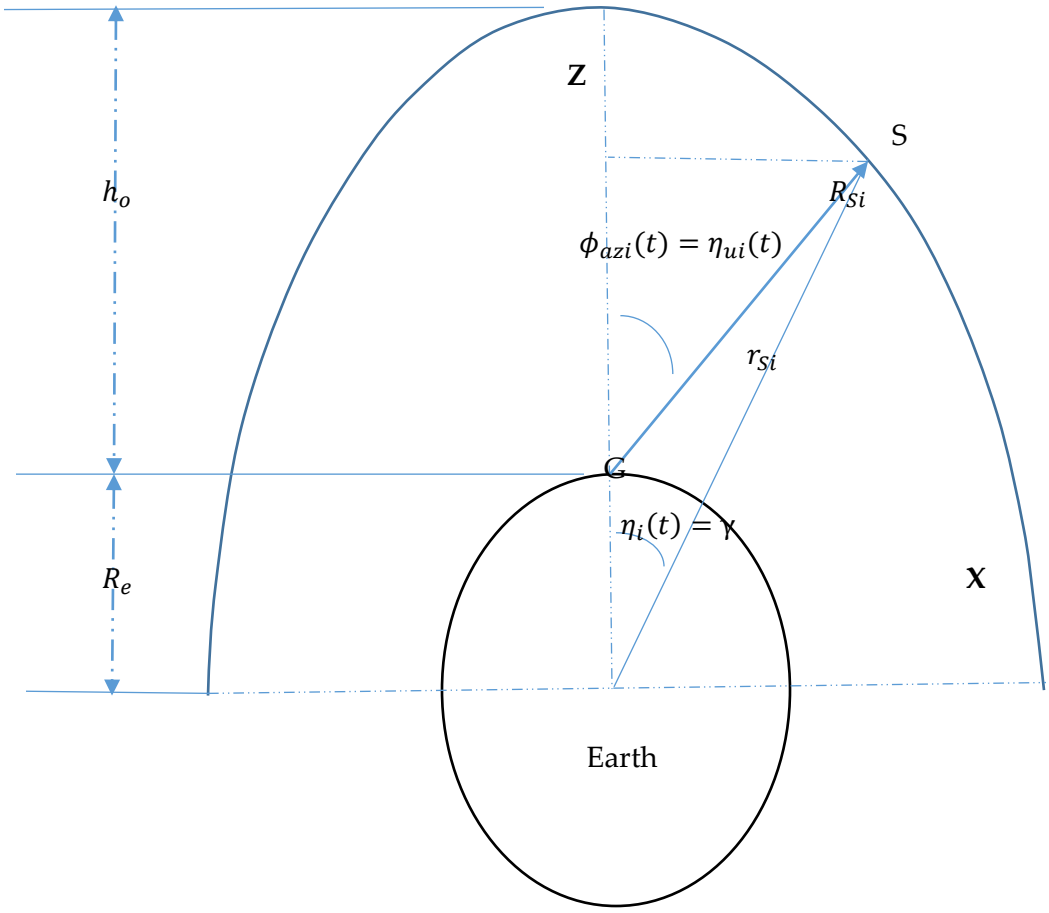

Figure (4.1) Earth station and satellite orbital path at elevation angle $\theta_{eli} = 0^0$ [11], [12].

4.4 Tracking Analysis (TTC and M station exactly at sub – satellite point)

Assume the ground station adaptive phased array antenna bore sight is pointed in the direction of $\theta_{eli} = 0^0$ which was given by the elevation angle formula of the i^{th}satellite in its orbit; and it was stated in eq. (4 – 2). Consider linear array for this case analysis and assume it is deployed at G in Figure (4.1) [11], [12]. Therefore, substituting ($L_{GSi} - L_{SATi}$) = Δ_i= o in to eq. (4 - 2) yields the elevation angle towards the i^{th}satellite zero degree [11].

$$\theta_{eli} = \tan^{-1} \frac{\left(\cos L_{GS\,i} \cos \Delta_i - \frac{R_e}{r_{si}}\right)}{\sqrt[2]{(1 - \cos^2(L_{GS\,i}) \cos^2(\Delta_i))}} = 0^0$$

Since the beam is steered on **XZ** Cartesian plane then the azimuth angle of arrival of the incident signal from the i^{th} satellite to the (TTC and M station) in the line of sight direction is $\phi_{azi}(t)/\eta_{ui}(t)$; and it is shown in Figure (4.1).The derived AOA by using the true anomaly of the i^{th}satellite is given by eq. (4 - 4).

$$\eta_{ui}(t) = \phi_{azi}(t) = \sin^{-1}\left[\frac{r_{si}(t) * \sin \eta_i(t)}{R_{Si}(t)}\right] \qquad (4-4)$$

Where $\eta_i(t) = \cot\left[\frac{\sqrt[2]{1-e^2}) \sin E_i(t)}{\cos E_i(t) - (e)}\right]$ and is given in eq. (4 – 11a)

By Substituting R_{Si} (t) and $r_{si}(t)$ from eq. (4 – 1) and eq. (4 – 3) into eq. (4 – 4) then the azimuth angle of arrival (AOA) of the beacon signal from the i^{th} satellite is given by the following expression [25], [28].

$$\eta_{ui}(t) = \phi_{azi}(t) = \sin^{-1} \frac{\left(\frac{a(1-e^2)}{(1 + e\cos\eta_i(t))} * \sin\eta_i(t)\right)}{\sqrt[2]{\left(R_e^2 + \left(\frac{a(1-e^2)}{(1 + e\cos(\eta_i(t)))}\right)^2 - 2R_e\left(\frac{a(1-e^2)}{(1 + e\cos(\eta_i(t)))}\right)\cos(\eta_i(t))\right)}} = \qquad (4-4)$$

Where $\gamma = \eta_i(t)$

4.4.1 AOA initially at t = t_0

Satellites which are deployed at lower earth orbit need to move at a certain angular speed. Therefore, when they rotate on their orbit, the TTC and M station antenna array tracks their beacon, so that they can be commanded and monitored as they are found on their orbital rotation.

In this thesis, the time instant t = t_0 is assumed to be the time instant at which the space borne tracking antenna sends the first beacon to the TTC and M station.

Since at t = t_0 we are assuming that the satellite is exactly at the perigee altitude then the true anomaly or the central angle is equal to 0^0 i.e. $\gamma = \eta_i(t_0) = 0^0$. Which implies the azimuth angle of arrival (AOA) of the beacon signal from the i^{th} satellite in the line of sight direction at

$t = t_0$ is zero. The substitution of the true anomaly value $\eta_i\,(t_0) \;=\; 0^0$ into eq. $(4-4)$ yields 0^0 azimuth angle of arrival (AOA) [25], [28].

$$\eta_{ui}(t_0) = \phi_{azi}(t_0) = \sin^{-1}\frac{\left(\frac{a(1\;-\;e^2)}{(1\;+\;e\;\cos(0^0))}\right) * \sin(0^0)}{\sqrt[2]{\left(R_e^2\;+\;\left(\frac{a(1\;-\;e^2)}{(1\;+\;e\;\cos(0^0))}\right)^2\;-\;2R_e\left(\frac{a(1\;-\;e^2)}{(1\;+\;e\;\cos(0^0))}\right)\cos(0^0)\right)}} = 0^0 \qquad (4-5)$$

4.4.2 AOA for $t \neq t_0$

At any instant, the dynamical angle of arrival (AOA) of the beacon signal from the i^{th} satellite is given by the summation of the value in eq. $(4-5)$ and the value at that instant and given by the eq. $(4-6)$.

$$\eta_{ui}(t) = \phi_{azi}(t) = \eta_{ui}(t_0) + \sin^{-1}\frac{\left(\frac{a(1\;-\;e^2)}{\left(1\;+\;e\;\cos\left(\eta_i\,(t)\right)\right)}\right) * \sin(\eta_i\,(t))}{\sqrt[2]{\left(R_e^2\;+\;\left(\frac{a(1\;-\;e^2)}{\left(1\;+\;e\;\cos\left(\eta_i\,(t)\right)\right)}\right)^2\;-\;2R_e\left(\frac{a(1\;-\;e^2)}{\left(1\;+\;e\;\cos\left(\eta_i\,(t)\right)\right)}\right)\cos\left(\eta_i\,(t)\right)\right)}} \qquad (4-6)$$

4.5 Investigation of the Models

In the previous section, the true anomaly $\eta_i\,(t)$ which was used to compute the instantaneous signal AOA describes the satellite orbital angular location with respect to the earth center. First let us now investigate the satellites location based on the spherical geometry. Assume the equatorial orbital plane, whose radius is extended to a far field region and the azimuth plane of the satellite tracking adaptive phased array antenna are parallel.

Having the two parallel planes assumption, it is evident that the observation site antenna's bore sight elevation angle is given by eq. (4 - 2) above [11], [12].

Since the true anomaly of the moving satellite is changed with time and hence the adaptive phased array antenna's azimuth angle has also changed adaptively with time. While the adaptive phased array antenna angle of elevation remain constant. Second, let us consider the signal analysis along with the satellite location based on the spherical geometry as it is stated above. Assume **K** complex signals with their equivalent source mean power p_i from **K** different directional moving sources intercepted by **M** by **N** rectangular array.

The array steering vector for each of the arrived signals in $(\theta_{eli}, \phi_{azi})$ direction forms the entire antenna system steering matrix $\mathbf{S}(\theta_{el}, \phi_{az})$ and we call this the array manifold [3].

Therefore, the total continuous time induced signal due to the **K** different directional sources is **X**(t) and the corresponding continuous time array output is **Y**(t), the discrete output is **Y**(k).

Therefore, the induced **K** signals are represented by $\mathbf{X}(t) = [(\mathbf{X_1}(t)), (\mathbf{X_2}(t)), \cdots, (\mathbf{X_k}(t))]$. If the angle of arrival (AOA) of each signal at time $t = t_0$ is designated as $(\theta_{eli}, \phi_{azi}(t_0))$ then at $t \neq t_0$ the angle of arrival (AOA) will be given as in eq. $(4-7)$.

$$(\theta_{eli}, \phi_{azi}(t)) = (\theta_{eli}, \phi_{azi}(t_0)) + \int_{t0}^{t} \frac{\partial(\theta_{eli}, \phi_{azi}(t))}{\partial t} dt \qquad (4-7)$$

Where $\int_{t0}^{t} \frac{\partial(\theta_{eli}, \phi_{azi}(t))}{\partial t} dt$ is the infinitesimal angle of arrival (AOA) of the beacon; which is the target satellite dynamical angular location relative to the ground station; where the reference frame is not the Earth center rather the reference frame is the TTC and M station. Therefore, the array steering matrix to the i^{th}beacon at $t \neq t_0$ is given by eq. (4 - 8).

$$\mathbf{S_i}(\theta, \phi(t)) = \mathbf{S}\left((\theta_{eli}, \phi_{azi}(t_0)) + \int_{t0}^{t} \frac{\partial(\theta_{eli}, \phi_{azi}(t))}{\partial t} dt \right) \qquad (4-8)$$

Since the target signal sources are located on the same orbital inclination then the signal impinging angles in the elevation are constant and the array system steering vector due to i^{th}beacon source will be expressed as follows.

$$\mathbf{S_i}(\theta, \phi_{azi}(t)) = \left[\mathbf{S_{M,1}}\left(\theta, \phi_{l,k}(t)\right), \ \mathbf{S_{M,2}}\left(\theta, \phi_{l,k}(t)\right), \ \cdots, \ \mathbf{S_{M,N}}\left(\theta, \phi_{l,k}(t)\right) \right] \qquad 4-9)$$

4.5.1 Premise #1 to compute the signal AOA from the satellite.

Based on the transdecental equation which relates the eccentricity anomaly with the mean anomaly as it is given by eq. (4 - 10) then the true anomaly of a satellite on its orbit is given by $\eta_i(t) = \cot g_i(t)$.

By taking the transdecental equation in eq. (4 - 10) into account, let us assume the ground station adaptive antennas' main beam bore sight is pointing to the satellite through the slant range in the line of sight direction.

Now consider the orbital parameters of the i^{th} satellite in Table (4.1) below. M_i (t) is the mean anomaly of the i^{th} satellite, it is the angular location of the satellite which is obtained by considering circular orbital path as a reference and is called Mean anomaly. E_i (t) is the eccentricity anomaly and given by eq. $(4-10)$, which is a transdecental equation that relates eccentricity anomaly with the mean anomaly.

Based on the above facts, the derivation of the true anomaly/η_i (t) of the i^{th} satellite is illustrated mathematically as follows and it helps us to derive the line of sight angle from ground station to the target [25], [29], [28].

$$E_i(t) = M_i(t) + e \sin E_i(t) \qquad (4-10)$$

$$\text{Since } \eta_i(t) = \cot\left[\frac{\sqrt[2]{1-e^2}\sin E_i(t)}{\cos E_i(t) - (e)}\right]$$

$$\text{Let } g_i(t) = \frac{\sqrt[2]{(1-e^2)}\sin E_i(t)}{\cos E_i(t) - (e)}$$

$$\text{then } \eta_i(t) = \cot g_i(t) \qquad (4-11a)$$

Since $\eta_{ui}(t) = \sin^{-1}\frac{r_{si} * \sin\eta_i(t)}{R_{Si}}$ given by eq. $(4-4)$ and substituting eq. $(4-11a)$ into eq. (4 - 4) for η_i (t) then the AOA of the beacon in the line of sight direction is given by eq. $(4-11b)$

$$\eta_{ui}(t) = \sin^{-1}\left[\frac{r_{si} * \sin[\cot g_i(t)]}{R_{Si}}\right] = \phi_{azi}(t) \qquad (4-11b)$$

4.5.2 Premise # 2 to estimate the adaptive weight of the array.

Consider the intercepted signals $\mathbf{X_{sat\,1}}(t)$ and $\mathbf{X_{sat\,2}}(t)$ from source 1 and 2 which are intercepted in two directions $(\theta_{el1}, \phi_{az1}(t))$, $(\theta_{el2}, \phi_{az2}(t))$ respectively. Having the previous signal and antenna array mathematical models, such as the antenna array element separation $\boldsymbol{d_x}$ and $\boldsymbol{d_y}$ in **X** and **Y** axis, arrival angle $(\theta_{eli}, \phi_{azi}(t))$, with the corresponding operating microwave frequency f and wave length λ in mind. Then the total induced electrical signal at the **M** by **N** antenna array due to the two satellites' is **X**(t) and it is given by eq. (4 -12) so the optimal weight, estimated at some discrete time is given be eq. (4 – 13).

$$\mathbf{X}(t) = \mathbf{X_{sat\,1}}(t) + \mathbf{X_{sat\,2}}(t) \qquad (4-12)$$

$$\mathbf{w}_{opt} = \left(\mathbf{X}(k)\mathbf{X}^{H}(k)\right)^{-1}\mathbf{X}(k)\,\mathbf{r}(k) \qquad (4-13)$$

4.6 Tracking Test

Using the investigation in the above sections, let us consider more than one satellite on the same orbital plane. Since Satellites' constellation on Figure (4.2) illustrates that they are at different angular position in their orbital plane. So different beacon signals arrived at different AOA, which are computed by the AOA equation in Eq. $(4-6)$ and the arrived signals from the satellites induce an electrical signal on the ground station adaptive antenna. Thereby the adaptive antenna signal processor used the received signal information so as to form the beams towards the target satellites.

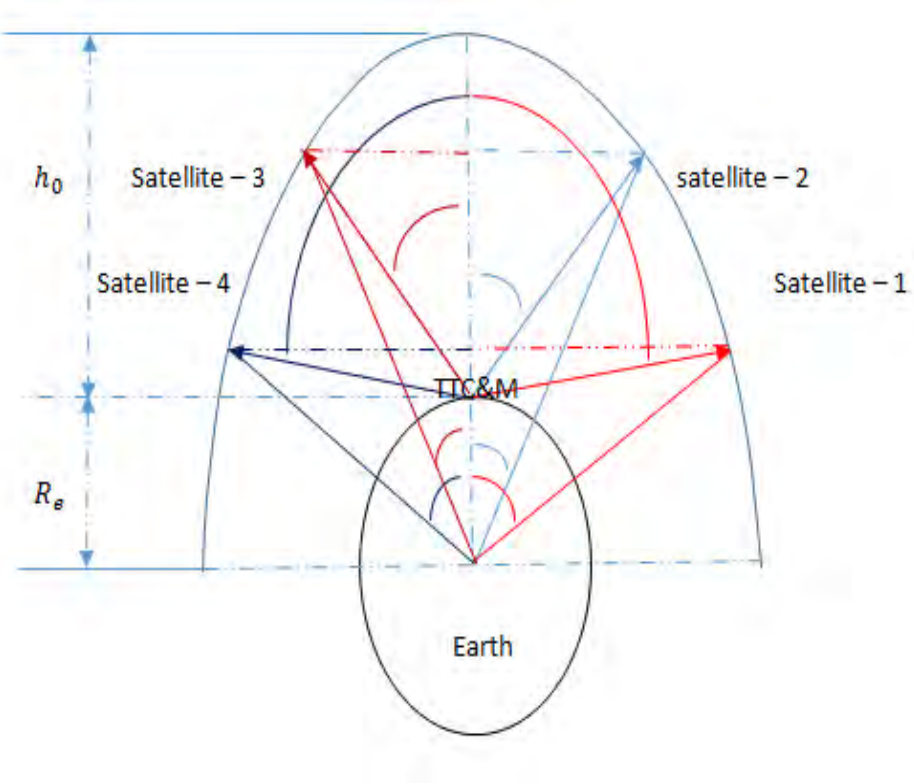

Figure (4.2) satellites constellations Model on their orbital plane [11], [12], [24].

Consider two target satellites on the same orbital plane as shown in Figure (4.2) with signal AOA constraint $\phi_{az2}(t) - \phi_{az1}(t) >= \text{FNBW}$ of the major lobe; and with their C_6 sets in Table (4.1). The time varying steering vector which are tracking the beacon signals from sat_1 and sat_2 are given by eq. $(4-14)$ and eq. $(4-15)$ respectively as it is stated in eq. (4 - 9).

Table (4.1) Two target satellites' six orbital element with the azimuths AOA for each.

Target	Major axis	RAAN	eccentricity	Inclination	$M_i\,(t)$	$E_i\,(t)$	$g_i\,(t)$	$\phi_{azi}\,(t)$	Argument of perigee
sat_1	a	Ω_1	e	i	$M_1\,(t)$	$E_1\,(t)$	$g_1\,(t)$	$\phi_{az1}\,(t)$	ω_1
sat_ 2	a	Ω_2	e	i	$M_2\,(t)$	$E_2\,(t)$	$g_2\,(t)$	$\phi_{az2}\,(t)$	ω_2

Where

1. a is the major axis length given in eq. (4-3) and ω(argument of perigee/angular measured value of the target from its perigee altitude), i(orbital inclination of the target), and e(eccentricity of the target satellite orbit)
2. $M_i\,(t)$ is the mean angular measured value of the i^{th}satellite and it is given in eq. (4-10)
3. $E_i\,(t)$ is the Eccentrity anomaly or the angular measured of the i^{th}satellite at eccentricity *e and it is given eq. (4-10).* RAAN is Ω *[Right ascension ascending node]*
4. $\phi_{azi}\,(t)$ is the AOA of the signal from i^{th} satellite and it is given in eq. (4- 11b)

Target1: $\mathbf{S_1}(\theta, \phi_{az1}\,(t)\,) = \left[\, \mathbf{S_{M,1}}\left(\theta, \phi_{l,k}(t)\right),\ \mathbf{S_{M,2}}\left(\theta, \phi_{l,k}(t)\right),\ \cdots,\ \mathbf{S_{M,N}}\left(\theta, \phi_{l,k}(t)\right)\right]$ $(4-14)$

Target2: $\mathbf{S_2}(\theta, \phi_{az2}\,(t)\,) = \left[\mathbf{S_{M,1}}\left(\theta, \phi_{l,k}(t)\right),\ \mathbf{S_{M,2}}\left(\theta, \phi_{l,k}(t)\right),\ \cdots,\ \mathbf{S_{M,N}}\left(\theta, \phi_{l,k}(t)\right)\right]$ $(4-15)$

$$\mathbf{S}\left(\theta, \phi(t)\right) = [\mathbf{S_1}(\theta, \phi_{az1}\,(t)\,),\ \mathbf{S_2}(\theta, \phi_{az2}\,(t)\,)] \qquad (4-16)$$

$$\mathbf{w}_{\text{opt}} = \left(\mathbf{X}(k)\mathbf{X}^{H}\,(k)\right)^{-1}\mathbf{X}(k)\mathbf{r}(k) \text{ and } \mathbf{X}(t) = \mathbf{X_{sat\,1}}(t) + \mathbf{X_{sat\,2}}(t)$$

$$\mathbf{w}(k+1) = \mathbf{w}(k) + \mu\, x(k)\left(e^{*}(k)\right) \qquad (4-17)$$

Then the beamformer for the two targets and the corresponding AOA estimator have made the functional DSP to steer the multiple beams in the targets line of sight directions. Taking the performance measure in AWGN channel the power output, the output SINR and the beam pointing error have been measured using MATLAB. The performance comparison of the adaptive beamforming algorithms based on (interferer nulling capacity, beam pointing accuracy and the computational convergence) have been measured and investigated.

In the next chapter, the beacon signal tracking simulation of the phased array antenna, by using the reference signal $\mathbf{r}(k)$, and by taking the Iridium and Global star satellites constellation and downlink signal characteristics as a test input data has been performed.

Chapter Five

Simulation Results

5.1 Introduction

In this chapter, antenna array parameters (element spacing and number) and adaptive beamforming algorithms (such as LMS, RLS, SMI, LSCMA) have been simulated for two satellite constellation systems at C and Ka band microwave frequency spectrum. The simulation has been performed in order to investigate the beamforming and steering ability, interference nulling and beacon signal tracking capability of the respective adaptive algorithms.

In this thesis, we take uniform linear array with different element number and spacing located at the TTC and M of the ground station, which is located exactly at the sub-satellite point. Since the array is at the sub satellite point then ($\theta_{el} = 0^0$).

In the simulation, we have tested the multiple beacon signals tracking ability of the adaptive beamforming algorithms such that the phased array antenna signal processor adjusts the weight of the array element by using a reference signal which is operating on the satellites' downlink microwave frequency spectrum.

In the middle of the simulation, the effect of varying element spacing and array number to optimize with the operating microwave frequency spectrum are investigated by taking walker star and delta satellite constellation.

5.2 Simulation Case-1(Iridium Satellite system)

In this case, before the simulation, the numerical analysis to compute the AOA of two Iridium Satellites have been performed. The computed AOA results have been used in the simulation. By using the Iridium satellite constellation and operating frequency, which are given in the summary Table (5.1) together with the computed AOA; then the tracking antenna array for 16 different element number and spacing combination has configured and used to perform the simulation.

This combined data have been used to investigate LMS, SMI, RLS and LS - CMA adaptive beamforming algorithms. The simulation results such as the phased array output SINR and beam pointing errors have also been tabulated in the comparision tables Table 5.7 and 5.8.

The Interference nulling and beacon tracking performance of LMS beamformer at 19.5GHz for different AOA from two target Iridium satellites and one interferer have been shown in the Part A of the simulation. The simulation has been performed for 16 different element number and spacing combination as it is shown in comparison Table 5.8.

Similarly, the tracking performances of SMI adaptive beamformig algorithm are shown in the Part B of the simulation. The simulation has been performed for 16 different element number and spacing combination as it is shown in comparison Table 5.7.

The simulation result of the RLS adaptive beamformer are also shown in the Part C of the simulation. That of the LS - CMA are shown in Part D of the simulation. The simulation has performed for 16 different element number and spacing combination and they are shown in the comparison Table 5.8 and Table 5.7 for RLS and LS - CMA. The performance evaluation of each algorithm has been simulated for 10, 75, 150 and 200 elements uniform linear array with elemental spacing of 0.5 λ, 2 λ, 8 λ and 16 λ.

The Simulation result in part I and part II show the adaptive weight convergence of LMS and RLS beamformers.

Table (5.1) Summary of key characteristics of Iridium satellites system used in simulation.

Characteristics	value or comments
Orbital Altitude	780 Km at LEO
Orbital geometry	polar orbit 84.6^0 inclination
Constellation	Walker Star
Number of orbits	6
Number of satellites per orbit	11
Total Number of satellites	66 with spare
No beams per satellite (Phased Array Antenna)	48 at L - Band
Gateway downlinks	19.4 – 19.6 GHz
Gateway uplinks	29.1 – 29.3 GHz
Inter satellite links	Ka – band 23.0 – 23.4 GHz adjacent satellites
Modulation	QPSK

5.2.1 Targets Tracking Flow chart

The tracking flow chart, which is shown in Figure (5.1) below, describes the pictorial representation of the steps and set of rules in solving two target satellite beacons tracking. In the flow chart, the process of tracking two target satellites is begun by accepting the satellite constellation information and the satellite downlink signal characteristics.

After that, each processing block such as calculating the slant range of the target, calculating the central angle/true anomaly, calculating the actual line of sight signal AOA towards the (TTC and M station) have been shown.

The Last conditional block checks the carrier frequency if it is either within Ka/C-band. Then the tracking process continues; and the error signal vector is generated by the difference of the reference signal and the array output. This error signal vector is used to derive the adaptive

weight control block so as to point the maxima towards the targets and the nulls towards the interferer. In such a way that the ground adaptive phased array antenna continuously tracks the two satellites by repeating the closed loop process.

It should be noted that, since the target tracking was started by inputting the satellites' constellation and signal characteristics information then the array output contains both the constellation and the where about information of the targets. Therefore, the error vector which is generated by taking the difference between the reference signal and the array output is the amount by which the amplitude and phase of the array element weight deviated from their optimal excitation; to point the maxima in the look directions.

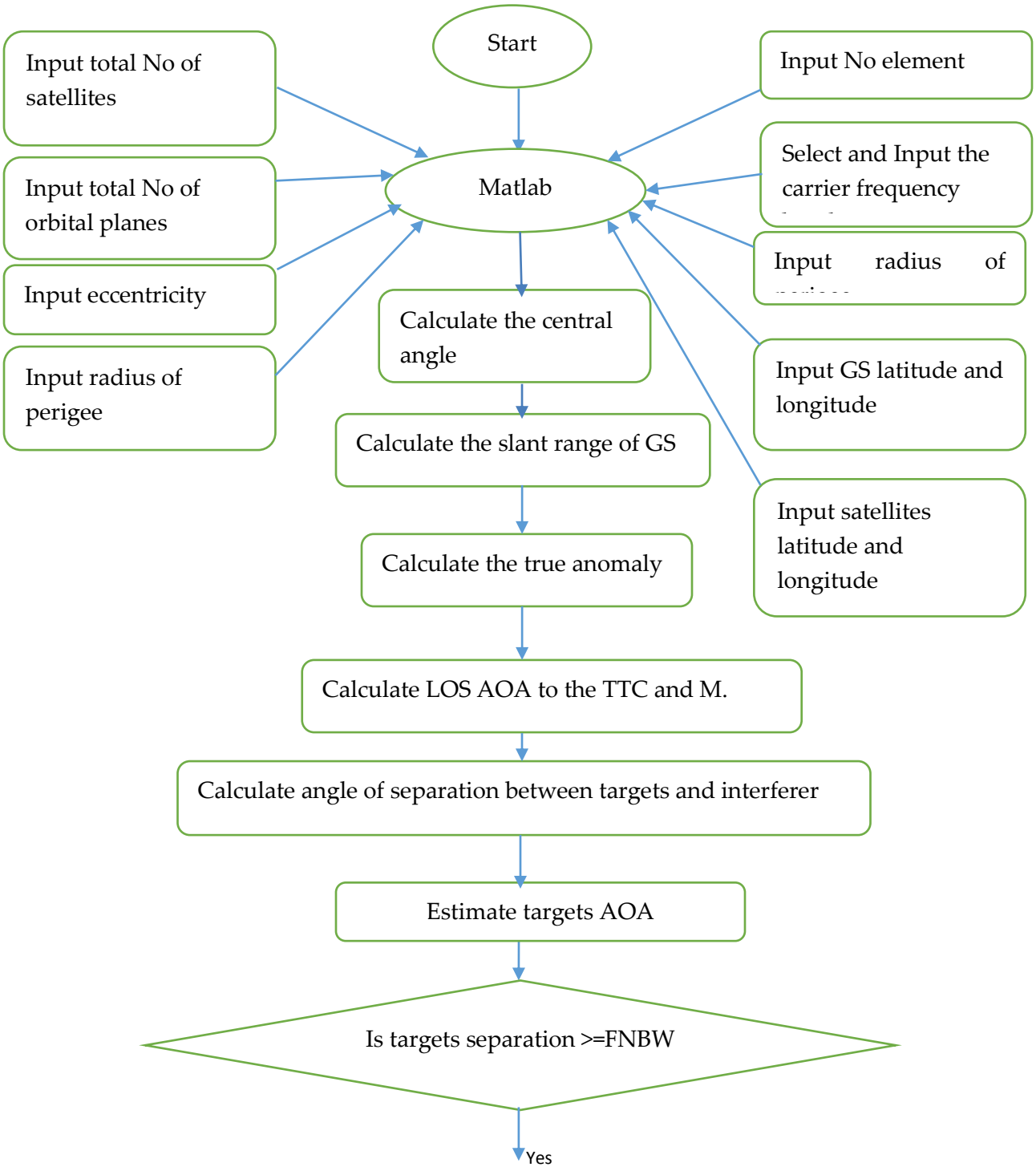

Figure (5.1) Two target tracking simulation flowchart.

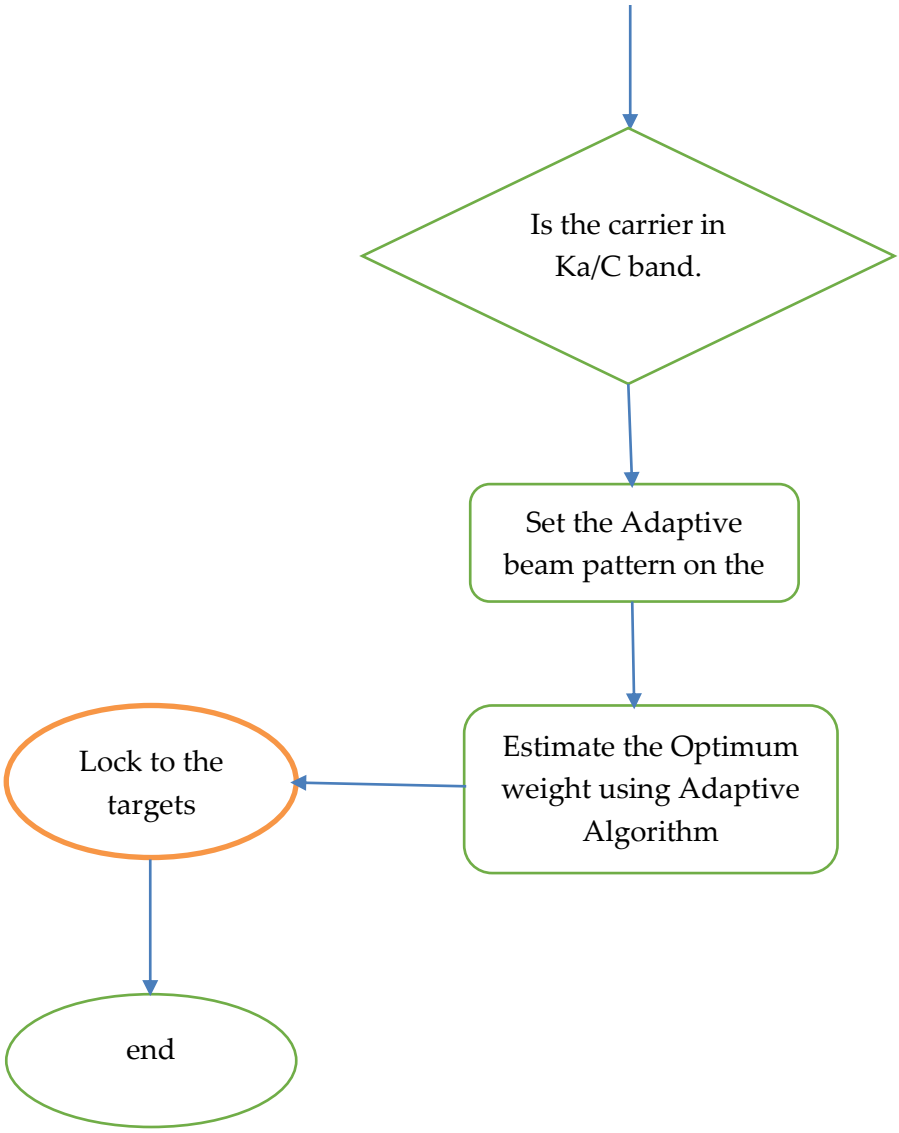

Continued from **Figure. (5.1)**

5.2.2 Two Iridium satellites orbital element numerical analysis to compute the AOA.

Table 5.2 Orbital element value of the first and second satellite with the computed AOA at 3 different instant.

Target	Major axis(km)	Eccentricity	Inclination	$M_1(t_0)$	$E_1(t_0)$	$g_1(t_0)$	$\phi_{az1}(t_0)$
Sat_1	7158	0.0029	84.4^0	0^0	0^0	0	0^0
Target	Major axis(Km)	Eccentricity	Inclination	$M_2(t_0)$	$E_2(t_0)$	$g_2(t_0)$	$\phi_{az2}(t_0)$
Sat_2	7158	0.0029	84.4^0	9.9995^0	10^0	0.1768	62.3751
Target	Major axis(km)	Eccentricity	Inclination	$M_1(t_1)$	$E_1(t_1)$	$g_1(t_1)$	$\phi_{az1}(t_1)$
Sat_1	7158	0.0029	84.4^0.	4.9997^0	5^0	0.0877	40.4397^0
Target	Major axis(km)	Eccentricity	Inclination	$M_1(t_2)$	$E_1(t_2)$	$g_1(t_2)$	$\phi_{az1}(t_2)$
Sat_1	7158	0.0029	84.4^0	-4.9997	-5	-0.0877	-40.4397
Target	Major axis(Km)	Eccentricity	Inclination	$M_2(t_1)$	$E_2(t_1)$	$g_2(t_1)$	$\phi_{az2}(t_1)$
Sat_2	7158	0.0029	84.4^0	14.9992^0	15	0.26	74.45
Target	Major axis (Km)	Eccentricity	Inclination	$M_2(t_2)$	$E_2(t_2)$	$g_2(t_2)$	$\phi_{az2}(t_2)$
Sat_2	7158	0.0029	84.4^0	-14.9992^0	-15^0	-0.2688	-74.4551^0

A. LMS adaptive algorithm simulation result.

Table (5.3) Iridium satellite tracking by LMS adaptive beamformer performance summary.

Performance	No. Element	spacing	Output SINR(dB)	Null(dB)	Error1	Error2
Best	150	0.5 λ	75.5	-73.03	0.0329	0.02
	200	0.5 λ	75.2	-50.4	0.06	0.07
	150	16 λ	93.33	-90.45	0.045	0.02
	200	2 λ	72.2	-69.37	0.08	0.03
worst	10	0.5 λ	2.9	-0.074	0.01	0.01

By using LMS adaptive beamformer, the best array configurations to track two Iridium satellites at Ka – band Microwave spectrum are the 150 by 0.5 λ and 200 by 0.5 λ. This performance criterion considers the physical space and the total number of element in the array.

The first array configuration i.e.150 by 0.5 λ, as it is shown in Figure (5.2) yields array output SINR of 75.5dB and it nulls the interferer at a level of -73.03dB. This array configuration has a beam pointing accuracy of 0.0329 towards the first satellite and 0.02 towards the second satellite.

Similarly, the second array configuration i.e. 200 by 0.5 λ, as it is shown in Figure (5.3) yields array output SINR of 75.2dB and nulls the interferer at a level of -50.4dB. This array configuration has a beam pointing accuracy of 0.06 and 0.07 towards the first and the second satellite respectively.

The third array configuration i.e.150 by 16 λ, as it is shown in Figure (5.4) yields array output SINR of 93.33dB and it nulls the interferer at a level of -90.45dB. This array configuration

has a beam pointing accuracy of 0.045 towards the first satellite and 0.02 towards the second satellite.

Array configuration such as 10 by 16 λ, 75 by 2 λ, 150 by 2 λ, 150 by 8 λ, 20 by 16 λ, 75 by 16 λ, 10 by 8 λ and 200 by 8λ are also the optimal arrangement which can be used to track two Iridium satellites at 16.5GHz.

The worst case array configuration, by LMS adaptive beamformer to track two iridium satellites at 19.5GHz is the 10 by 0.5 λ which yields array output SINR of 2.9dB and its nulling level is almost -0.074dB which is unacceptable and it is shown in Figure (5.5).

One of the important fact, we have discovered in the simulation is that, two Iridium satellite tracking by using LMS adaptive beamformer has not array power wastage through grating lobes at 19.5GHz provided that the 16 different element number and spacing combination considered in this thesis.

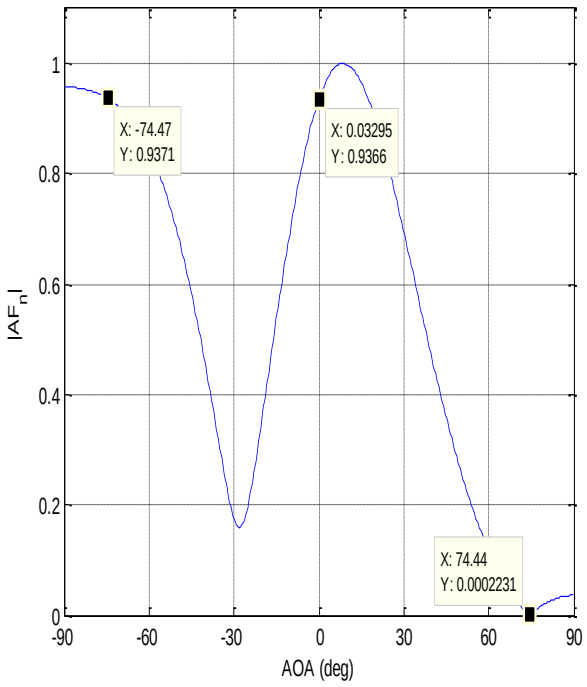

Figure (5.2) *LMS 150 by 0.5(λ) two targets tracking at 19.5GHz.*

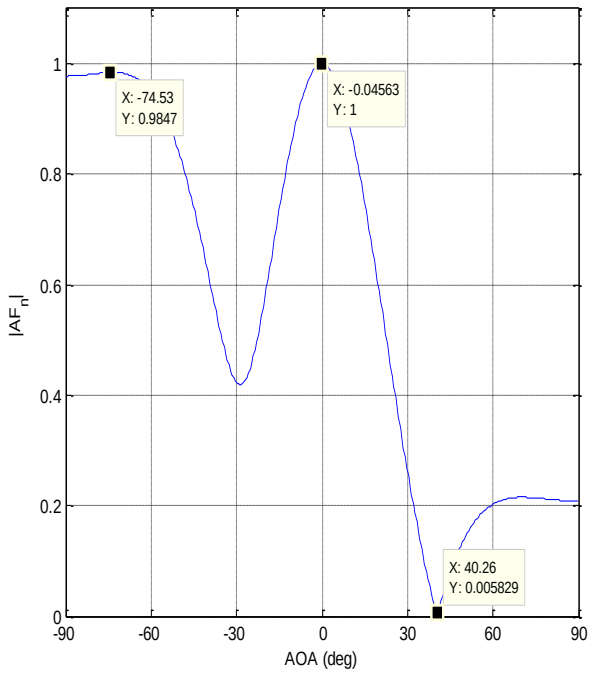

Figure (5.3) *LMS 200 by 0.5(λ) two targets tracking at 19.5GHz.*

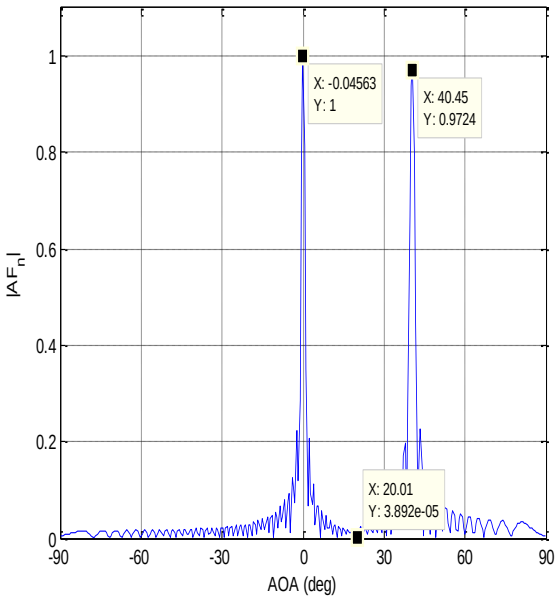

Figure (5.4) *LMS 150 by 16(λ) two targets tracking at 19.5GHz.*

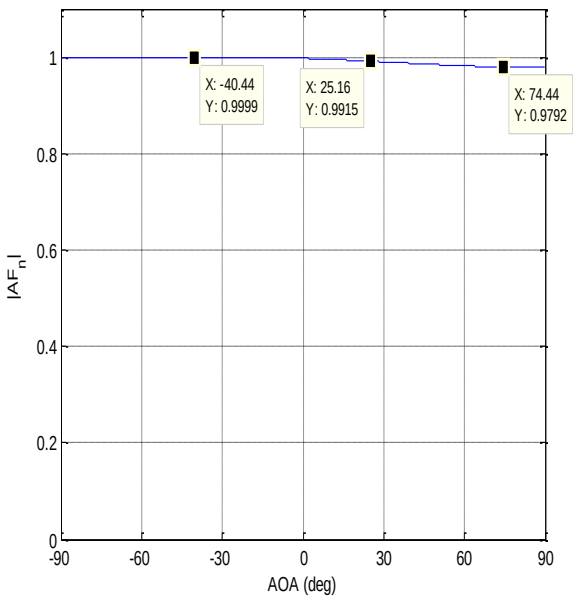

Figure (5.5) *LMS 10 by 0.5(λ) two targets tracking at 19.5GHz.*

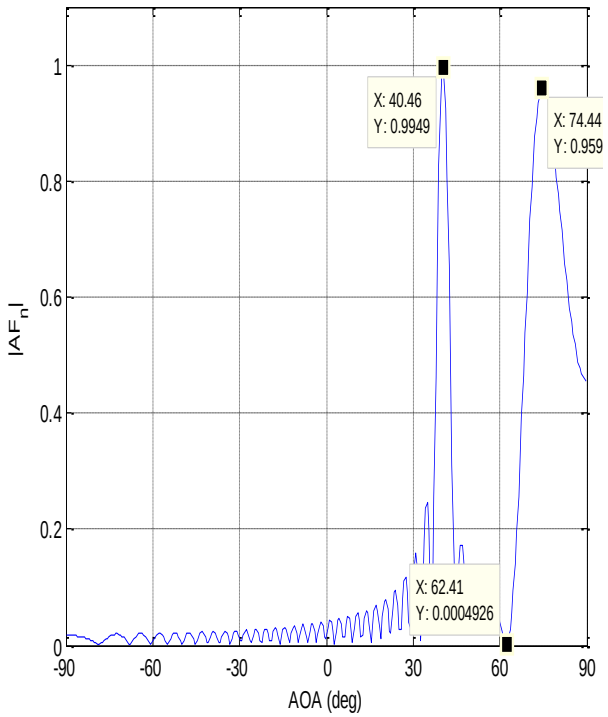

Figure (5.6) *LMS 150 by 8(λ) two targets tracking at 19.5GHz.*

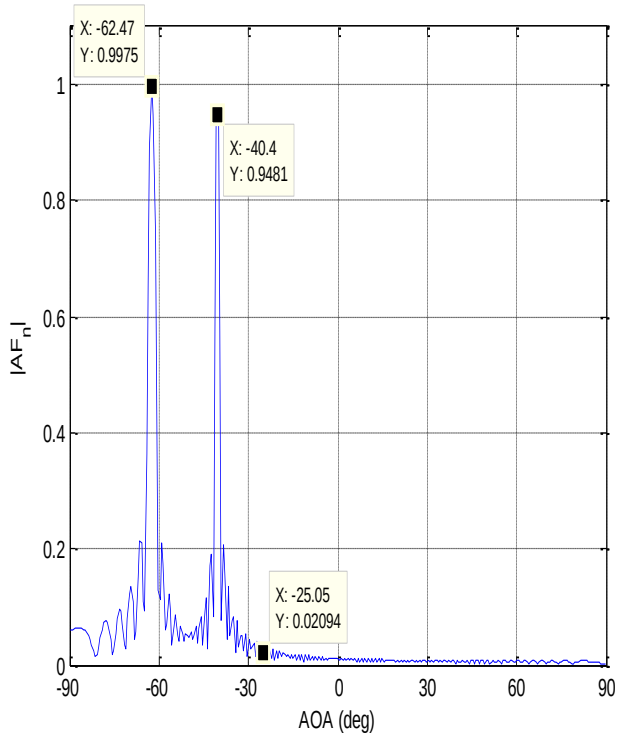

Figure (5.7) *LMS 200 by 16(λ) two targets tracking at 19.5GHz.*

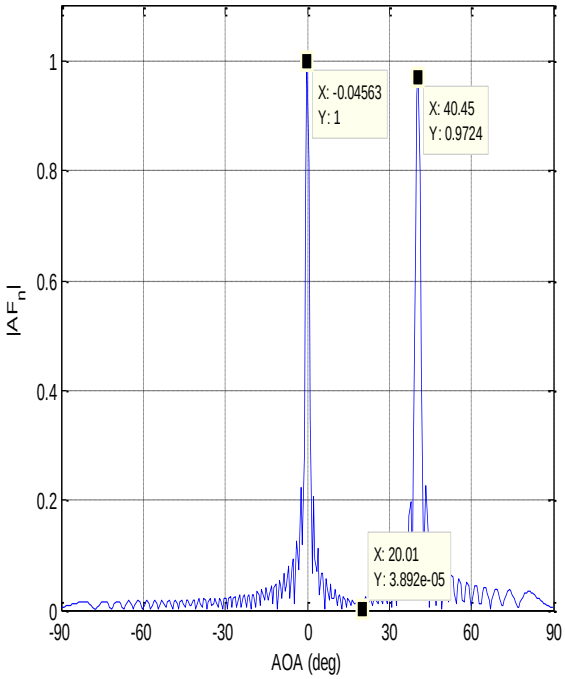

Figure (5.8) *LMS 150 by 16(λ) two targets tracking at 19.5GHz..*

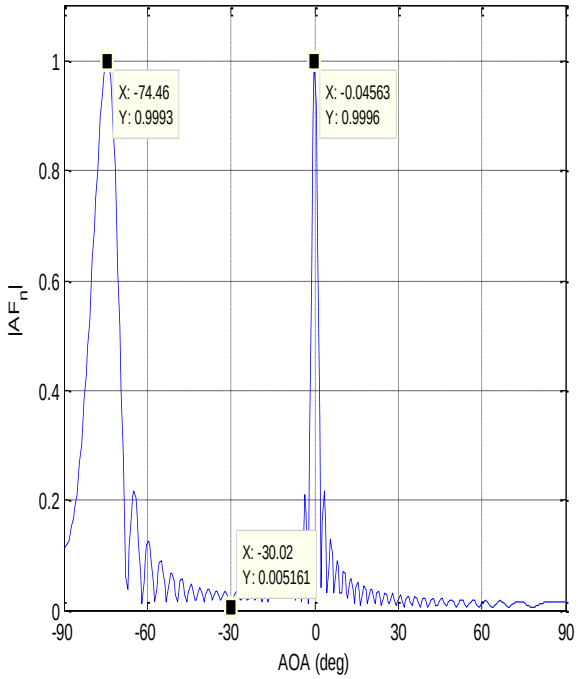

Figure (5.9) *LMS 200 by 8(λ) two targets tracking at 19.5GHz.*

B. SMI adaptive algorithm simulation result.

Table (5.4) Iridium satellite tracking by SMI adaptive beamformer performance summary.

Performance	No. Element	Spacing(m)	Output SINR(dB)	Null(dB)	Error1	Error2
Best	10	16 λ	44.5	-41.9	0.045	0.02
	75	16 λ	40.2	-38.4	0.04	0.005
Optimal	75	8 λ	41.99	-40.53	0.045	0.02
	75	2 λ	71.4	-69.3	0.03	0.01
Worst	200	8 λ	0.094	-8.4	0.01	0.005

By using SMI adaptive beamformer, the best array configurations to track two Iridium satellites at Ka – band Microwave spectrum are the 10 by 16 λ and 75 by 16 λ . This performance criteria considers the beamformed in the target direction and the number of elements in the array.

The first best array configuration i.e.10 by 16 λ, yields array output SINR of 44.5dB and it nulls the interferer at a level of -41.9dB. This array configuration has a beam pointing accuracy of 0.045 towards the first satellite and 0.02 towards the second satellite.

The optimal array configuration i.e.75 by 8 λ and 75 by 2λ yield array output SINR of 41.9dB and 71.4dB, respectively; which can be used to track two Iridium satellites at 16.5GHz by SMI adaptive beamformer.

The worst case array configuration by SMI adaptive beamformer to track two Iridium satellites at 19.5GHz is the 200 by 8 λ; which yields array output SINR of 0.094dB and its nulling level is almost -8.4dB which is unacceptable.

One of the important fact, we have realized in the simulation is that, two Iridium satellite tracking by using SMI adaptive beamformer has shown poor performance as the number of elements increased.

Array configuration such as 10 by 16 λ, 200 by 0.5 λ, 10 by 0.5 λ, 75 by 2 λ, 75 by 16 λ and 10 by 8 λ are also the optimal arrangement which can be used to track two Iridium satellites at 16.5GHz.

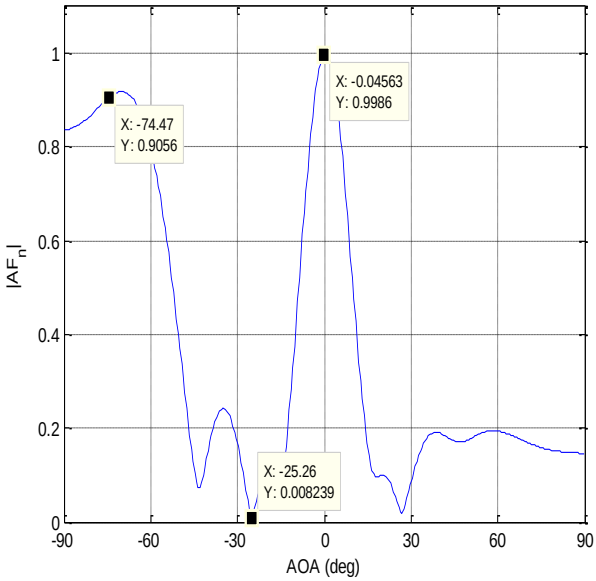

Figure (5.10) *SMI 10 by 16(λ) two targets tracking at 19.5GHz.*

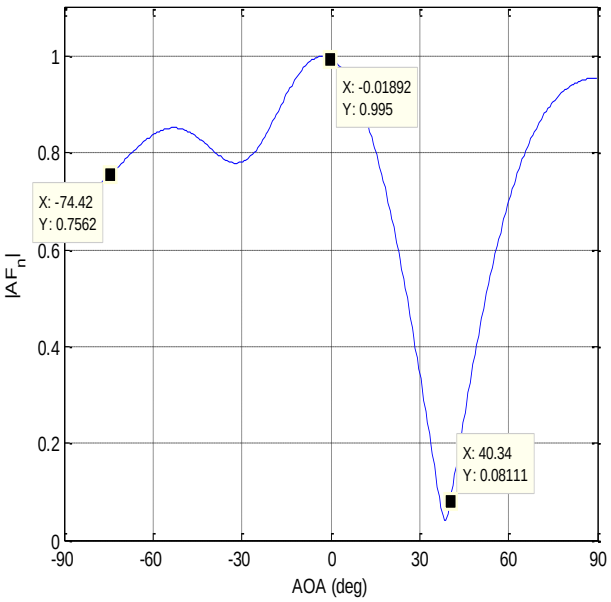

Figure (5.11) *SMI 200 by 0.5(λ) two targets tracking at 19.5GHz.*

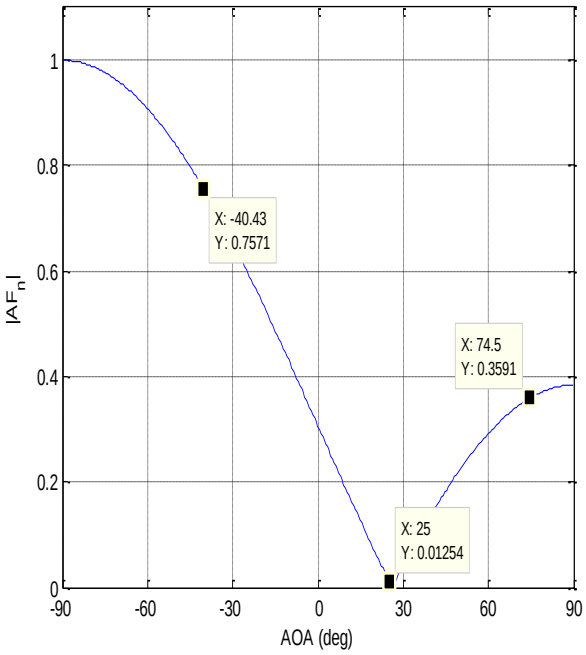

Figure (5.12) *SMI 10 by 0.5(λ) two targets tracking at 19.5GHz.*

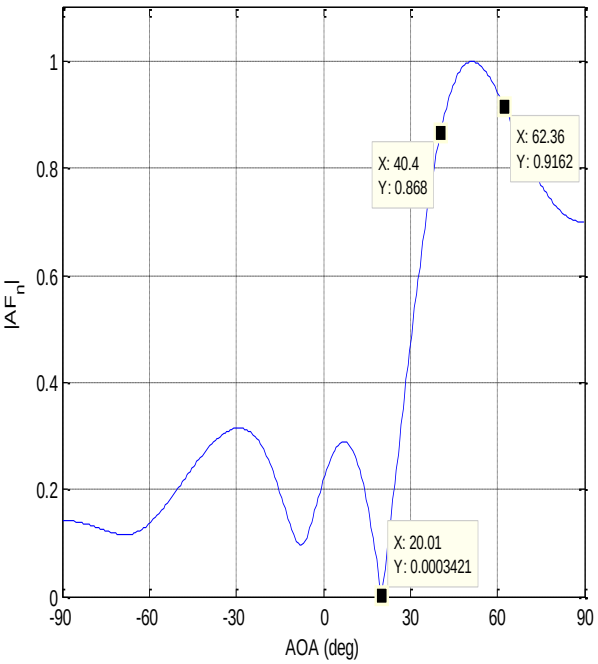

Figure (5.13) *SMI 75 by 2(λ) two targets tracking at 19.5GHz.*

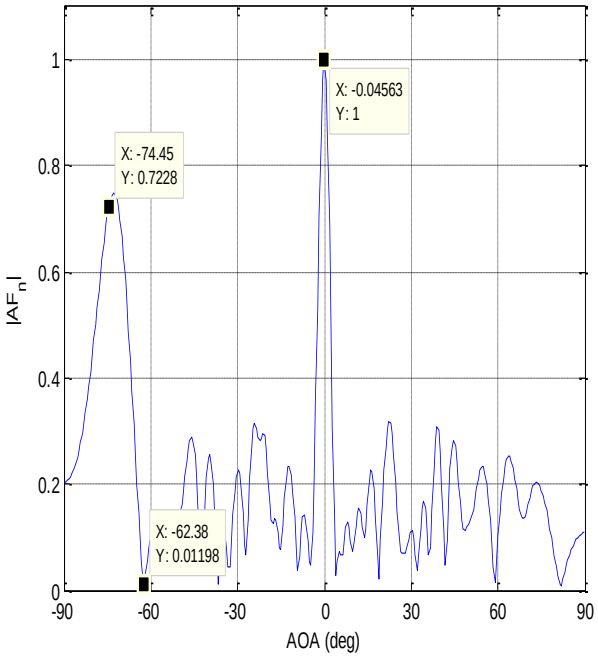

Figure (5.14) *SMI 75 by 16(λ) two targets tracking at 19.5GHz.*

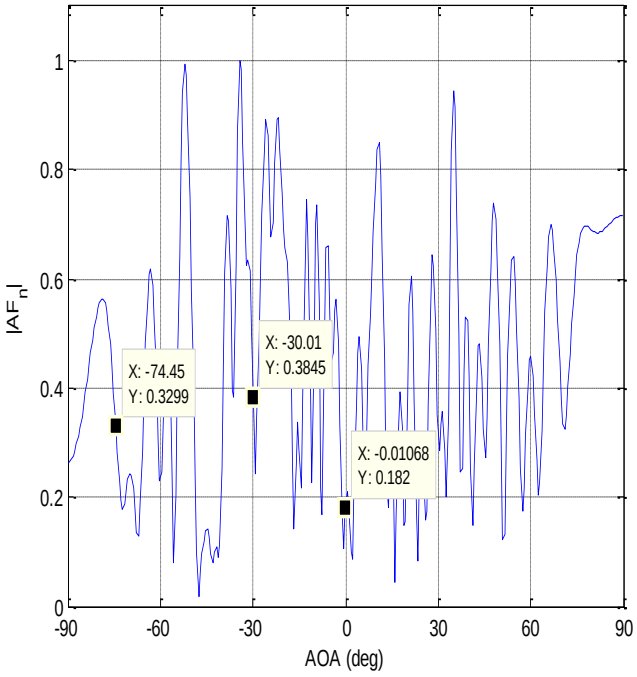

Figure (5.15) *SMI 10 by 8(λ) two targets tracking at 19.5GHz.*

C. RLS adaptive algorithm simulation result.

Table (5.5) Iridium satellite tracking by RLS adaptive beamformer performance summary.

Performance	No. Element	spacing	Output SINR(dB)	Null (dB)	Error1	Error2
Best	10	16 λ	44.55	-41.9	0.045	0.02
	10	8 λ	49	-46.74	1	0.02
	75	16 λ	48	-47.95	0.04	0.08
worst	150	16 λ	1.7	-5.3	0.05	0.05
	200	2 λ	0.16	-1.3	0.04	0.005

In the case of RLS adaptive beamformer, we have discovered that array configurations 10 by 16 λ , 10 by 8 λ and 75 by 16 λ are the best array configuration to track the two Iridium satellites. The first array configuration, which is 10 by 16 λ yields array output SINR of 44.5 dB with the highest nulling capacity of -41.9dB. The beams pointing error of this array configuration are 0.045 and 0.02 towards the first and the second Iridium satellites, respectively.

The 10 by 8 λ and 75 by 16 λ array configuration are also the best and yield array output SINR of 49dB and 48dB respectively. Similarly, the 10 by 8 λ yields array output SINR of 49dB with the nulling level at -46.74dB. The beam pointing errors of this array configuration are 1 and 0.02 towards the first and the second satellites, respectively.

The 75 by 16 λ array configuration yields array output SINR of 48dB with a nulling level at -47.95dB and the beams pointing errors of this array configuration are 0.04 and 0.08 towards the first and the second target satellites, respectively.

The second array configuration which results the worst performance, has an array output SINR of 1.7dB with a nulling level at -5.35dB. This array configuration has beams pointing error of 0.05 towards the two satellites.

The worst array configurations in the case of RLS beamformer are 200 by 2 λ and 150 by 16 λ. The 200 by 2 λ array configuration yields array output SINR of 0.16dB. This has nulling level at -1.3dB; with beams pointing errors of 0.04 and 0.005 towards the first and the second satellites, respectively.

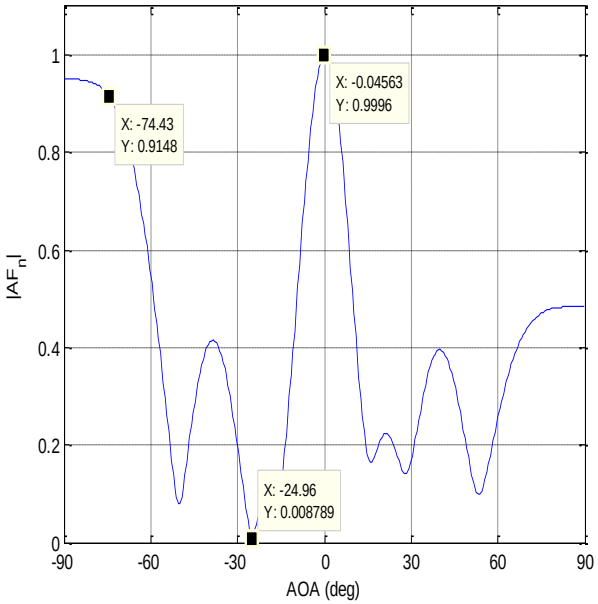

Figure (5.16) RLS 10 by 16(λ) two targets tracking at 19.5GHz.

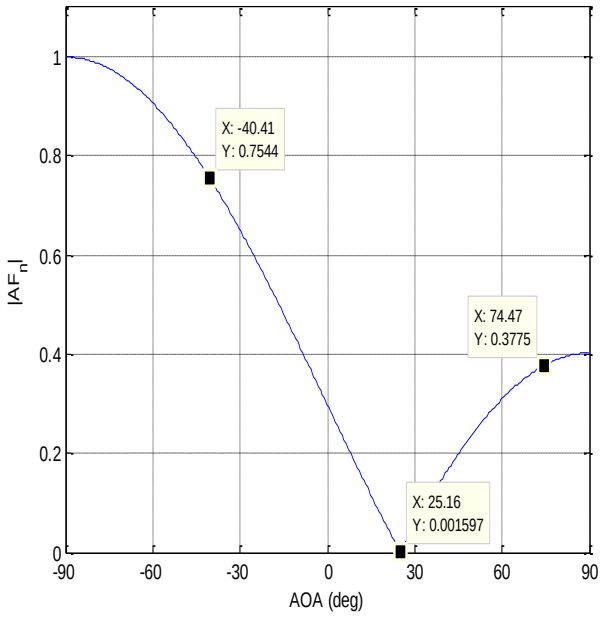

Figure (5.17) RLS 10 by 0.5(λ) two targets tracking at 19.5GHz.

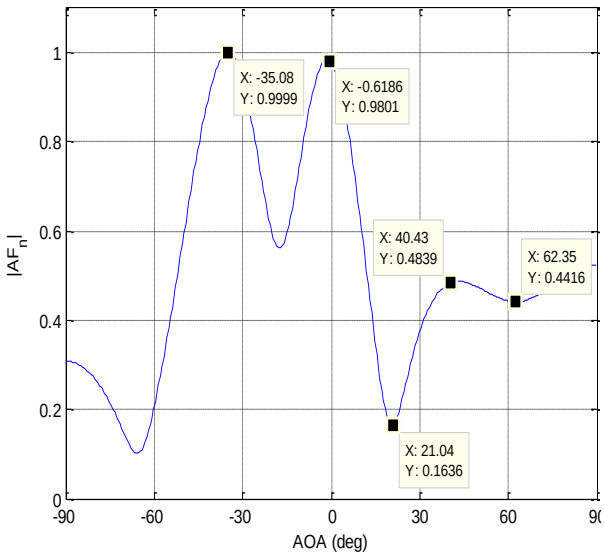

Figure (5.18) RLS 75 by 2(λ) two targets tracking at 19.5GHz.

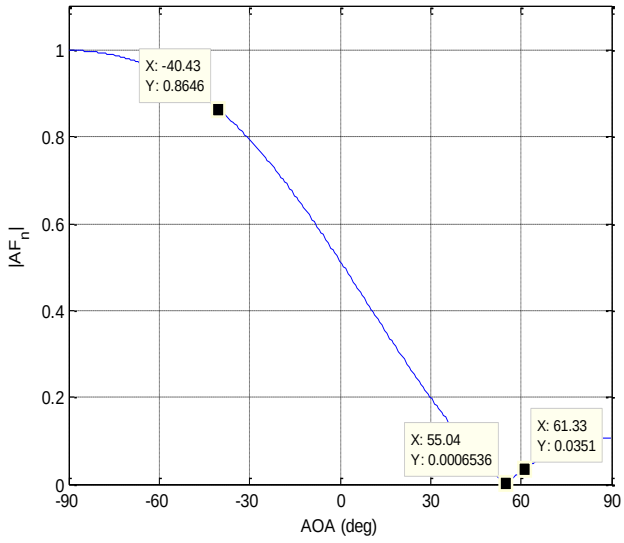

Figure (5.19) RLS 10 by 2(λ) two targets tracking at 19.5GHz.

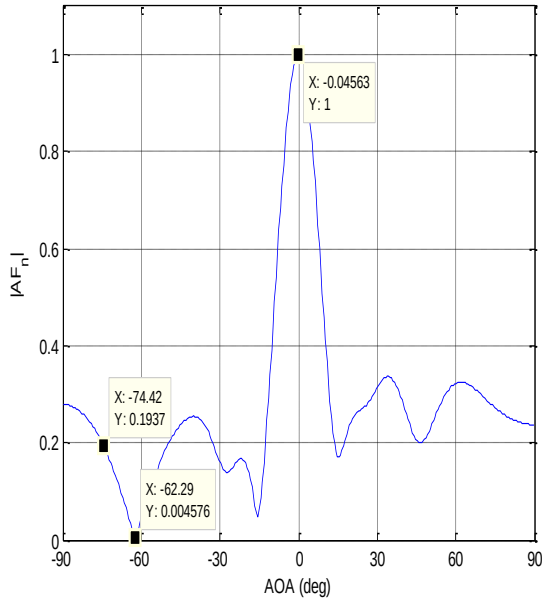

Figure (5.20) RLS 75 by 16(λ) two targets tracking at 19.5GHz.

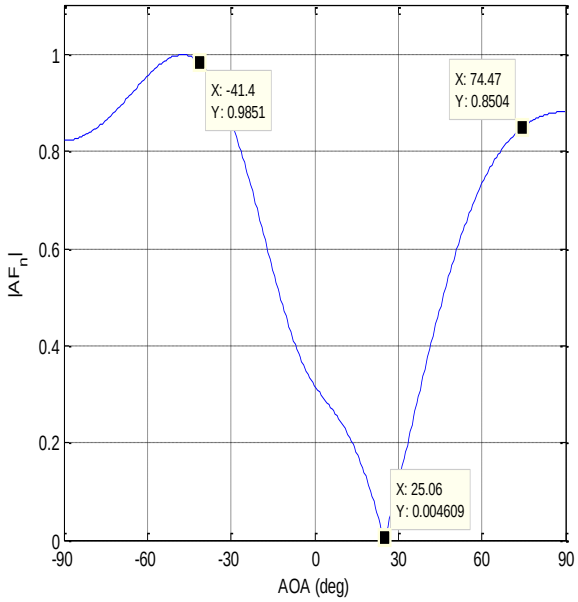

Figure (5.21) RLS 10 by 8(λ) two targets tracking at 19.5GHz.

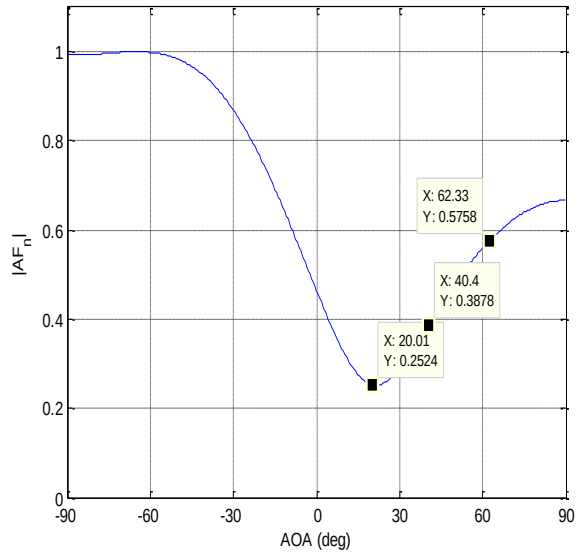

Figure (5.22) RLS 75 by 0.5(λ) two targets tracking at 19.5GHz.

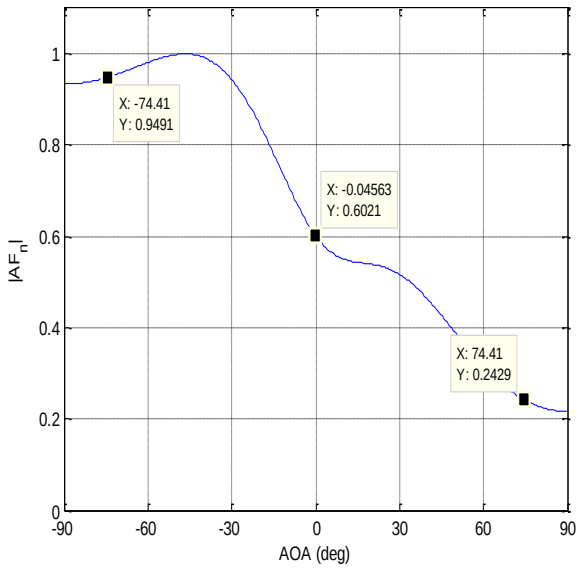

Figure (5.23) RLS 150 by 0.5(λ) two targets tracking at 19.5GHz.

D. LS - Constant Modulus adaptive algorithm simulation result.

Table (5.6) Iridium satellite tracking by LSCMA adaptive beamformer performance summary.

Performance	No. Element	spacing	Output SINR(dB)	Null1(dB)	Null2(dB)	Error$_1$	Error$_2$
Best	200	2 λ	62.9	-90.4	-60	0.007	0.04
	150	2 λ	55.8	-60	-53.9	0.03	0.02
	150	16 λ	53.2	-73.9	-50.4	0.01	0.019
Worst	10	0.5 λ	3.2	-6.19	-7.7	0.01	0.005
	10	2 λ	0.95	-10.4	-0.08	0.03	0.02

In the case of LS - CMA adaptive beamforming simulation, the following array configurations are the best and optimal. First, the 200 by 2 λ array configuration yields a deep null values at -90.45dB and -60dB as it is show in Figure (5.31). The array output SINR of this configuration is 62.9dB with a beam pointing errors of 0.007 and 0.04 towards the first and the second satellite as it is shown in Figure (5.31).

The second best array configuration is 150 by 2 λ, which yields array output SINR of 55.8dB by nulling the two interferers at -60dB and -53.9dB level. This array configuration has a beam pointing errors of 0.03 and 0.02 towards the first and the second satellite as it is shown in Figure (5.26).

The third best array configuration is the 150 by 16 λ, which yields 53.27dB array output SINR by nullifying the two interferers at a level of -73.9dB and -50.4dB.This array configuration has a beam pointing errors of 0.01 and 0.019 towards the first and the second satellites as it is shown in Figure (5.30).

The fourth best array configuration is the 75 by 16 λ which yields 51.65db array output SINR and it nullifies the two interferers at level of -53.9db and -50.4db.This array configuration has a beam pointing error of 0.04 and 0.02 towards the first and the second satellites as it is shown in Figure (5.29).

The fifth best array configuration is the 200 by 8 λ and it yields array output SINR of 50.7dB and it nullifies the two interferers at a level of -47.9 and -61.9dB. This array configuration has a beam pointing errors of 0.04 and 0.03 towards the first and the second satellites.

In LS – CMA adaptive beamformer, the 10 by 0.5 λ and the 10 by 2 λ array configuration are the two worst array configurations; such that they yield array output SINR of 3.2dB and 0.95dB respectively.

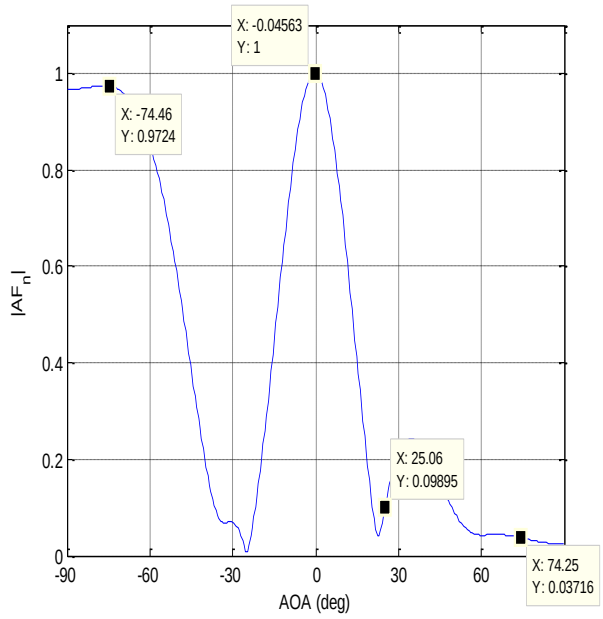

Figure (5.24) *LSCMA 10 by 16(λ) two targets tracking at 19.5GHz.*

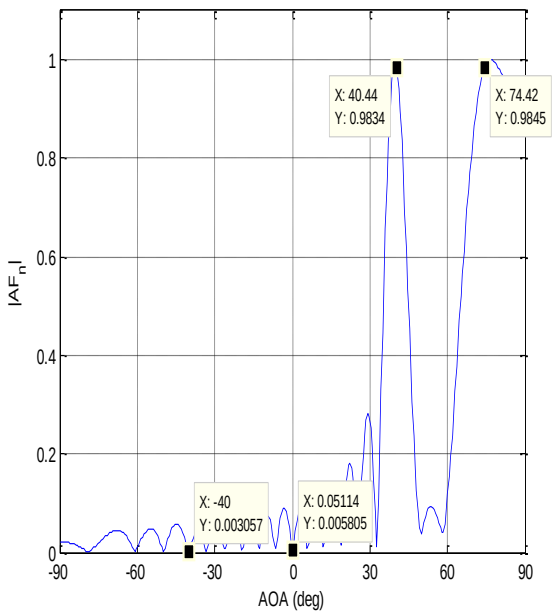

Figure (5.25) *LSCMA 75 by 8(λ) two targets tracking at 19.5GHz.*

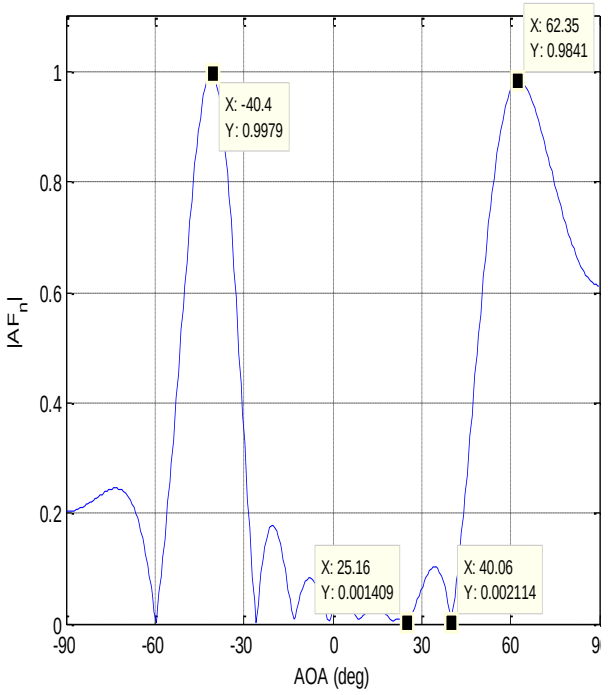

Figure (5.26) *LSCMA 150 by 2(λ) two targets tracking at 19.5GHz.*

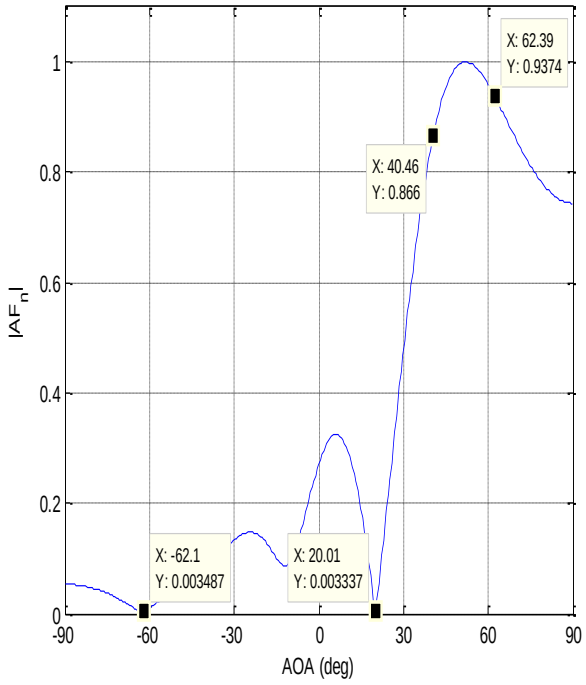

Figure (5.27) *LSCMA 75 by 2(λ) two targets tracking at 19.5GHz.*

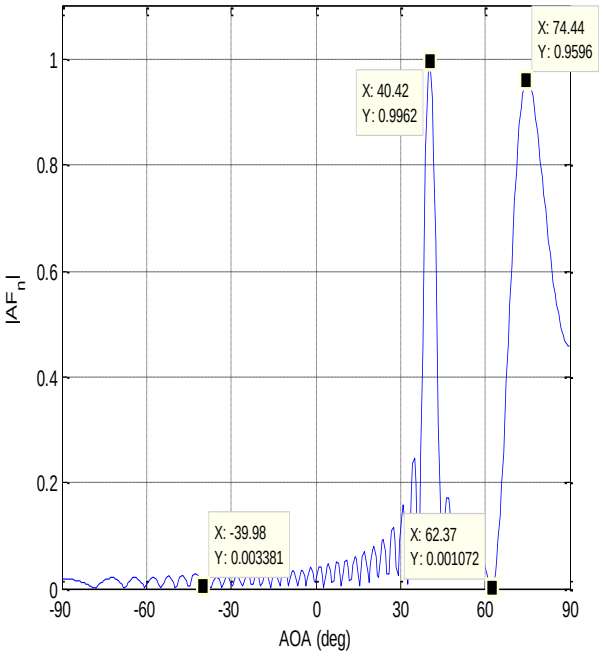

Figure (5.28) *LSCMA 150 by 8(λ) two targets tracking at 19.5GHz.*

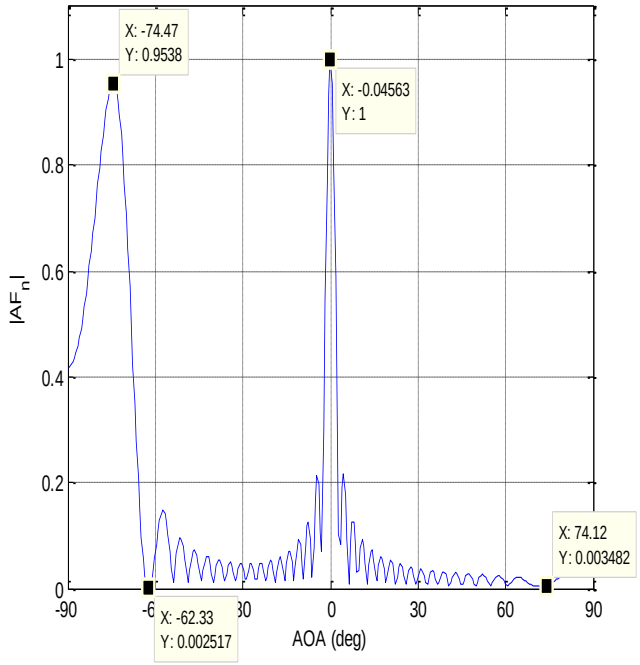

Figure (5.29) *LSCMA 75 by 16(λ) two targets tracking at 19.5GHz.*

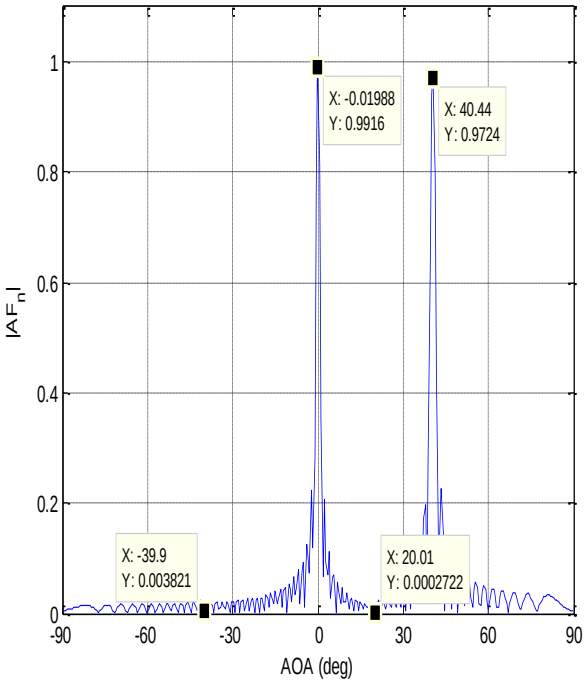

Figure (5.30) *LSCMA 150 by 16(λ) two targets tracking at 19.5GHz.*

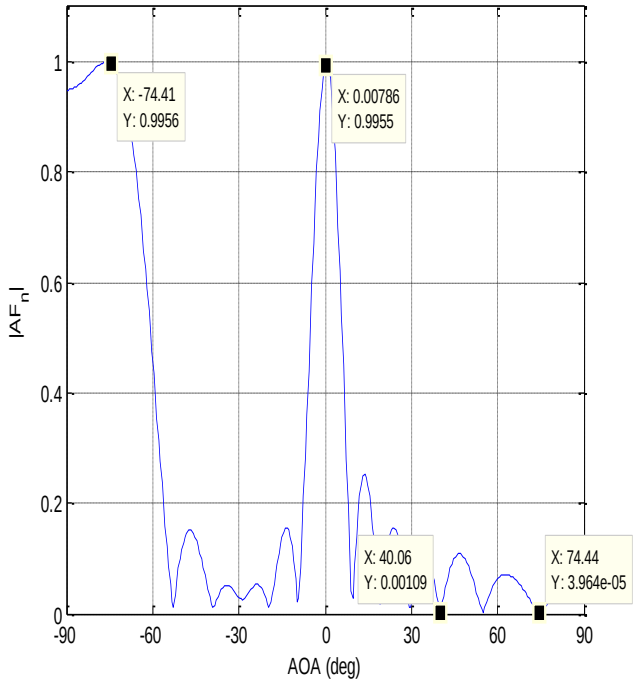

Figure (5.31) *LSCMA 200 by 2(λ) two targets tracking at 19.5GHz.*

Adaptive beamformer comparison (SMI with RLS and LMS with LS - CMA)

The green shaded records in Table (5.7) show us that, SMI and RLS have the maximum output SINR of 63.1dB and 60.dB respectively. As we have seen in the record, when the number of elements increased in the array system then the performance SMI and RLS algorithms have degraded.

The minimum SINR which is recorded by SMI is -0.094dB and that of the RLS is 0.16dB. Generally, the overall performance of RLS and SMI are better provided that minimum no. element.

Table (5.7) comparison SMI with RLS

Array configuration		SMI				RLS			
		Interferer Nulling(dB)	Beam pointing Accuracy		Array output power SINR(dB)	Interferer Nulling(dB)	Beam pointing Accuracy		Array output power SINR(dB)
No. Element	Spacing		$Error_1$ (0^0)	$Error_2$ (0^0)			$Error_1$ (0^0)	$Error_2$ (0^0)	
10	16(λ)	-41.9382	0.045	0.02	44.5083	-41.9382	0.045	0.02	44.5534
75	8(λ)	-40.5374	0.009	0.01	41.9960	-6.0729	0.009	0.01	4.3595
150	2(λ)	-6.7448	0.01	0.03	7.0807	-2.1916	0.01	0.04	3.2941
200	0.5(λ)	-21.9382	0.01	0.03	23.8738	-3.4785	0.045	0.01	2.5585
10	0.5(λ)	-38.0618	0.009	0.05	36.5252	-60	0.02	0.02	58.4936
75	2(λ)	-69.3704	0.03	0.01	71.4111	-15.9176	0.009	0.02	12.1913
150	8(λ)	-11.8692	0.02	0.01	3.3387	-5.3521	0.01	0.04	5.0672
200	16(λ)	-20.9151	0.01	0.01	14.7522	-13.9794	0.01	0.07	8.5830
10	2(λ)	-61.5144	0.04	0.02	60.3140	-64.4370	0.009	1.04	63.1341
75	16(λ)	-38.4164	0.04	0.005	40.2426	-47.9588	0.04	0.08	48.1128
150	16(λ)	-27.9588	0.001	0.01	23.6840	-5.3521	0.05	0.05	1.7679
200	2(λ)	-18.4164	0.045	0.03	15.6920	-1.3100	0.04	0.005	0.1659
10	8(λ)	-46.0206	0.02	0.04	48.6603	-46.7448	1	0.02	49.0054
75	0.5(λ)	-61.2096	0.04	0.02	60.1311	-12.0412	0.03	0.04	8.7557
150	0.5(λ)	-8.4962	0.025	0.005	10.5810	-12.3958	0.04	0.04	13.4081
200	8(λ)	-8.4043	0.01	0.005	-0.0943	-6.5580	0.04	0.01	5.5759

Table 5.8 comparison LMS with LS - CMA

Array configuration		LMS				LS – CMA				
		Interferer Nulling(dB)	Beam pointing Accuracy		Array output power SINR(dB)	Interferer -1 nulling(dB)	Interferer - 2 nulling(dB)	Beam pointing Accuracy		Array output power SINR(dB)
No. element	spacing		$Error_1$ (0^0)	$Error_2$ (0^0)				$Error_1$ (0^0)	$Error_2$ (0^0)	
10	16(λ)	-12.5491	0.0051	0.0083	15.4721	-36.4782	-30.4576	0.04	0.01	32.3685
75	8(λ)	-51.8999	0.02	0.01	54.7347	-46.0206	-50.4576	0.01	0.03	44.5102
150	2(λ)	-72.3129	0.06	0.07	75.2359	-60	-53.9794	0.03	0.02	55.8894
200	0.5(λ)	-44.7314	0.0456	0.08	47.6549	-50.4576	-40	0.03	0.02	42.3733
10	0.5(λ)	-0.0741	0.010	0.01	2.9533	-6.1961	-7.7443	0.01	0.005	3.2008
75	2(λ)	-57.0774	0.01	0.005	59.2272	-50.4576	-50.4576	0.03	0.02	49.5007
150	8(λ)	-66.1961	0.03	0.01	68.9875	-60	-50.4576	0.01	0.01	52.7476
200	16(λ)	-33.5805	0.039	0.4	36.3280	-33.9794	-70.4576	0.009	0.01	36.6360
10	2(λ)	-12.0412	0.02	0.01	11.5802	-10.4576	-0.0873	0.03	0.02	0.9524
75	16(λ)	-60	0.00308	0.02	62.7476	-53.9794	-50.4576	0.04	0.02	51.6538
150	16(λ)	-90.4576	0.045	0.02	93.3376	-73.9794	-50.4576	0.01	0.019	53.2736
200	2(λ)	-69.3704	0.08	0.03	72.2934	-90.4576	-60	0.0078	0.04	62.9191
10	8(λ)	-43.6091	0.04	0.05	45.8343	-24.4370	-5.6799	0.009	0.01	7.5950
75	0.5(λ)	-6.4114	0.009	0.03	8.1038	-18.4164	-9.8970	0.01	0.025	9.0831
150	0.5(λ)	-73.0339	0.0329	0.02	75.5068	-47.9588	-33.9794	0.04	0.02	34.9652
200	8(λ)	-45.8486	0.045	0.01	48.8111	-47.9588	-61.9382	0.04	0.03	50.7857

As we have seen in the comparison Table 5.8, the maximum output SINR of LMS is 93.33dB and its deep nulling point is at a level of -90dB. It also attains a minimum beam pointing error of 0.005. Similarly, the maximum output SINR of LSCMA is 62.9dB and its deep nulling point is at a level -70.45dB. It also attains the minimum beam pointing error of 0.005.

Generally, the overall signal tracking, interferers nulling and the beam pointing accuracy of LMS and LSCMA adaptive algorithms are comparable; and we have concluded that these two algorithms are the best, so they can be applied for multiple satellite tracking within Microwave frequency spectrum.

5.2.3 Weighting convergence of the adaptive algorithms

I. LMS adaptive beamformer element weight convergence.

In the simulation of two Iridium satellites tracking, the array element weighting convergence, by using LMS adaptive beamformer has presented below.

The adaptive weight convergence simulation of the LMS adaptive beamformer, has been simulated to five of the array elements. The Mean square error vs. Iteration. No and the weigh magnitudes of the five array elements vs. the No. Iteration have been shown on every pair of the following figures.

Every pair figures represent a particular array configuration corresponding to the element number and spacing. The iteration is simulated by starting from initial value of 1 up to the final value of 100, where the mean square error iteratively tries to converge based on the array configuration and the induced signal characteristics.

The normalized array factor is plotted based on the final mean square error value. If the mean square error and the elements weight convergence then the performance of the LMS beamformer will be maximized.

Each array configuration which was analyzed and compared before in the part A has its own specific weighting convergence behavior as it is illustrated below. The worst case scenario which we have discovered before has its own effect on the weighting process.

The best array configuration in LMS such as 150 by 0.5 λ has shown its best weighting convergence in Figure 5-33. Similarly, the 150 by 2λ and 150 by 8 λ array configuration show its best performance correspondingly.

The LMS adaptive weight and mean square error simulation qualitative result of the two Iridium satellite tracking are summarized in Table (5.9).The worst array configuration which we have discovered before has also revealed its poor performance. The weighting convergence and the mean square error simulation of the array configuration such as 10 by 0.5 λ as it is shown in Figure 5.37, has mean square error value of 0.76 at the 96th iteration, whereas the magnitude of the element's weigh oscillate and have not been converged.

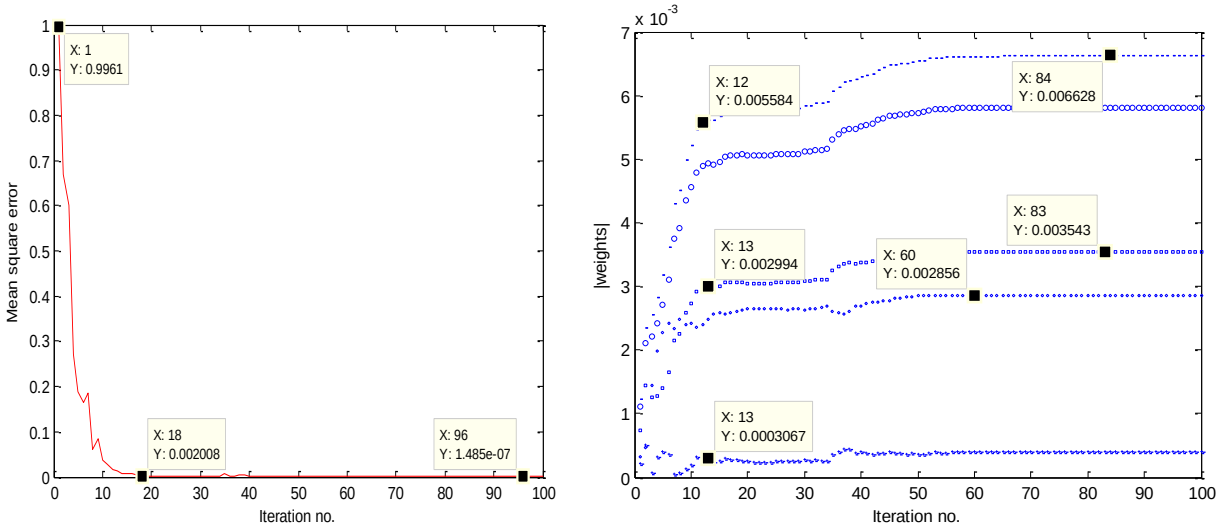

Figure 5.32 LMS *mean square error vs. Iteration.no (left). Weight vs. iteration.no (right) at 19.5GHz by 150 element and 16(λ)*

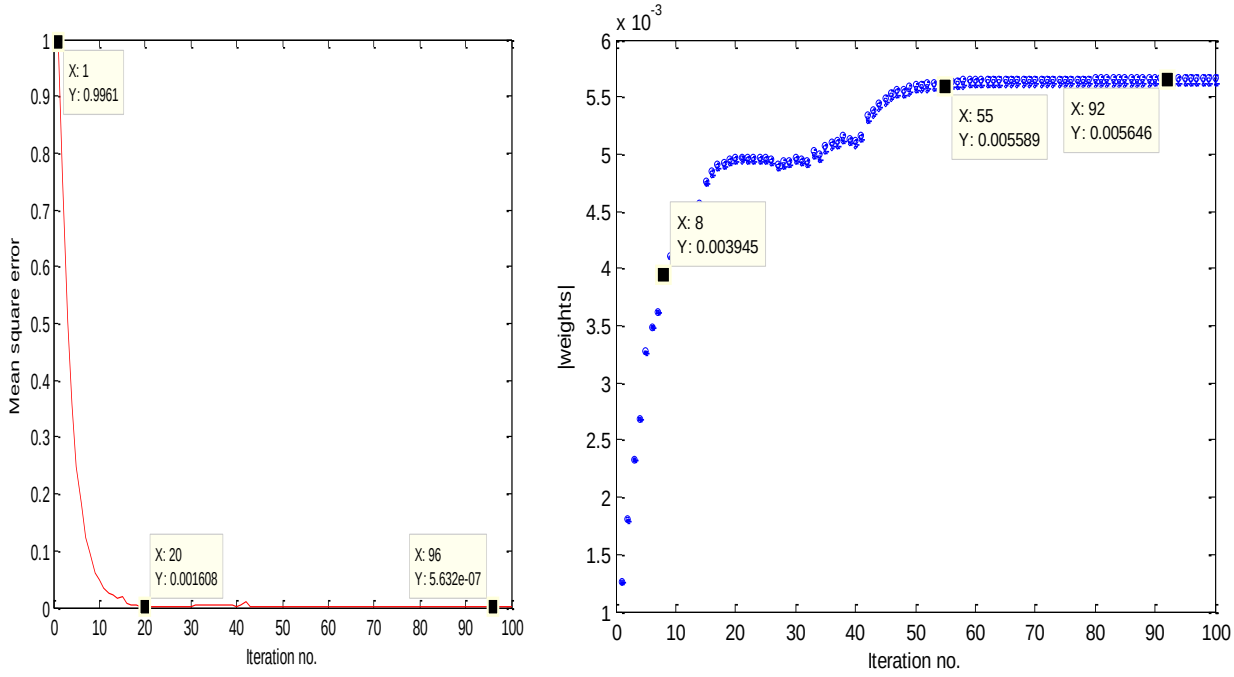

Figure 5.33 LMS *mean square error vs. Iteration.no (left). Weight vs. iteration.no (right) at 19.5GHz by 150 element and 0.5(λ)*

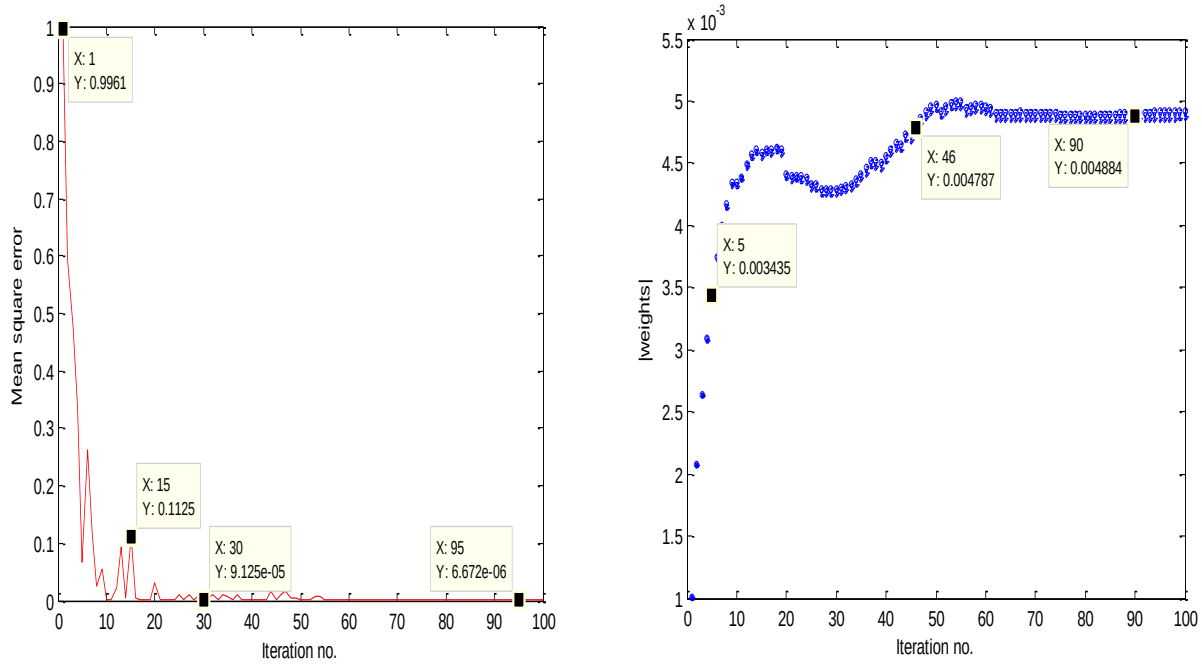

Figure 5-34 LMS *mean square error vs. Iteration.no (left). Weight vs. iteration.no (right) at 19.5GHz by 200 element and 0.5(λ)*

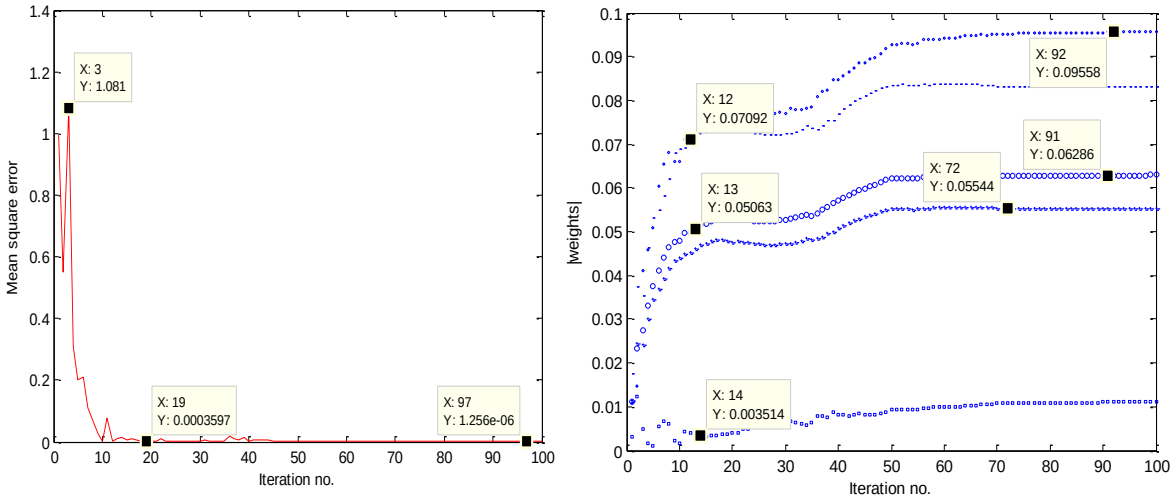

Figure 5.35 LMS *mean square error vs.Iteration.no (left).Weight vs.iteration.no (right) at 19.5GHz by 10 element and 16(λ).*

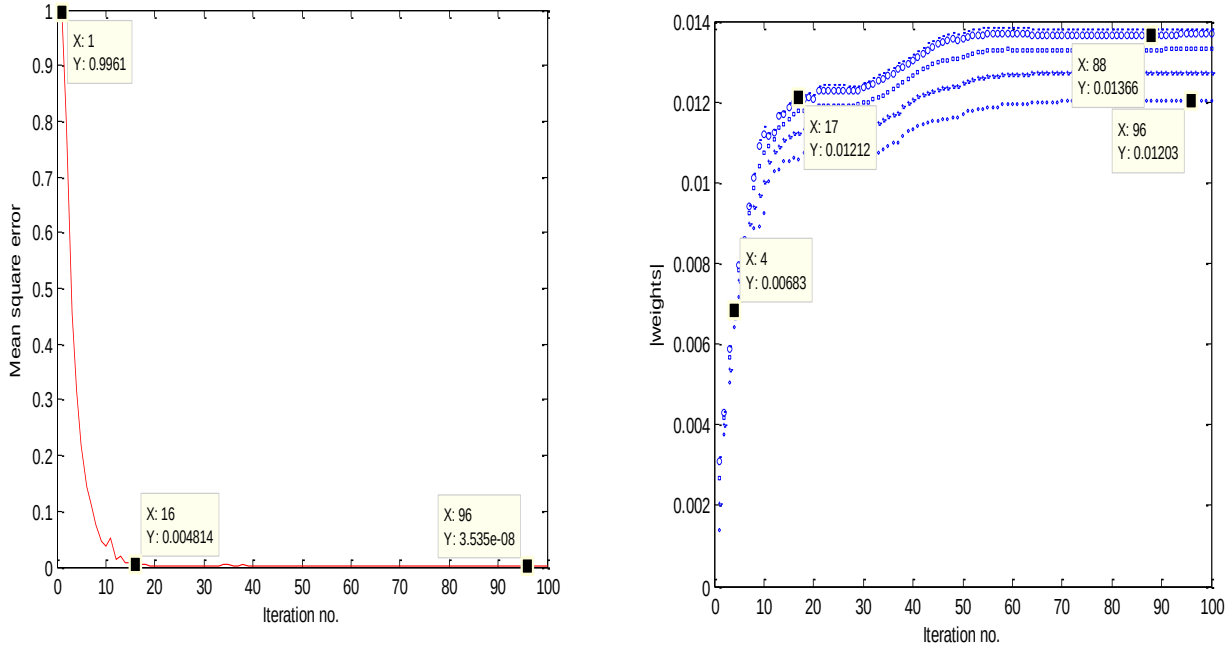

Figure 5-36 LMS *mean square error vs. Iteration.no (left). Weight vs. iteration.no (right) at 19.5GHz by 75 element and 2(λ).*

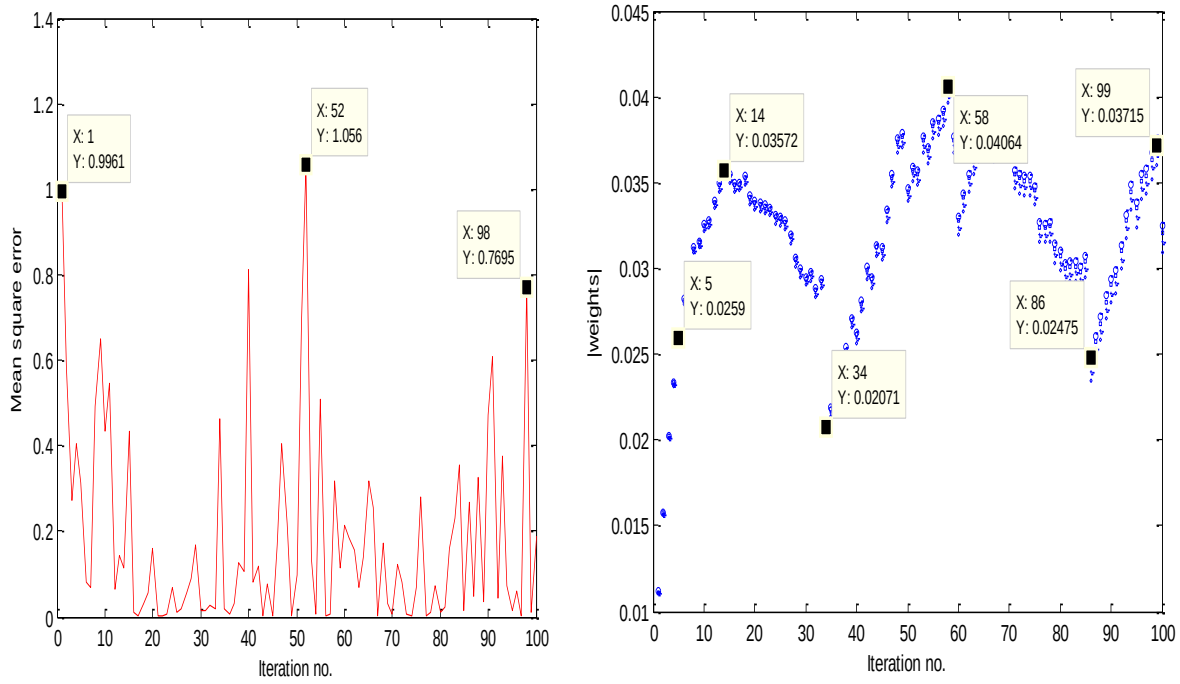

Figure 5.37 LMS *mean square error vs. Iteration.no (left). Weight vs. iteration.no (right) at 19.5GHz by 10 element and 0.5(λ)*

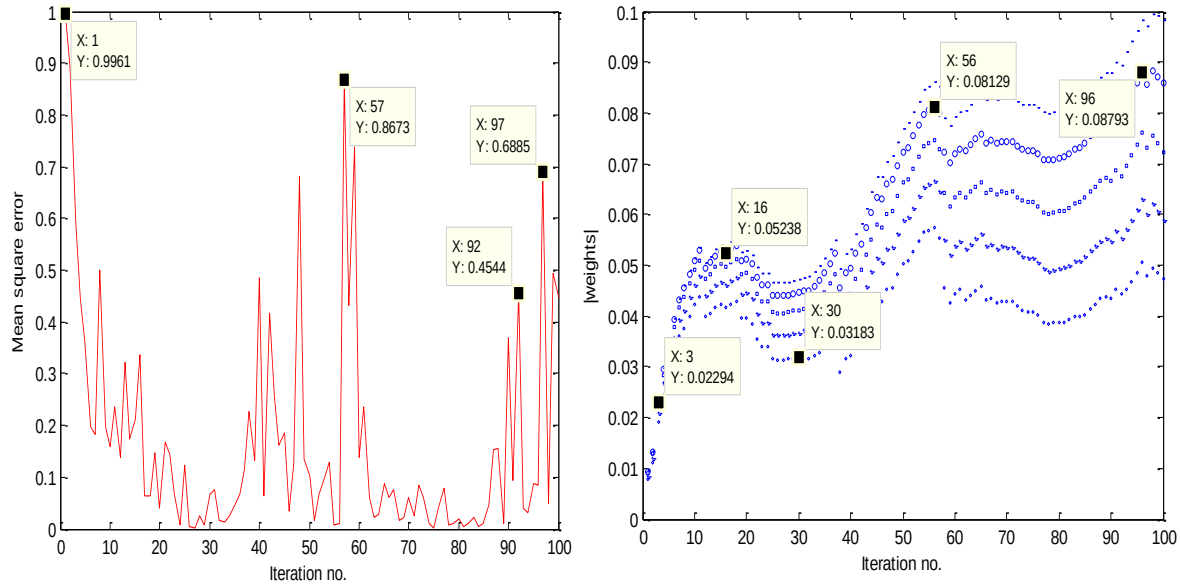

Figure 5.38 LMS *mean square error vs. Iteration.no (left). Weight vs. iteration.no (right) at 19.5GHz by 10 element and 2(λ)*

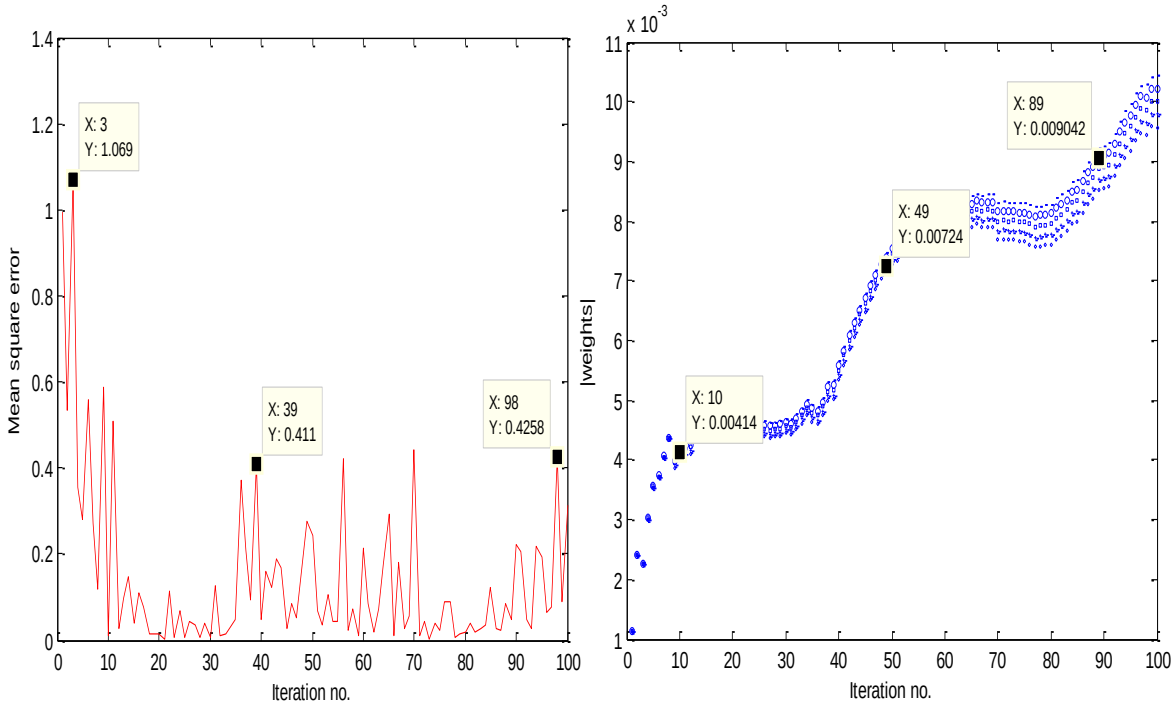

Figure 5-39 LMS *mean square error vs. Iteration.no (left). Weight vs. iteration.no (right) at 19.5GHz by 75 element and 0.5(λ)*

Table (5.9) Summary of MSE vs. array configuration by LMS beamformer to track two Iridium satellites

Performance	No. Element	spacing	Iteration	MSE
Best	150	16 λ	18 to 96	0.002 to $1.4 * 10^{-07}$
	150	0.5 λ	20 to 96	0.0016 to $5.6*10^{-07}$
Optimal	200	0.5 λ	15 to 95	0.1 to $6.6*10^{-06}$
	10	16 λ	19 to 97	0.0003 to $1.25*10^{-06}$
	75	2 λ	16 to 96	0.004 to $3.5*10^{-8}$
Worst	10	0.5 λ	98	0.769
	10	2 λ	97	0.68
	75	0.5 λ	98	0.42

II. RLS array element weighting convergence

Two Iridium satellite tracking, array element weighting convergence by RLS adaptive beamformer has presented below, and illustrated in the following figures. The weighting process is simulated to the maximum number of element in the array. The best array configuration of RLS beamformer such as the 75 by 16 λ, 10 by 8 λ and 10 by 2 λ have also revealed their best performance in the weighting process.

It is necessary to note that, in the below figures, the weighting convergence behavior has harmonized with the result presented on the performance investigation of the adaptive beamformer. For example, the array configuration i.e. the 75 by 16 λ in Figure 5.42 has the best performance and the beamformer has array output SINR of 48dB within the iteration interval of

(9^{th} – 49^{th}). The summary of two satellite tracking, weighting convergence by RLS adaptive algorithm has presented in Table (5.10) below.

Table (5.10) Summary of array configuration vs. elements weight by RLS to track two Iridium satellites

Performance	No. Element	spacing	Iteration	weight
Best	10	2 λ	9 to 49	0.09 – 0.11
	10	8 λ	14 to 49	0.06 – 0.085
	75	16 λ	9 to 49	0.06 – 0.08
Optimal	10	16 λ	15 to 50	0.018 – 0.006
	10	0.5 λ	10 to 45	0.05 – 2.08
Not practical	75	2 λ	1 to 10	0 - diverged
	75	0.5 λ	1 to 15	0 - diverged
	75	8 λ	1 to 15	0 - diverged
Not practical	150	2 λ	1 to 10	0 - diverged
	150	8 λ	1 to 15	0 - diverged
	150	16 λ	1 to 49	0 - diverged

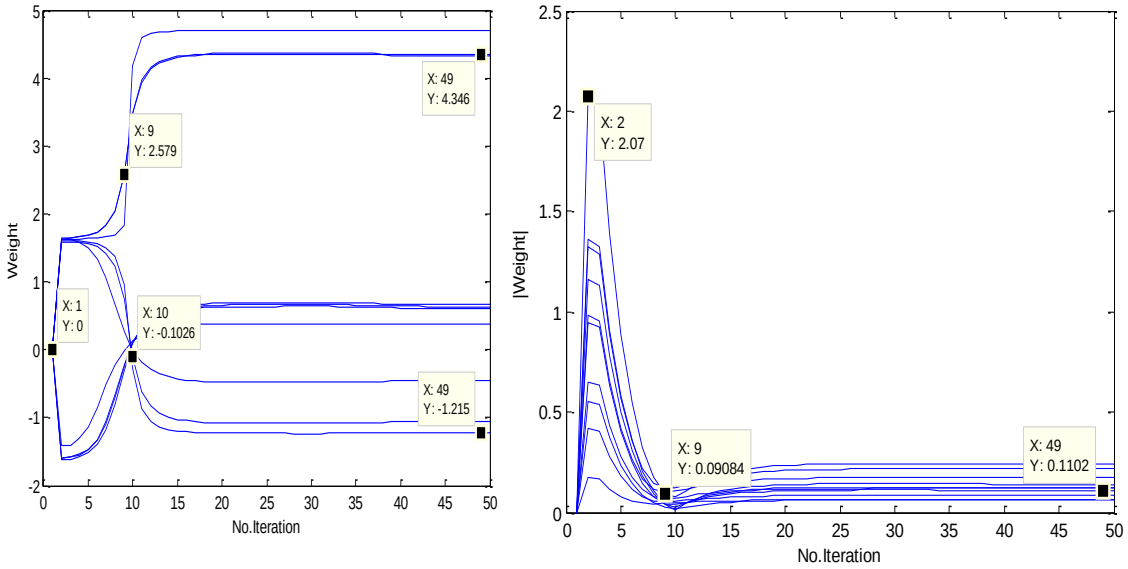

Figure [5.40] RLS *weight vs. Iteration.no (left).* |Weight| *vs. iteration.no (right) at 19.5GHz by 10 element and 8(λ).*

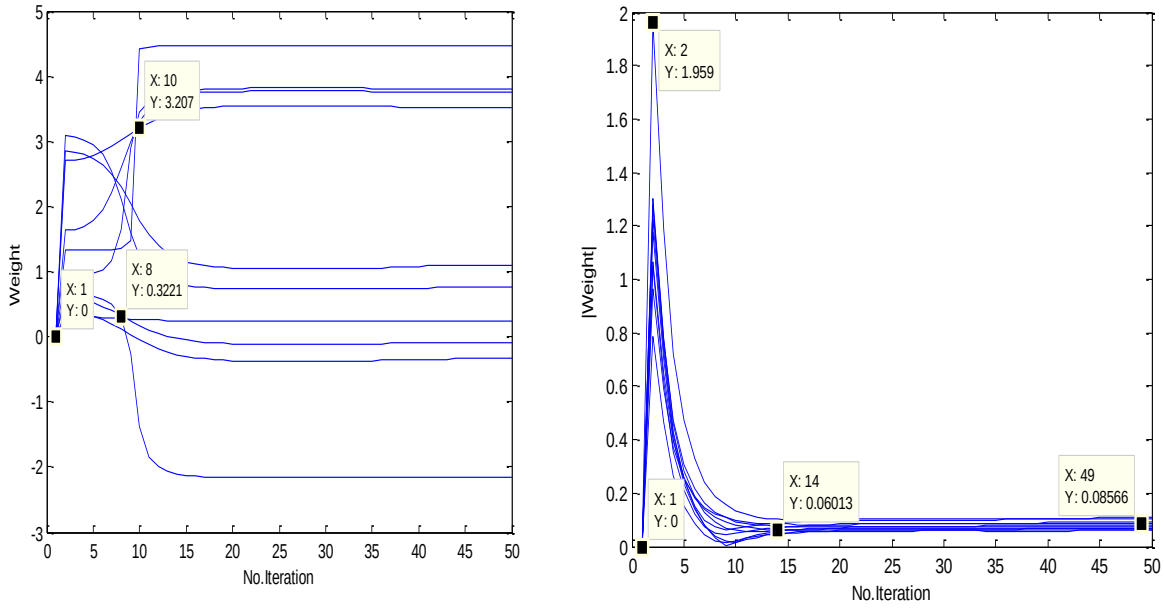

Figure [5.41] RLS *weight vs. Iteration.no (left).* |Weight| *vs. iteration.no (right) at 19.5GHz by 10 element and 8(λ).*

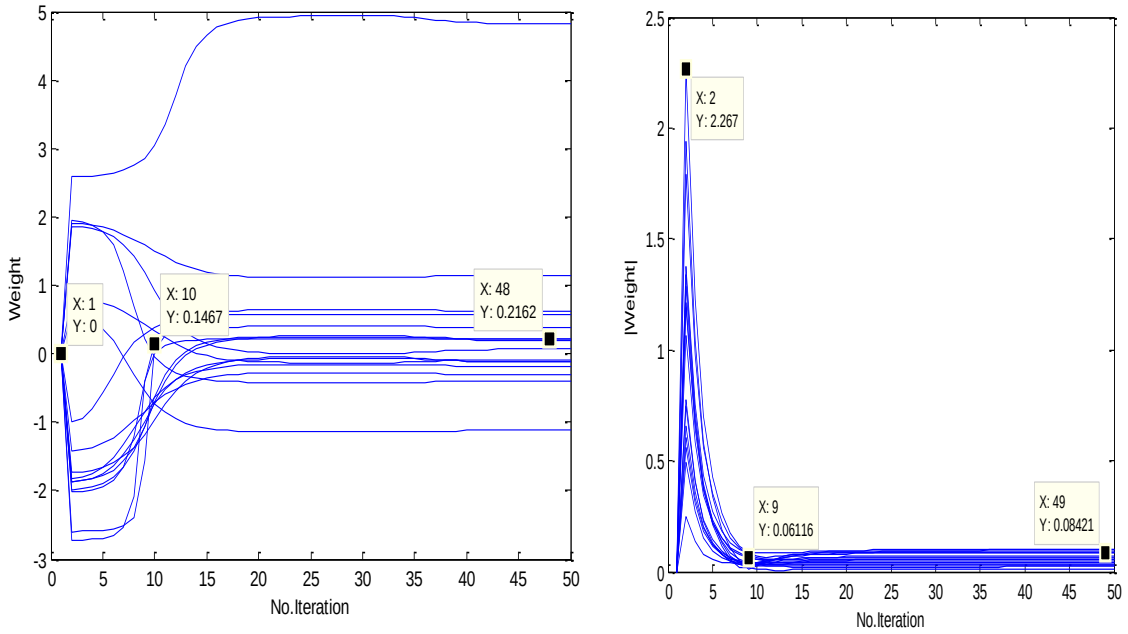

Figure [5-42] RLS *weight vs. Iteration.no (left).* |Weight| *vs. iteration.no (right) at 19.5GHz by 75 element and 16(λ).*

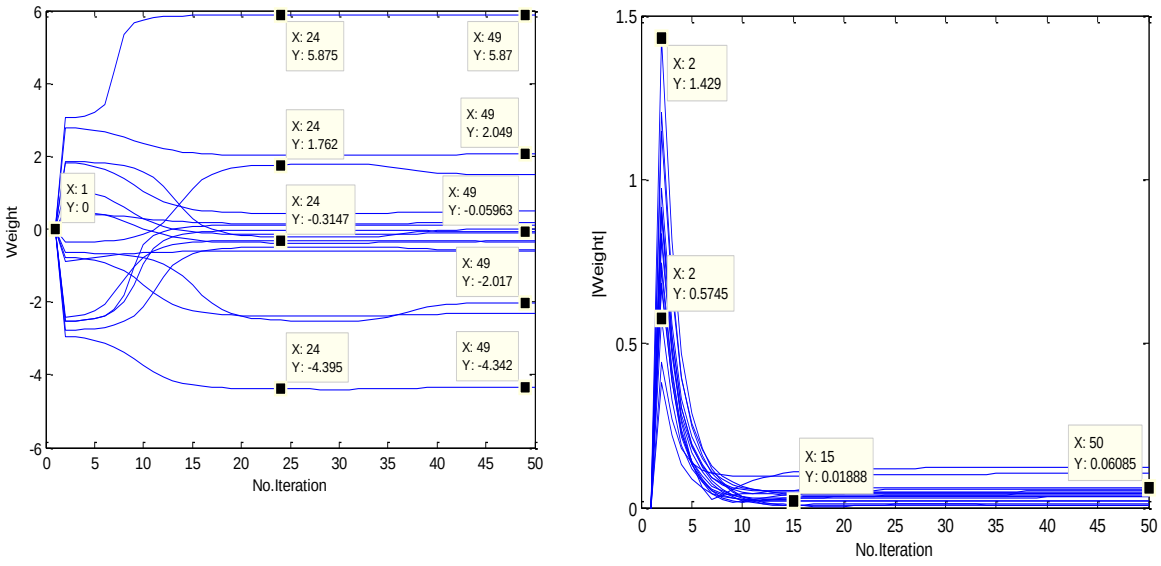

Figure [5.43] RLS *weight vs. Iteration.no (left).* |Weight| *vs. iteration.no (right) at 19.5GHz by 10 element and 16(λ).*

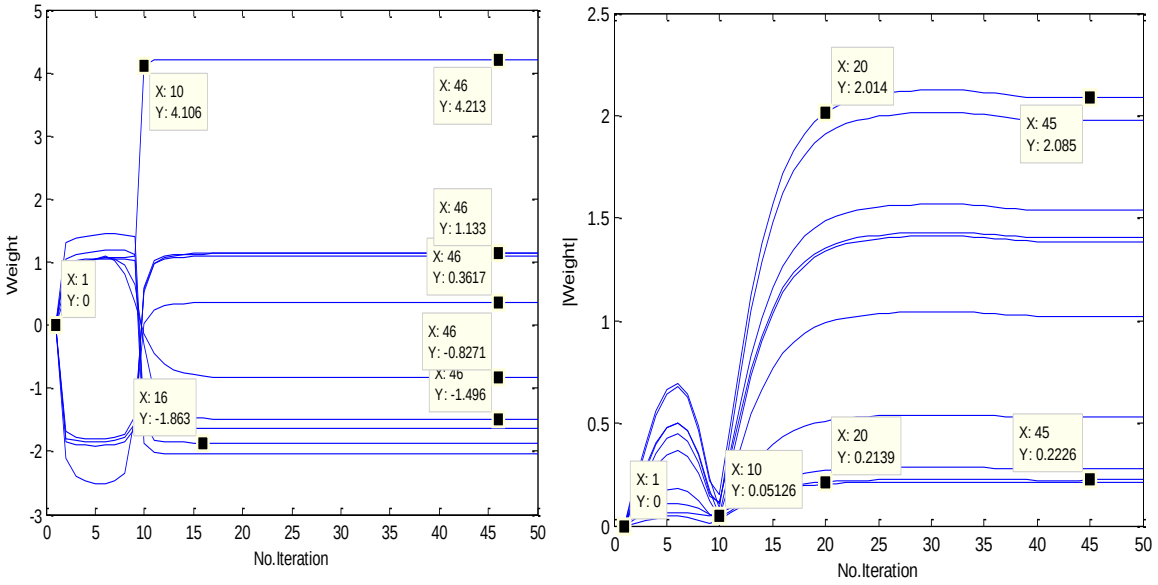

Figure [5.44] RLS *weight vs. Iteration.no (left).* |Weight| *vs. iteration.no (right) at 19.5GHz by 10 element and 0.5(λ).*

1.3 Simulation Case-2 (Global Star Satellite System)

In the second case of the simulation, the numerical analysis to compute the AOA of two Global Star Satellites have been performed. Then computed the AOA result have been used in the simulation. By using the Global Star satellite constellation and operating frequency data, which are given in the summary Table (5.11) with the computed AOA data, then the input data such as downlink beacon signal characteristics and tracking antenna array has configured and used to perform the simulation to investigate LMS and LS – CMA, respectively.

The Interference nulling and beacon tracking performance of LMS at 5GHz for different AOA from two target Global Star satellites and one interferer have been shown in the Part A of the simulation. Similarly, of the LS - CMA are shown in the Part B of the simulation. Finally, the comparison of LMS with LS - CMA based on interferer nulling level (dB), beam pointing accuracy towards the targets and the array output SINR have been shown in Table (5.17).

Table (5.13) Summary of key characteristics of Global star satellites system used in simulation

Characteristics	**value or comments**
Orbital Altitude	1,401 km at LEO
Orbital geometry	52^0 inclination
Constellation	Walker Delta
Number of orbits	6
Number of satellites per orbit	8
Coverage latitude and longitude	latitude up to about 70^0
Total Number of satellites	48
No. Beams per satellite (Phased array antenna)	48 at L – band, Earth to Space
Gateway downlinks	5 GHz
Gateway uplinks	7 GHz

5.3.1 Two Global Star satellites orbital element and computed the AOA.

Table 5.14 Orbital element value of the first and second satellite with the computed AOA at 3 different instant.

Target	Major axis (km)	eccentricity	Inclination	$M_1(t_0)$	$E_1(t_0)$	$g_1(t_0)$	$\phi_{az1}(t_0)$
Sat_1	*7779*	*0.0003*	52^0	0^0	0^0	0	0^0
Target	Major axis (Km)	eccentricity	Inclination	$M_2(t_0)$	$E_2(t_0)$	$g_2(t_0)$	$\phi_{az2}(t_0)$
Sat_2	*7779*	*0.0003*	52^0	9.9999^0	10^0	0.1764	46.5309^0
Target	Major axis (Km)	eccentricity	Inclination	$M_1(t_1)$	$E_1(t_1)$	$g_1(t_1)$	$\phi_{az1}(t_1)$
Sat_1	*7779*	*0.0003*	52^0	5.0000^0	5^0	0.0875	26.3454^0
Target	Major axis(Km)	eccentricity	Inclination	$M_1(t_2)$	$E_1(t_2)$	$g_1(t_2)$	$\phi_{az1}(t_2)$
Sat_1	*7779*	*0.0003*	52^0	-4.9997^0	-5^0	-0.0878	-40.4397^0
Target	Major axis (Km)	eccentricity	Inclination	$M_2(t_1)$	$E_2(t_1)$	$g_2(t_1)$	$\phi_{az2}(t_1)$
Sat_2	*7779*	*0.0003*	52^0	14.9999^0	15^0	0.2680	60.6186^0
Target	Major axis Km)	eccentricity	Inclination	$M_2(t_2)$	$E_2(t_2)$	$g_2(t_2)$	$\phi_{az2}(t_2)$
Sat_2	*7779*	*0.0003*	52^0	-14.9999^0	-15^0	-0.2680	-60.6186^0

A. LMS adaptive algorithm simulation result.

Table (5.15) Global Star satellite tracking by LMS adaptive beamformer performance summary

Performance	No. Element	spacing	Output SINR(dB)	Null(dB)	Error$_1$	Error$_2$
Best	150	2 λ	56.9	-53.9	0.003	0.003
	200	2 λ	53.3	-50.4	0.01	0.03
Optimal	150	8 λ	48.8	-46	0.00	0.01
	10	8 λ	44.1	-41.9	0.03	0.003
	75	0.5 λ	43.9	-41.9	0.03	0.01
	75	16 λ	43.2	-40.9	0.004	0.09
Worst	10	0.5 λ	3.6	-1.01	0.04	0.02
Worst with a grating lobes	10	16 λ	-33.9794	36.5082	0.07	1.1
	200	16 λ	-40	39.2942	0.03	0.00
	75	16 λ	-40.9151	43.2033	0.004	0.09
	150	16 λ	-40	42.5691	0.02	0.03

By using LMS adaptive beamformer, the best array configuration to track two Global Star satellites at C – band Microwave spectrum are the 150 by 2 λ and 200 by 2 λ.The first best array configuration i.e.150 by 2 λ , as it is shown in Figure (5.45) yields array output SINR of 56.9dB and it nulls the interferer at a level of -53.9dB. This array configuration has a beam pointing accuracy of 0.003 towards the two satellites.

Similarly, the second best array configuration i.e. 200 by 2 λ, as it is shown in Figure (5.46) yields array output SINR of 53.3dB and nulls the interfere at a level of -50.45dB. This array

configuration has a beam pointing accuracy of 0.01 and 0.003 towards the first and the second satellite respectively.

The optimal array configuration i.e.150 by 8 λ , as it is shown in Figure (5.47) yields array output SINR of 48.8dB and it nulls the interferer at a level of -46dB. This array configuration has a beam pointing accuracy of 0.00 towards the first satellite and 0.001 towards the second satellite.

Array configurations such as 10 by 8 λ, 75 by 0.5 λ, 75 by 16 λ and 150 by 16 λ are also the optimal arrangement which can be used to track two Global Star satellites at 5GHz.

The worst case array configuration, by LMS adaptive beamformer, to track two Global star satellites at 5GHz is the 10 by 0.5 λ; which yields array output SINR of 3.6dB and its nulling level is almost -1.01dB which is an acceptable. Similarly, the array configurations such as 10 by 16 λ, 200 by 16 λ , 75 by 16 λ and 150 by 16 λ have poor performance since they have wasted the useful power through their grating lobes.

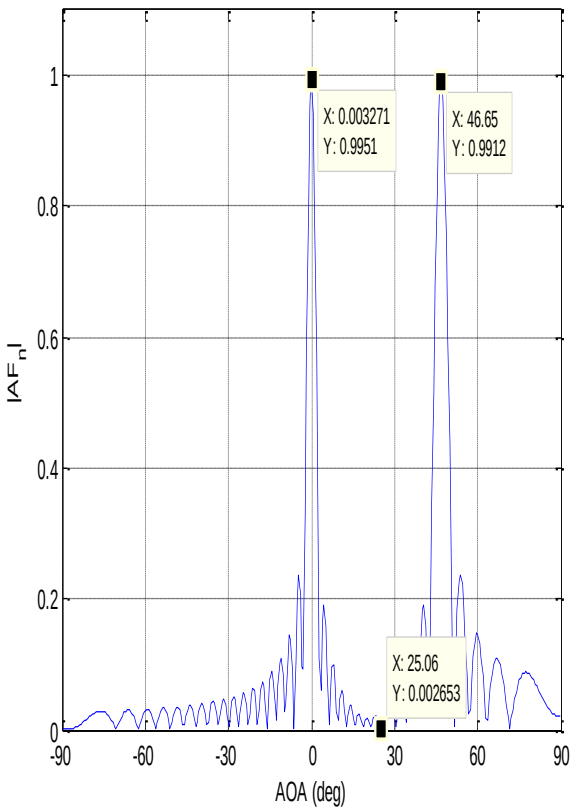

***Figure** (5.45) LMS two signals 150 by 2(λ) at 5 GHz.*

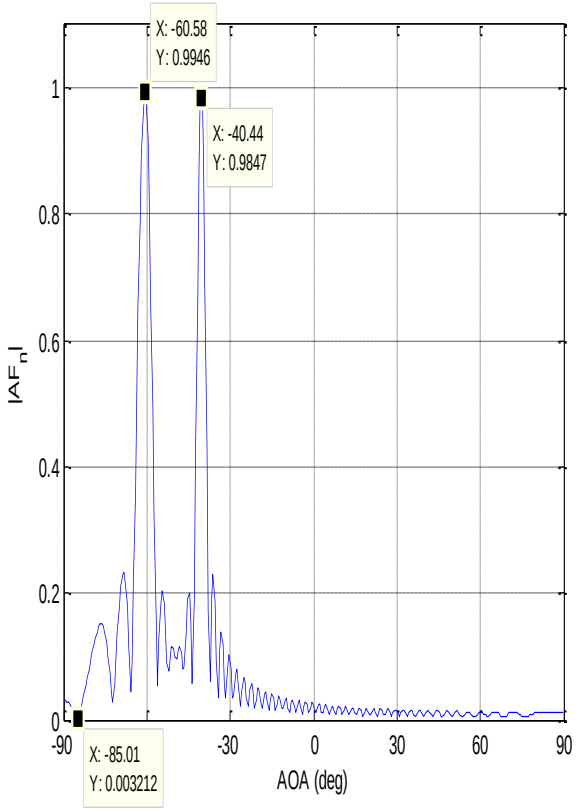

***Figure** (5.46) LMS two signals 200 by 2(λ).at 5 GHz.*

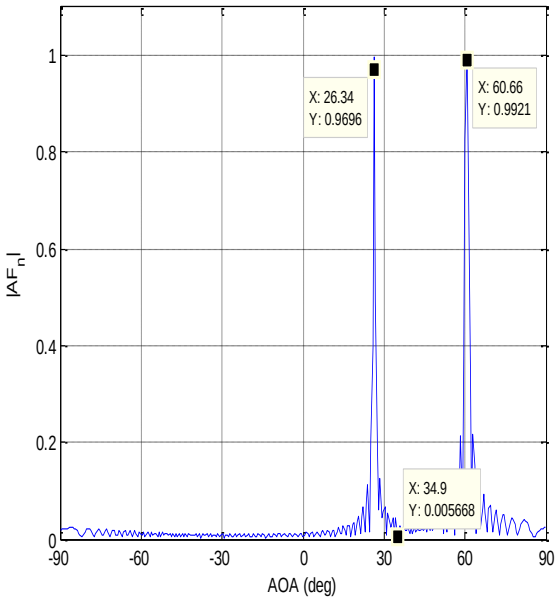

***Figure** (5.47) LMS two signals 150 by 8(λ) at 5 GHz.*

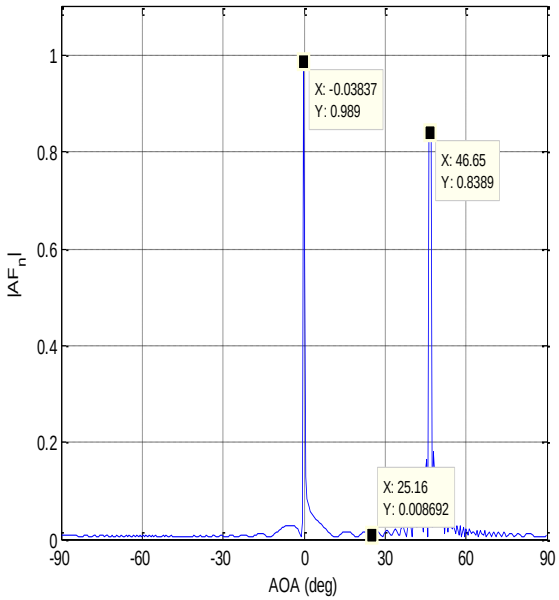

***Figure** (5.48) LMS two signals 200 by 8(λ) at 5 GHz.*

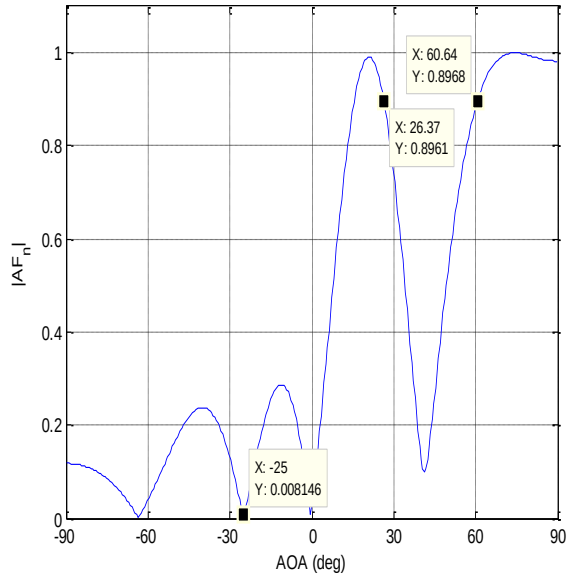

***Figure** (5.49) LMS two signals 75 by 0.5(λ) at 5 GHz.*

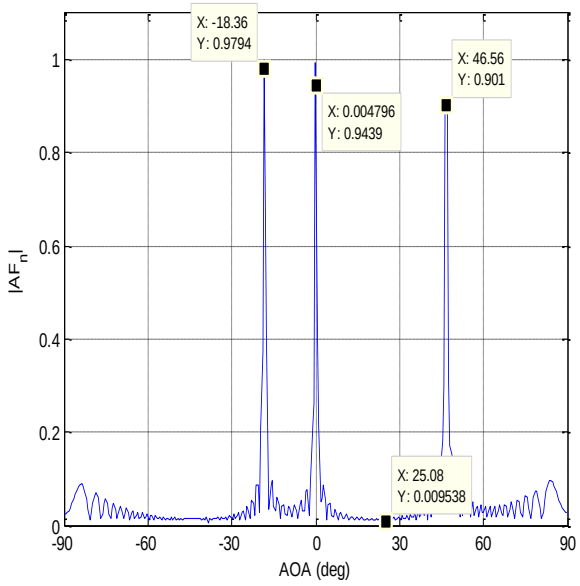

***Figure** (5.50) LMS two signals 75 by 16(λ) at 5 GHz.*

B. LS – CMA adaptive algorithm

By using LSCMA adaptive beamformer, the best array configuration to track two Global Star satellites at C – band Microwave spectrum are the 200 by 2 λ, 75 by 2 λ and 75 by 8 λ.The first best array configuration i.e.200 by 2 λ , as it is shown in Figure (5.51) yields array output SINR of 60.3dB and it nulls the interferers at a level of -60.9dB and -60dB. This array configuration has a beam pointing accuracies of 0.00 towards the first satellite and 0.01 towards the second satellite.

Similarly, the second best array configuration i.e. 75 by 2 λ, yield array output SINR of 55.9dB and nulls the interferes at a level of -53.9dB and -60dB. This array configuration has a beam pointing accuracy of 0.04 and 0.005 towards the first and the second satellite, respectively.

The optimal array configuration i.e.150 by 0.5 λ, yields array output SINR of 49.7dB and it nulls the interferers at a level of -47.9dB and -60dB. This array configuration has a beam pointing accuracy of 0.03 towards the first satellite and 0.02 towards the second satellite. Array configuration such as 200 by 8 λ is also the optimal arrangement which can be used to track two Global star satellites at 5GHz by using LSCMA adaptive beamformer.

The worst case array configuration, by LSCMA adaptive beamformer to track two Global star satellites at 5GHz are the 75 by 10 λ , 75 by 0.5 λ , 10 by 0.5 λ and 10 by 2 λ which yield array output SINR of 25.4dB, 20.5dB, 20.45dB and 20.4dB respectively. The results which are shown in Figure (5.53), Figure (5.54) and (Figure 5.55) have poor performance since they have wasted the useful power through their grating lobes.

Table (5.16) Global star satellite tracking by LSCMA adaptive beamformer performance summary

Performance	No. Element	spacing	Output SINR(dB)	Null1(dB)	Null2(dB)	$Error_1$	$Error_2$
Best	200	2 λ	60.3	-60.9	-60	0.00	0.01
	75	2 λ	55.9	-53.9	-60	0.04	0.05
	75	8 λ	55.8	-60	-53.9	0.03	0.06
Optimal	150	0.5 λ	49.7	-47.9	-60	0.03	0.02
	200	8 λ	48.07	-46	-60	0.04	0.02
Worst	75	10 λ	25.4	-23	-40	0.03	0.04
	10	0.5 λ	20.5	-20	-24	0.01	0.01
	75	0.5 λ	20.45	-40	-20.9	0.02	0.01
	10	2 λ	20.4	-46	-33.9	0.03	0.09

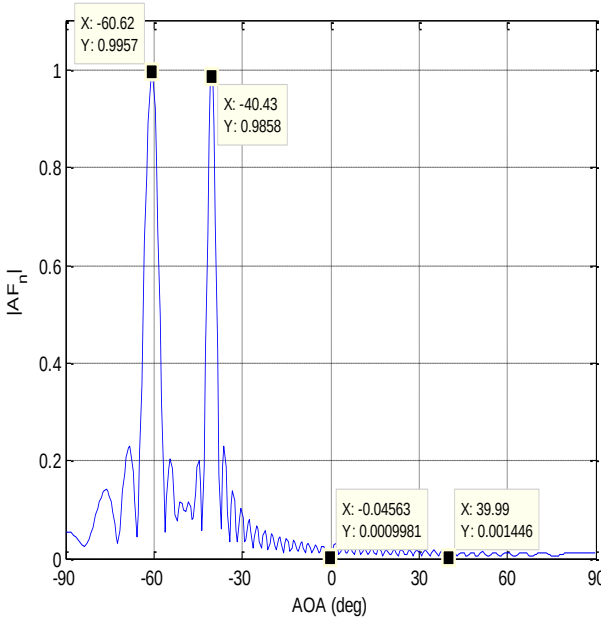

***Figure** (5.51) LSCMA two signals 75 by 8(λ) at 5 GHz.*

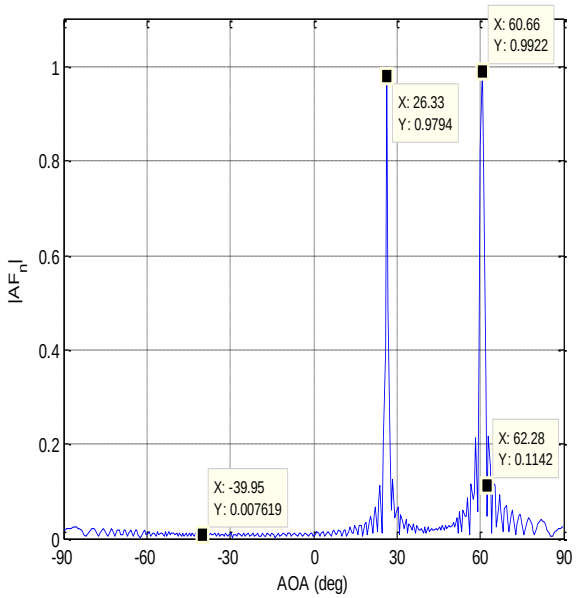

***Figure** (5.52) LSCMA two signals 150 by 8(λ) at 5 GHz.*

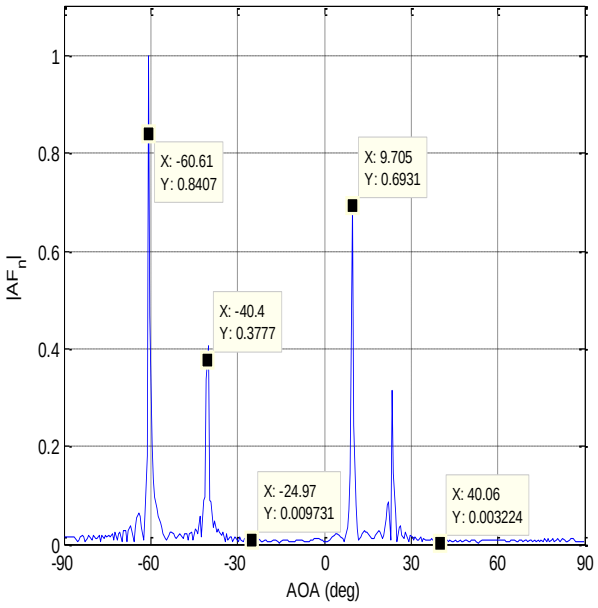

***Figure** (5.53) LSCMA two signals 200 by 16(λ)at 5 GHz.*

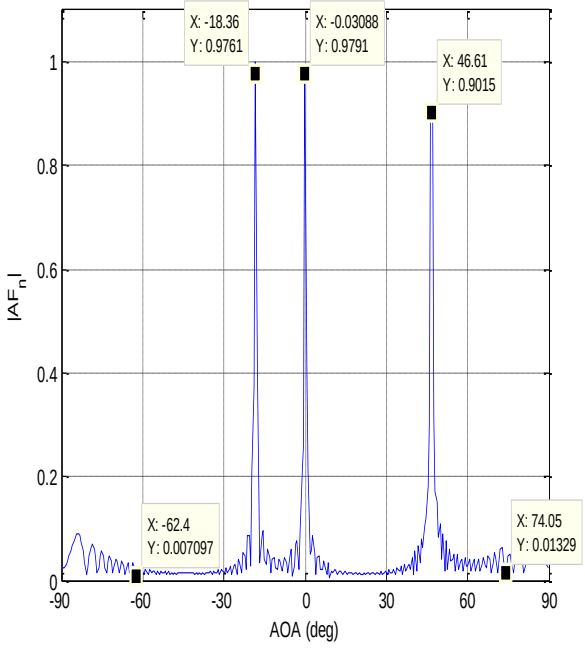

***Figure** (5.54) LSCMA two signals 75 by 16(λ) at 5 GHz.*

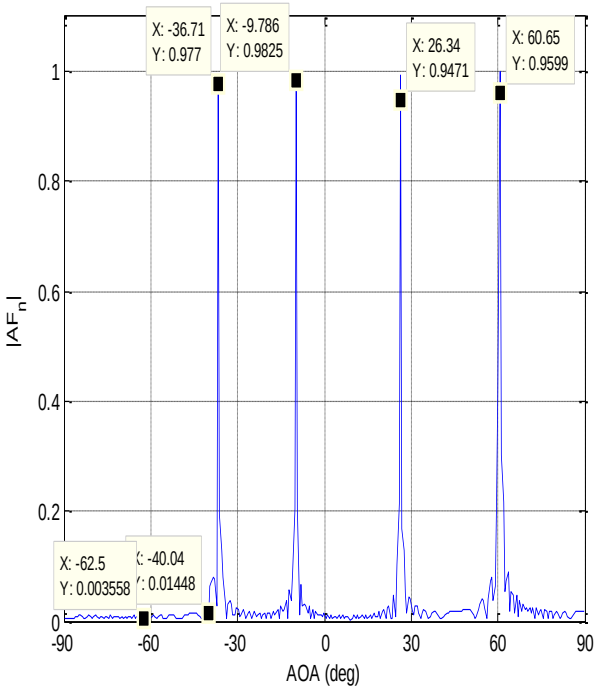

***Figure** (5.55) LSCMA two signals 150 by 16(λ) at 5 GHz.*

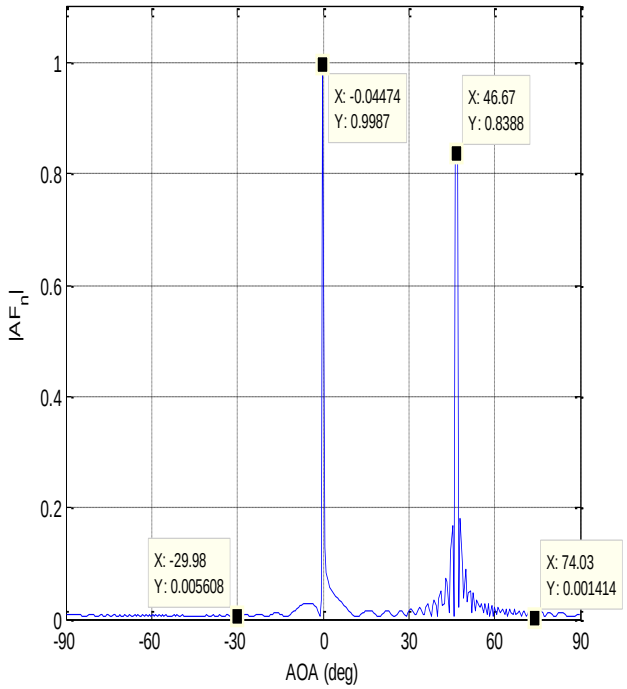

***Figure** (5.56) LSCMA two signals 200 by 8(λ) at 5 GHz.*

Table 5.17 Comparison LMS with LS – CMA for Global star satellites AOA

Array Configuration		LMS				LS – CMA				
		Interferer	Beam pointing Accuracy		Array output power	Interferer	Interferer	Beam pointing Accuracy		Array output power
No. element	Spacing	Nulling(dB)	$Error_1$	$Error_2$	SINR(dB)	nulling(dB)	Nulling(dB)	$Error_1$	$Error_2$	SINR(dB)
10	16(λ)	-33.9794	0.07	1.1	36.5082	-26.0206	-18.4164	0.04	0.03	20.4230
75	8(λ)	-31.7005	0.03	0.00	34.4467	-60	-53.9794	0.03	0.06	55.8017
150	2(λ)	-53.9794	0.003	0.003	56.9024	-30.4576	-60	0.0009	0.03	33.3758
200	0.5(λ)	-33.9794	0.01	0.04	36.6832	-44.4370	-30.4576	0.03	0.01	31.8976
10	0.5(λ)	-1.0122	0.04	0.02	3.6698	-20	-24.4370	0.01	0.01	20.5322
75	2(λ)	-37.7211	0.04	0.06	40.6441	-53.9794	-60	0.04	0.05	55.9772
150	8(λ)	-46.0206	0.00	0.01	48.8120	-41.9382	-43.0980	0.01	0.01	42.3045
200	16(λ)	-40	0.03	0.00	39.2942	-40.9151	-50.4576	0.03	0.00	39.7133
10	2(λ)	-24.4370	0.02	0.01	25.5794	-46.0206	-33.9794	0.03	0.09	36.3275
75	16(λ)	-40.9151	0.004	0.09	43.2033	-23.0980	-40	0.03	0.04	25.4429
150	16(λ)	-40	0.02	0.03	42.5691	-50.4576	-40	0.00	0.00	42.1448
200	2(λ)	-50.4576	0.01	0.03	53.3367	-60.9151	-60	0.00	0.01	60.3024
10	8(λ)	-40	0.04	0.01	42.7476	-40	-33.9794	0.04	0.00	35.9337
75	0.5(λ)	-41.9382	0.03	0.01	43.9363	-26.0206	-18.4164	0.02	0.01	20.4551
150	0.5(λ)	-33.9794	0.02	0.00	36.0746	-60	-53.9794	0.03	0.02	49.7907
200	8(λ)	-41.9382	0.03	0.003	44.1112	-30.4576	-60	0.04	0.02	48.0748

Chapter Six

Conclusion and recommendation for future work

6.1 Summary

In this thesis, a detail investigation of adaptive phased antenna and satellite constellation theories have been performed. In the adaptive phased antenna section, the two essential functional blocks of the digital signal processor which are the AOA estimator and the adaptive beamformer along with their adaptive beamforming algorithms have been used to track two satellites' signals within Ka and C – band microwave frequency spectrum.

In the section of satellite constellation, the ground TTC and M station mathematical modeling, by taking a polar satellite orbit into account, and along with the assumption that regards the deployment of the tracking adaptive phased antenna exactly at the sub – satellite point have been performed. This TTC and M mathematical modeling is used in order to derive a formula which is used to compute the AOA of the signals from two target satellites' in the LoS directions.

In the simulation, we have used the computed AOA from two target satellites along with the 16 different array element number and spacing combination as an input. This combined data have been used to simulate two target satellites' signals tracking by single TTC and M station located at the sub – satellite point. Then the simulation result of the 16 different array configurations for LMS, SMI, RLS and LS – CMA adaptive algorithms within microwave frequency spectrum have been performed.

Finally, the signal tracking performance, interferer nulling ability, the phased array output SINR and beampointing accuracy towards the targets of each adaptive beamformer have been presented and used as a conclusion to verify the ability of phased array antenna in tracking multiple moving satellites by single TTC and M station.

6.2 Conclusion

Based on the mathematical modeling analysis in Chapter four; the angle of arrival of the beacon signals in the line of sight direction, which are coming from the target satellites have been computed. In addition the observation on the simulation result shows us that the number of element and spacing in the antenna array have effects on the pattern formed by the adaptive algorithms.

In addition, from the simulation result of case 1, we have concluded that the tracking performance of the phased array system depends on antenna element number and spacing. That is to operate at 16.5GHz or Ka – band microwave spectrum the maximum antenna spacing is about sixteen times the wave length given that the antenna element is held at minimum value of 10. Whereas to make the antenna element spacing to half of the wavelength then the number of antenna element should be increased to a maximum of 20 times more elements than that of the phased array system which is simulated for larger spacing.

At C – band frequency spectrum, which is the downlink operating band of the global star satellite, the adaptive phase array antenna, by controlling its element number and spacing and by using LMS and LSCMA adaptive beamformer can track two Global Star satellites, and its performance has been shown in the simulation result of the previous section.

In addition, from the simulation result of case 2, we have concluded that, the tracking performance of the phased array system depends on the element number and spacing just like Case 1. Generally, in adaptive phased array antenna by controlling the inter element spacing and array number, it is also possible to track multiple moving Global Star Satellites which are working within microwave frequency spectrum like C – band.

As a general conclusion for the two cases, in adaptive phased array antenna by controlling the inter element spacing and array number, it is possible to track multiple moving satellites which are working within microwave frequency spectrum like C – band and Ka – band.

6.3 Recommendations for future Work

In this thesis, the initial condition to verify the adaptive tracking capability of the phased array antenna is performed by assuming the ground station is exactly located on the sub satellite point. That means the antenna bore sight elevation angle is zero or the satellites orbital inclination $i = 90^0$, therefore for future work the research can be further investigated by setting the elevation angle at some angular constant value $\theta_{el} \neq 0^0$ or orbital inclination $i \neq 90^0$. In such a case the array lattice and the adaptive signal processing algorithm will become two dimensional.

In addition, the initial assumption in this thesis has been set by suppressing the Doppler shift and array coupling effect. So that the research can also be further investigated by taking the Doppler shift and array element coupling effects into account.

The analytical and simulation result analysis of the beam pointing accuracy of the phased array system have not been performed. So the research can be further investigated by proposing a solution to increase the pointing accuracy of the antenna array system. Generally, the research can be broadened by considering different wireless communication parameters in the uplink and downlink channels.

6.4 Recommendations

Satellite tracking method in the present and earlier time involves rotating large dish antenna towards the target. This method of tracking is prone to errors, which is induced from wind vibration and system deterioration. It is also applicable to only single target tracking. Therefore, as it is verified in this thesis adaptive phased array antenna, which involves the AOA estimator and the adaptive beamformer can easily track multiple moving satellites on non – geosynchronous orbit.

Therefore, we recommend to replace large dish antenna by the adaptive phased array antenna system as an effective method of multiple satellites/spacecraft tracking.

References

[1]. G. J. Hawkins, D. J. Edwards, Prof. J. P. McGeehan, "Tracking systems for satellite communications." *IEE Proc.*, Vol. 135, pt. F. No.5, Oct. 1988.

[2]. Lal Chand Godara, "Smart Antennas." Boca Raton, Florida: *CRC press*, 2004, pp. 67 – 80.

[3]. Frank B. Gross, "Smart antenna for wireless communications." USA: *McGraw*, 2005 pp.169 –252.

[4]. Naftali (Tuli) Herscovic, Christas Christodoul, "Smart Antennas." *IEEE Antenna and propagation Magazine*, Vol. 42, No. 3, June 2000.

[5]. Fahad Alradday, "Steering Vector and Interference Cancellation of Two – Dimensional Arrays."*International Journal of Advanced Research in computer Engineering and Technology (IJARCET)* Vol.3, Issue 11, Nov.2014.

[6]. Amara Prakasa Rao, N.V.S.N. Sarma, "Adaptive Beamforming Algorithms for Smart Antenna Systems." *WSEAS Transactions on Communications*, Vol. 13, 2014.

[7]. Muhammad Amir Shafiq Ejaz and Ahmed, "Real Time Implementation of Adaptive Beamformer for Phased Array Radar over DSP kit." *International Journal of Signal processing* (SPU), Vol.1, 2013.

[8]. L.E. Brennan, "Angular Accuracy of a Phased Array Radar." *U.S. Air force project Rand Research Memorandum* RM – 2467 October 22, 1959.

[9]. Constantine A. Balanis, "Antenna Theory Analysis and Design." USA: *A. John Wiley and Sons Inc.*, 2005 pp. 27 – 108, 2005, Third edition.

[10]. Sangeeta kaboj, and Dr. Ratna Dahiya, "Adaptive Antenna Array for Satellite Communication Systems." *Proceedings of the International Multi – Conference of Engineering and Computer Scientists'* vol.2, IMECS 2008, 19 – 21 March, 2008, Hong Kong.

[11]. Michael O. Kolawole, "Satellite Communication Engineering." New York: *Marcel Deker*, Inc. 2002, pp. 32- 45.

[12]. Bruce R. Elbert, "The Satellite Communication Ground Segment and Earth Station Handbook. "Boston. London: *Artech House Inc*. 2001.

[13]. M. B Narrollahnejad, S. Arabi Nowdeh, Y. Mokhtari and P. Moharlooet, "LEO Satellite Tracking using Monopulse." *Middle – East Journal of Scientific Research*, *IDDSI publications*, 2012.

[14]. B. Atrouz, A. Alimohad, B. Aissa, "An effective Jammers Cancellation by means of a Rectangular Array Antenna and a sequence block LMS Algorithm: case of mobile sources." *Progress in Electromagnetics Research,* Vol.7, 193 – 207, and 2009.

[15]. D. K Yeomans and P. W. Chodas, G. Sitarski, S. Szutowicz, and M. Krolikowska,"Cometary Orbit Determination and Non-Gravitational Forces." Jet propulsion laboratory/California Institute of Technology, *Space Research center of the polish Academy of science*.

[16]. Herve Lebret and Stephen Boyd, "Antenna Pattern Synthesis via Convex Optimization." *IEEE Transactions on Signal Processing* vol.45, No. 3, March 1997.

[17]. Professor Simon Haykin, Dr. John Litva, Dr. Terence J. Shephered," Radar Array Processing." Berlin Heidelberg: s*pringer* - Verlag, 1993, first edition, 1993.

[18]. Gerd Sommerkom, Dirk Hampicke, Ralf klukas, Adreas Richter Alex Schneider Reiner Thoma, " Uniform rectangular Antenna Array Design and Calibration Issues for 2- D ESPRIT Application." *EPMCC* 2001 Venna, February 20 -22, 2001.

[19]. Constantine A. Balanis, "Introduction to Smart Antenna." Lecture#5, *Morgan and Claypool*, 2007.

[20]. Taylor and Francis Group, LLC," Radar Signal Analysis and Processing using MATLAB." 2009

[21]. S. F Shaukat, Mukhtar Hassani, R. Farooq, H.U Saeed and Z. Saleem. "Sequential Studies of Beamforming Algorithms for Smart Antenna Systems." *World Applied science Journal*, 2009

[22]. Kristine L. Bell, Yaris Ephraim, Fellow, IEEE, and Harry L. Van Trees, Life Fellow, IEEE, "A Bayesian Approach to Robust Adaptive Beamforming. "*IEEE Transactions on Signal Proc*., Vol.48 Feb. 2000.

[23]. R. Jain and G S. Mani," Dynamic Thinning of Antenna Array Using Genetic Algorithm." *Progress in*

[24]. Bruce R. Elbert," The Satellite communication Applications Handbook." Boston. London: *Artech House Inc.* 2^{nd} edition, 2004.

[25]. Soung Sub Lee, "Dynamic and Control of Satellite Relative Motion: Design and Applications." *PhD. Dissertation* March 20, 2009 Blacks Burg, Virginia.

[26]. R. Raol, N.K. Sinha, Member IEEE, "On the Orbit Determination Problem." *IEEE Transactions on Aerospace and Electronics Systems* Vol. ACS – 21, No 3 May 1985. *Electromagnetic research* B, vol.32, 1-20, and 2011.

[27]. Amarnadh polur, Ashish kumar, "Beam Steering in Smart Antenna by using low complex Adaptive Algorithm." *International Journal of Research in Engineering Technology*. Vol. 02, 2013.

[28]. Dr. Lyoyd Wood, "Introduction to Satellite Constellations." Guest lecture, *Isu* session July 2006.

[29]. Marina Ruggier; Mauro De Sanctis, Tommasu Rossi, Marco Lucente, Daniele Mortari, Christian Bruccolen, Pietro Salvini, Valerio Nicolai," The Flower Constellation Set and its Possible Applications Final Report." *ESA Research* Fellow/Technical Officer Dario Izzo. Vol. 44, July, 2008.

[30]. K. Strong," Earth Observation from Space." *Sydney.edu.au/engineering/aeomech*.

[31]. Adrian Jaggi," Satellite Orbit Determination." *Astronomical Institute University of Bern*.

[32]. Theresa W. beech and Genevlive Dutruel – Lecohier, "A study of Three Satellite Constellation Design Algorithms." Madrid, Spain, *Calle Issac Newton* 11, PTM – Tres Cantos, 28760.

[33]. Koteswara Rao. Thokala Chjana Prakash, "Steering an Adaptive Antenna Array by LMS, NLMS and BBNLMS Algorithms." *Global Journal of Advanced Engineering Technologies*, Vol.1 – Issue 3 – 2012.

[34]. Leiwang," Array Signal Processing Algorithms for Beamforming and Direction finding." *Communications Research Group Department of Electronics*, University of York, December 2009.

[35]. Ravati Joshi, AshwiniKumar Dhande, "Adaptive Beamforming using LMS Algorithm", Vol.03, *IJRET*, Issue 05 May 2014.

[36]. Daniele Mortari, IEEE, and Mathew P. Wilkins, "The Flower Constellation set Theory Part1." *IEEE Transactions on Aerospace and Electronics*, 2008.

[37]. V. Y. Lo, "Ka – Band Monopulse Antenna – Pointing Systems Analysis and Simulation." *TDA progress Report* 42 – 124, *Communications systems and Research Section*, February 15, 1996.

[38]. Eran Fisher, Member, IEEE, Alexander Haimovich, Senior Member, IEEE, Ricks. Blum, Fellow, IEEE, Leonard J Cimini, Jr. Fellow, IEEE, Dmitry Chizhik, and Reinado A. Valenzuela, Fellow IEEE, "Spatial Diversity in Radars – Models and Detection Performance." *IEEE transactions on Signal Processing*, Vol.54 No.3 March 2006.

[39]. Jerome R. Vetter, "Fifty years of Orbit Determination: Development of Modern Astrodynamics Methods." *John Hopkins Apl. Technical Digest*, Volume 27, November 3, 2007.

[40]. Viktor Zaharov, Angel Gonzalez, James Acosta and Marvi, "Implementing a Vector RLS

Smart Antenna Beamformer using Xilinx system Generator. "*IEEE*, Feb 5-7. 2007

[41]. Dean D. Howard, "Radar Handbook." Locas. Inc., *Kaman corp*. page 18.1 – 18.25.

[42]. Klaus Hugi, Juha Laurila, Erns Bonek, "Smart Antenna a Downlink Beamforming for uncorrelated Communication Links." *European space Agency* 2000.

[43]. Hervi Lebret and Stephen Byd, "Antenna Array Pattern Synthesis via Convex Optimization." *IEEE Transactions on Signal Processing*, Vol.45, No.3 March 1997.

[44]. Lal C. Godara and M. R. Jahromi," Broadband Antenna Array Pattern Synthesis with Specified Nulls Using Eigenvector Constraints." *In Proc. of ISAP* 2005, Seoul, Korea.